Université de Montréal

Supercomplexes multifonctionnels chez les mitochondries, et chez *E. coli*

par

Rachid Daoud

Département de Biochimie,
Faculté de Médecine

Thèse présentée a la Faculté des études supérieures en vue de l'obtention du grade de Philosophie Doctor (Ph. D.) en biochimie.

Septembre, 2011

Université de Montréal
Faculté des études supérieures et postdoctorales

Cette thèse intitulée :

Supercomplexes multifonctionnels chez les mitochondries, et chez *E. coli*

Présentée par :
Rachid Daoud

a été évaluée par un jury composé des personnes suivantes :

Dr. Stephen Michnick, président-rapporteur
Dr. B. Franz Lang, directeur de recherche
Dr. Nikolaus Heveker, membre du jury
Dr. Christian Landry, examinateur externe
Dr. Lapointe Jean-Yves, représentant du doyen de la FES

Résumé

Les processus mitochondriaux tels que la réplication et la traduction sont effectués par des complexes multiprotéiques. Par contre, le métabolisme et la voie de maturation des ARN mitochondriaux (p. ex précurseurs des ARNt et des ARNr) sont habituellement traités comme une suite de réactions catalysées par des protéines séparées. L'exécution fidèle et optimale de ces processus mitochondriaux, exige un couplage étroit nécessaire pour la canalisation des intermédiaires métaboliques. Or, les évidences en faveur de l'interconnexion postulée de ces processus cellulaires sont peu nombreuses et proviennent en grande partie des interactions protéine-protéine.

Contrairement à la perception classique, nos résultats révèlent l'organisation des fonctions cellulaires telles que la transcription, la traduction, le métabolisme et la régulation en supercomplexes multifonctionnels stables, dans les mitochondries des champignons (ex *Saccharomyces cerevisiae, Aspergillus nidulans* et *Neurospora crassa*), des animaux (ex *Bos taurus*), des plantes (*B. oleracea* et *Arabidopsis thaliana*) et chez les bactéries (ex *E. coli*) à partir desquelles les mitochondries descendent. La composition de ces supercomplexes chez les champignons et les animaux est comparable à celle de levure, toutefois, chez les plantes et *E. coli* ils comportent des différences notables (ex, présence des enzymes spécifiques à la voie de biosynthèse des sucres et les léctines chez *B. oleracea*).

Chez la levure, en accord avec les changements dûs à la répression catabolique du glucose, nos résultats révèlent que les supercomplexes sont dynamiques et que leur composition en protéines dépend des stimulis et de la régulation cellulaire. De plus, nous montrons que l'inactivation de la voie de biosynthèse des lipides de type II (FASII) perturbe l'assemblage et/ou la biogenèse du supercomplexe de la RNase P (responsable de la maturation en

5’ des précurseurs des ARNt), ce qui suggère que de multiples effets pléiotropiques peuvent être de nature structurale entre les protéines.

Chez la levure et chez *E. coli*, nos études de la maturation *in vitro* des précurseurs des ARNt et de la protéomique révèlent l’association de la RNase P avec les enzymes de la maturation d’ARNt en 3’. En effet, la voie de maturation des pré-ARNt et des ARNr, et la dégradation des ARN mitochondriaux semblent êtres associées avec la machinerie de la traduction au sein d’un même supercomplexe multifonctionnel dans la mitochondrie de la levure. Chez *E. coli*, nous avons caractérisé un supercomplexe similaire qui inclut en plus de la RNase P: la PNPase, le complexe du RNA degradosome, l’ARN polymérase, quatre facteurs de transcription, neuf aminoacyl-tRNA synthétases, onze protéines ribosomiques, des chaperons et certaines protéines métaboliques. Ces résultats supposent l’association physique de la transcription, la voie de maturation et d’aminoacylation des ARNt, la dégradation des ARN.

Le nombre de cas où les activités cellulaires sont fonctionnellement et structurellement associées est certainement à la hausse (ex, l’éditosome et le complexe de la glycolyse). En effet, l’organisation en supercomplexe multifonctionnel représente probablement l’unité fonctionnelle dans les cellules et les analyses de ces super-structures peuvent devenir la prochaine cible de la biologie structurale.

Mots-clés : processus mitochondriaux, *E. coli*, supercomplexe multifonctionnel, canalisation métabolique, maturation des précurseurs des ARNt, aminoacylion des ARNt matures, dégradation des ARN.

Abstract

It is known that processes such as transcription, translation and intron splicing require a multitude of proteins (plus a few non-protein components) organized in large 'molecular machines'. But, according to traditional views, processing of RNA precursors (e.g., tRNA and rRNA) and metabolic pathways are pools of individual enzymes (single proteins or small complexes), with sequential enzymatic reaction steps connected *via* diffusible metabolites. This perception is incompatible with the 'molecular crowding' in most cellular compartments (e.g., 60% in the mitochondrial matrix). It is also not in line with the cumulating indirect evidence from comprehensive studies of protein-protein interactions and affinity purification, showing that numerous protein complexes involving different metabolic and regulatory processes are interconnected. However, direct evidence of extensive cross-talk among diverse cellular processes remains to be clearly demonstrated.

Here we show that in mitochondria of yeast and other fungi (*Neurospora crassa* and *Rhizopus oryzae*), animal (*Bos taurus*), plant (*Brassica oleracea*), and in *E. coli* (standing for the "bacterial ancestor" of mitochondria), metabolism is physically interlinked (in supercomplexes) with translation, replication, transcription and RNA processing. Further, the supercomplexes also contain a variety of helper proteins, in support of earlier reports that describe such proteins as important structural units assisting complex assembly. Whereas the composition of supercomplexes in fungi (e.g., *Neurospora crassa*), animals and yeast is relatively similar, plants and *E. coli* present substantial compositional differences (e.g., plant-specific enzymes involved in the biosynthesis of sugars and secondary metabolites).

In yeast, the supercomplex pattern of glucose-repressed cells is completely different from that of cells grown on galactose/glycerol, and the protein composition perfectly correlates with known regulatory changes

under glucose repression. The destabilization of the complex organization is also illustrated by the deletion of genes in the mitochondrial fatty acid type II biosynthetic pathway (mutant strain oar1Δ). Mutants have both, a defect in fatty acid synthesis and in 5' processing of mitochondrial tRNA, and no longer have a supercomplex containing Oar1p and components of RNase P (5' tRNA processing). The pleiotropic mutant phenotype is best explained by a structural (assembly) defect.

Also in yeast mitochondria, we demonstrate that RNase P and tRNA Z activities are part of a large complex, which further includes the RNA degradosome complex, five additional RNA processing proteins, and several other mitochondrial pathways. 5' and 3' tRNA processing enzymes are also associated in a large, multifunctional supercomplex in *E. coli* that includes six out of the seven proteins of the RNA degradosome, nine aminoacyl-tRNA synthases, RNA polymerase plus four transcription factors, eleven ribosomal proteins plus four translation factors, several components of protein folding and maturation, and a small set of metabolic enzymes. Apparently, not only is RNA processing coordinated, but it is also structurally connected to aminoacylation, transcription and other cellular functions.

The number of documented cases where functionally related activities are structurally integrated is definitely increasing (e.g., editosome, glycolysis complex, etc). Indeed, structural integration of related functions and pathways may turn out to be a principle and the analyses of such super-structures may become a next structural biology frontier.

Keywords : process of mitochondria, *E. coli,* multifunctional supercomplexes, metabolic channeling, maturation of tRNA precursors, tRNA aminoacylation, RNA dégradation.

Table des matières

Liste des figures

Liste des abréviations

ATP	Adenosine triphosphate
BN-PAGE	Blue native polyacrylamide gel electrophoresis
bp	Paire de base
C5p	Sous-unité protéique de la RNase P d' *E. coli*
cDNA	ADN complémentaire
ADN	Acide desoxyribonucleotides
DTT	dithiothreitol
E. coli	*Escherichia coli*
EDTA	ethylenediaminetetraacetic acid
kb	Kilobase
kDa	Kilodalton
LC/MS/MS	Liquid chromatography tandem mass spectrometer
M	Molaire
M1 RNA	Sous-unité ARN de la RNase P d'*E. coli*
ADNmt	ADN mitochondrial
mM	Millimolaire
mt-P RNA	Sous-unité ARN de la RNase P mitochondriale
mt-RNase P	RNase P mitochondriale
nt	nucléotides
pmol	picomole
ARN	Acide deoxyribonucleotide
RNase P	Ribonucléase P
ADNr	ADN ribosomal
ARNr	ARN ribosomal
TCA	acide tricarboxylique
ARNt	ARN de transfert

قُلْ إِنَّ صَلَاتِي وَنُسُكِي
وَمَحْيَايَ وَمَمَاتِي لِلَّهِ
رَبِّ الْعَالَمِينَ ﴿١٦٢﴾
لَا شَرِيكَ لَهُ ۖ
وَبِذَٰلِكَ أُمِرْتُ
وَأَنَا أَوَّلُ الْمُسْلِمِينَ ﴿١٦٣﴾
قُلْ أَغَيْرَ اللَّهِ أَبْغِي رَبًّا
وَهُوَ رَبُّ كُلِّ شَيْءٍ ۚ
وَلَا تَكْسِبُ كُلُّ نَفْسٍ
إِلَّا عَلَيْهَا ۚ وَلَا تَزِرُ
وَازِرَةٌ وِزْرَ أُخْرَىٰ ۚ
ثُمَّ إِلَىٰ رَبِّكُم مَّرْجِعُكُمْ
فَيُنَبِّئُكُم بِمَا
كُنتُمْ فِيهِ تَخْتَلِفُونَ ﴿١٦٤﴾

*Je dédicace cette thèse à mes parents (**Mohammed et Maria**), à ma femme, **Nihade**, à mon fils **Soulaiman**, mes **frères**, mes **sœurs** et à toute ma **famille**: toutes ces personnes chères qui m'ont soutenu tout au long de ces années d'études.*

Remerciements

Je tiens à saluer ici les personnes qui, de près ou de loin, ont contribué à la concrétisation de ce travail de thèse de doctorat.

Tout d'abord, je tiens à exprimer ma profonde gratitude au Dr. B Franz Lang qui m'a encadré avec beaucoup de patience et de (esprit, commentaire) critique tout au long de ces années d'étude. Au fil de nos discussions, il m'a apporté une compréhension plus approfondie des divers aspects du sujet, l'art de la présentation et de la rédaction scientifique. Je salue aussi avec admiration la curiosité, la souplesse et l'ouverture d'esprit de Franz; il a su me laisser une grande marge de liberté, sans pression, pour mener à bien ce travail de recherche.

Je remercie Dr. Stephen Michnick, qui m'a fait l'honneur de présider le jury de ma thèse de doctorat, pour l'intérêt et le soutien chaleureux dont il a toujours fait preuve (tout au long de mon doctorat et au sein de mon comité de thèse) pour discuter des aspects scientifiques et techniques du sujet. Je suis très reconnaissant envers le Dr. Christian Landry et le Dr. Nikolaus Heveker d'avoir accepté d'être membres de mon jury.

J'adresse aussi ma gratitude à mon oncle, Dr. El-Maaroufi Mohammed, et à mon frère, Dr. Daoud Rahim, pour leur soutien inconditionnel durant mes années d'études. Je tiens à les remercier pour leur parrainage pendant toutes les années de mes études en Europe et lors de ma venue au Canada. Je tiens à exprimer ma profonde gratitude au Dr. Sabar Mohammed tout d'abord pour son amitié, son aide pratique, son initiation aux études des complexes, pour ces réponses à des questions pratiques, techniques, ou scientifiques, que je me suis posé.

Je tiens à exprimer ma reconnaissance très sincère à Lise Forget pour son soutien indéfectible durant mes années de thèse, les améliorations suggérées pour cette thèse, ainsi que pour l'aide et les conseils techniques. Egalement, je tiens à la remercier pour son amitié, son soutien moral et les discutions que nous avons partagées. Je remercie Shona Teijeiro pour son soutien et pour les améliorations du texte de cette thèse ainsi que pour son amitié. Je tiens à remercier tous les membres présents et passés du laboratoire de Franz, de Gertraud, d'Hervé et de Nicolas. Malika Daoud, Noureddine Daoud, Abdaljabar Daoud, Abdelatif Daoud, Mohammed Daoud, Abdelbaki Daoud, Rachid El-Kraimi, Majid El-Kraimi, Mohamed Aoulad Aissa, Faysal Ouenzar, Khalid Hilmi, Pasha, Elias, Siva, Patrice, Sophie et Ioana. Je souhaite également remercier le personnel du département de biochimie, Dr. Daniel Chevrier, Monique Vasseur et Sylvie Beauchemin.

Mes remerciements aux Dr Gertraud Burger, Dr Hervé Philippe, Dr. Nicolas Lartillot, Dr. Henner Brinkmann, Dr. Emmanuel Levy, Dr. Pascal Chartrand, Dr. Daniel Zanklusen, Dr. Marlene Oeffinger, Dr. Eric Bonneil et Dr. Isabelle Rouiller pour leurs conseils et leurs discutions des aspects scientifiques du sujet.

Préface

Mon travail au laboratoire a commencé par l'étude comparative de l'organisation en complexes de la RNase P (maturation en 5' et 3' des précurseurs des ARNt (pré-ARNt)), sur plusieurs systèmes mitochondriaux des eucaryotes (ex *Saccharomyces cerevisiae*) et chez *E. coli.* Ainsi, suite à la caractérisation chez la levure de l'association en complexe (130 protéines) de la RNase P avec des protéines de différentes fonctions (incluants maturation des ARN ribosomiques, métaboliques, chaperons, transports, traduction, maintenance de génome), nous avons décidé pour la suite du projet d'élargir notre champ d'étude et d'explorer l'organisation des processus mitochondriaux et d'*E. coli* (ex transcription, traduction et métabolisme) en général.

Dans l'introduction de cette thèse, je vais discuter l'organisation en complexes des protéines, les principaux exemples connus au sujet du couplage entre les fonctions cellulaires, la maturation des précurseurs des ARNt, et ensuite décrire les objectifs du projet de mon doctorat. Cependant, puisqu'il y a très peu d'exemples de l'organisation en supercomplexe multifonctionnel dans la mitochondrie (appart les liens physiques entre les complexes de la chaîne respiratoire/ phosphorylation oxydative), j'ai choisie de faire une revue de la littérature plus générale qui tient compte des principaux exemples connus à travers les espèces.

Chapitre 1. Introduction

Introduction

Certaines fonctions de la cellule comme la réplication et la dégradation des protéines sont connues pour être accomplies par des machines moléculaires, stables et/ou transitoires. Celles-ci sont composées de protéines, d'ADN, d'ARN et d'autres molécules (ex lipides, sucres et ions) et sont hautement structurées (Alberts 1998; Adelmant and Marto 2009). Des études récentes démontrent que ces complexes représentent probablement l'unité fonctionnelle dans la cellules des bactéries et des eucaryotes (Hartwell, Hopfield et al. 1999; Spirin and Mirny 2003; Pereira-Leal, Enright et al. 2004; Gavin, Maeda et al. 2010).

Afin d'identifier tous les complexes cellulaires d'une manière systématique, des techniques génétiques, biophysiques, biochimiques et *in silico* ont été appliquées (Figure 1) (Kohn, Aladjem et al. 2006; Kocher and Superti-Furga 2007). Ainsi, par l'utilisation des stratégies biochimiques (ex co-immunoprécipitation; chromatographie d'affinité des protéines étiquetées suivie par la spectrométrie de masse (AP-MS) (Chien, Bartel et al. 1991; Kohn, Aladjem et al. 2006); crosslinking chimique suivie par la spectrométrie de masse et chromatographie), des centaines de petits complexes ont été identifiés (Hartwell, Hopfield et al. 1999; Gavin, Bosche et al. 2002; Ho, Gruhler et al. 2002; Gavin and Superti-Furga 2003; Spirin and Mirny 2003; Bouwmeester, Bauch et al. 2004; Pereira-Leal, Enright et al. 2004; Butland, Peregrin-Alvarez et al. 2005; Gavin, Aloy et al. 2006; Kohn, Aladjem et al. 2006; Krogan, Cagney et al. 2006; Ewing, Chu et al. 2007; Kocher and Superti-Furga 2007; Adelmant and Marto 2009; Gavin, Maeda et al. 2010). Chaque stratégie est associée à d'important taux de faux-positifs et faux-négatifs (von Mering, Krause et al. 2002). Chez *S. cerevisiae* par exemple, en fonction de la technique d'investigation utilisée, les nombres des interactions protéine-protéine varient entre 10 000-17 000 et 25 000 -35 000 (Parrish, Gulyas et al. 2006). En plus, les 1038 complexes caractérisés par les études de chromatographie d'affinité des protéines étiquetées, suivie par la spectrométrie de masse, n'incluent pas 74 complexes qui sont pourtant biochimiquement bien identifiés et reportés dans la littérature (Pu, Vlasblom et al. 2007; Wodak, Pu et al. 2009). De plus, l'organisation de plusieurs fonctions (ex métabolisme, maturation des protéines, ARNt synthétases et voie de maturation des

ARNt) reste en grande partie sans réponse (Williamson and Sutcliffe 2010). Les raisons pour le manque d'identification de ces processus sont: (i) qu'ils soient systématiquement éliminés de la liste des protéines, car les auteurs considèrent qu'elles sont liées d'une façon non spécifique à plusieurs complexes; ceci à cause de leurs niveau d'expression cellulaire souvent élevé (ex l'aconitase, une protéine métabolique dont on retrouve jusqu'à 96,700 copies pare cellule (Ghaemmaghami, Huh et al. 2003)), de même, les enzymes de la glycolyse (connues pour être associées elles-mêmes en complexes (Winkel 2004)), et les protéines ribosomiques (connues pour être impliquées dans des fonctions autres que la traduction (Wool 1996; Krause, von Mering et al. 2004)) ont été éliminées de la liste des complexes identifiés par AP-MS chez la levure; (ii) leur expression cellulaire est très faibles (ex la Rpm2p (RNase P; maturation en 5' des précurseurs des ARNt mitochondriaux a seulement ~1,000 copies par cellule (Ghaemmaghami, Huh et al. 2003)), donc leur identification par ces techniques est difficile.

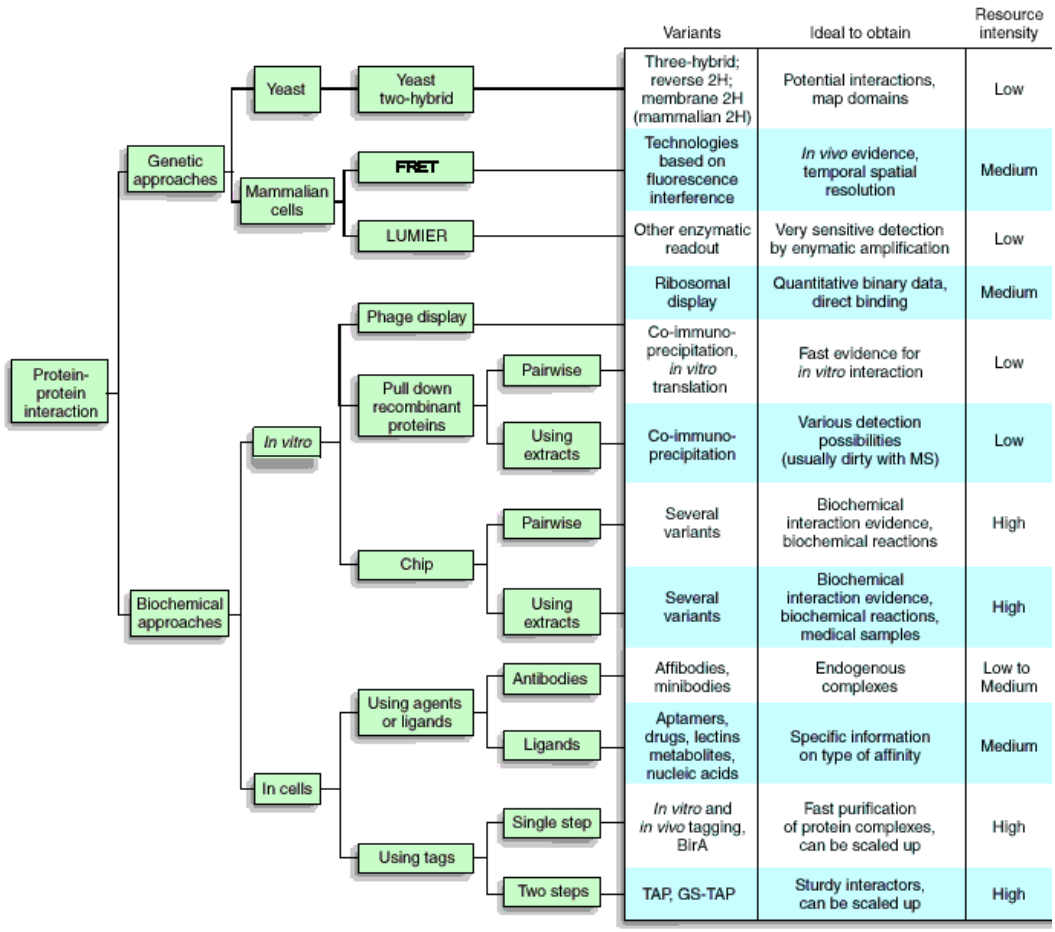

Figure 1. Liste des approches expérimentales pour les études *in vivo* et *in vitro* d'interactions protéine-protéine. Les variantes, les types des interactions identifiées (génétique et/ou biochimique) et l'estimation du rendement de chaque stratégie sont indiqués.

Figure tirée de (Kocher and Superti-Furga 2007).

A. Association des protéines cellulaires en machineries moléculaires multifonctionnelles

L'assemblage et la biogenèse des machines moléculaires comme le ribosome impliquent des étapes de la régulation transcriptionnelle, ainsi que des modifications post-traductionnelles et conformationnelles qui dépendent de chaperons et de la disponibilité d'énergie en forme d'ATP. Ils requièrent aussi le recrutement de protéines et/ou de molécules non peptidiques (ex ARN) (Kruger, Kloetzel et al. 2001; Grandi, Rybin et al. 2002; Kusmierczyk and Hochstrasser 2008). D'autre part, l'exécution fidèle et optimale des processus cellulaires, tels que la traduction, exige le couplage étroit de la synthèse des précurseurs des protéines (ex acides aminés et ARNt aminoacylés), du ribosome et de l'énergie (Kruger, Kloetzel et al. 2001; Grandi, Rybin et al. 2002; Kusmierczyk and Hochstrasser 2008). Or, les évidences en faveur de l'interconnexion postulée de ces processus cellulaires sont peu nombreuses (voir détails plus bas). Toutefois, la composition des complexes protéiques révélés par les interactions protéine-protéine et les études AP-MS suggère des interconnexions entre divers processus cellulaires tels que transcription, traduction, métabolisme et régulation (Krause, von Mering et al. 2004). En d'autres termes, les fonctions cellulaires semblent êtres organisées en superstructures multifonctionnelles (Kuhner, van Noort et al. 2009; Burmann, Schweimer et al. 2010; Proshkin, Rahmouni et al. 2010). Par exemple, suite à la comparaison des modèles structuraux des complexes (ex ribosome) aux images obtenues par la microscopie électronique et aux structures établies par la tomographie de la bactérie *Mycoplasma pneumoniae*, des associations sont révélées entre le ribosome et le complexe de pyruvate déshydrogénase (PDH), entre l'ARN polymérase et la PDH, et entre les trois, soient ribosome, l'ARN polymérase et la PDH (Figure 2) (Kuhner, van Noort et al. 2009).

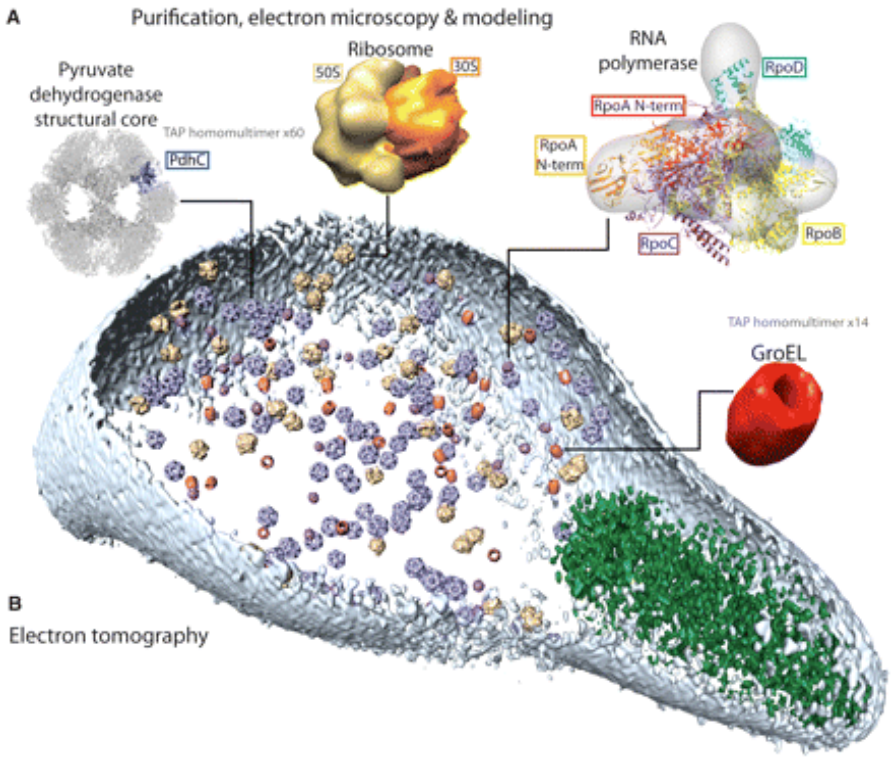

Figure 2. De la protéomique à la cellule. Par la combinaison de la reconnaissance de forme et d'algorithme de classification, les modèles structuraux des complexes protéiques de *M. pneumoniae* ont été comparés aux images obtenues par la microscopie électronique et à des structures définies par la tomographie. (A) tomographies du ribosome en jaune (~26 nm), du PDH en bleu (~23 nm), du chaperon homo-multimère GroEl (HSP60) en rouge (~20 nm) et de l'ARN polymérase en violet (~17 nm) (B) tomographie de la cellule. Les dimensions cellulaires sont ~300 nm par 700 nm. La membrane cellulaire est représentée en bleu clair. Les complexes individuels (A) ne sont pas à l'échelle, mais ils le sont par rapport à la cellule bactérienne (B).
Figure tirée de (Kuhner, van Noort et al. 2009).

A.I. Supercomplexes multiprotéiques incluant la machinerie de réplication et le métabolisme des nucléotides

Chez les eucaryotes, le couplage étroit de la synthèse des nucléotides avec la réplication est nécessaire pour franchir la contrainte de la durée limitée de la phase S durant la quelle se fait la duplication du génome (Hubscher, Maga et al. 2002). En fait, les quantités de désoxynucléotides (dNTP) distribués dans toute la cellule sont de quatre à cinq fois inférieures au Km apparent (50 µM) de l'ADN polymérase (Reddy and Mathews 1978; Reddy and Fager 1993); donc elles ne peuvent supportées la vitesse à laquelle les fourches de réplication se déplacent chez les eucaryotes (4 millions de nucléotides / seconde / cellule). De plus, l'ensemble du pool cellulaire de dNTPs devait être épuisé au maximum après une minute du début de la synthèse d'ADN. Ces observations suggèrent que les dNTPs devraient être (i) synthétisées dans le cadre et au rythme du mouvement de la fourche de réplication, et (ii) compartimentés et concentrés dans les sites de réplication de l'ADN en vue d'atteindre une concentration qui supporte la vitesse de l'ADN polymérase. Connaissant les valeurs des Km et Vmax de certaines enzymes clés du métabolisme des désoxynucléotides, il est postulé que ces enzymes devraient interagir les unes avec les autres pour former un complexe multienzymatique capable de soutenir la vitesse rapide de la synthèse des dNTP, correspondant à celle de la réplication (Reddy, Singh et al. 1977; Reddy and Fager 1993). En fait, chez *E. coli* et les mammifères des résultats biochimiques (co-purification) et de microscopie électronique (Figure 3a) suggèrent des interactions entre les protéines de la machinerie de réplication (réplisome) et celles de la synthèse des nucléotides (dNTP synthétase). Ainsi, leur organisation en complexe multienzymatique et multiprotéique "réplitase" a été proposée (Figure 3b) (Prem veer Reddy and Pardee 1980; Alberts 1987; Wheeler, Ray et al. 1996; Murthy and Reddy 2006).

(a) (b)

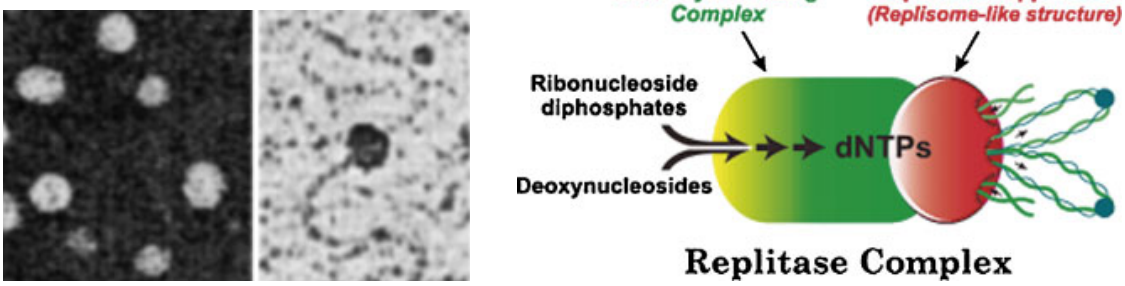

Figure 3. Microscopie électronique du réplitase. (a) association entre le complexe de la dNTP synthétase et de la machine de réplication, isolée à partir de l'extrait nucléaire des cellules du thymus (Murthy and Reddy 2006). (b) Modèle de l'association entre le complexe de dNTP synthétase et de la machine de réplication formant la réplitase (Murthy and Reddy 2006).

Figure tirée de (Murthy and Reddy 2006)

A.II. Jonction physique entre la transcription, la maturation des ARN et l'assemblage des complexes ribonucléoprotéiques

Sur la base de données protéomiques (p. ex chromatographie d'affinité) et d'immunoprécipitation de la chromatine, chez les eucaryotes, il semble que la maturation des ARNr et des ARNm est physiquement couplée à l'assemblage du ribosome et du splicéosome respectivement, de même qu'à la transcription de leurs ARN respectifs (Granneman and Baserga 2005; Pandit, Wang et al. 2008). Ainsi, il a été démontré que les protéines de synthèse de la coiffe en 5' des ARNm, de l'épissage des ARNm, et de la formation de 3'des ARNm sont liées à l'ARN polymérase II (ARNPII) et aux facteurs de transcription (Figure 4) (Bentley 2005; Buratowski 2005)(Maniatis and Reed 2002; Proudfoot, Furger et al. 2002; Saunders, Core et al. 2006; Das, Yu et al. 2007). Toutefois, l'ARNPII purifié ne contient pas tous les facteurs de la maturation d'ARN, ce qui suggère qu'à la suite du fractionnement biochimique seule une partie des interactions plus stables sont identifiées (Bentley 2005; Buratowski 2005; Maniatis and Reed 2002; Proudfoot, Furger et al. 2002; Saunders, Core et al. 2006; Das, Yu et al. 2007).

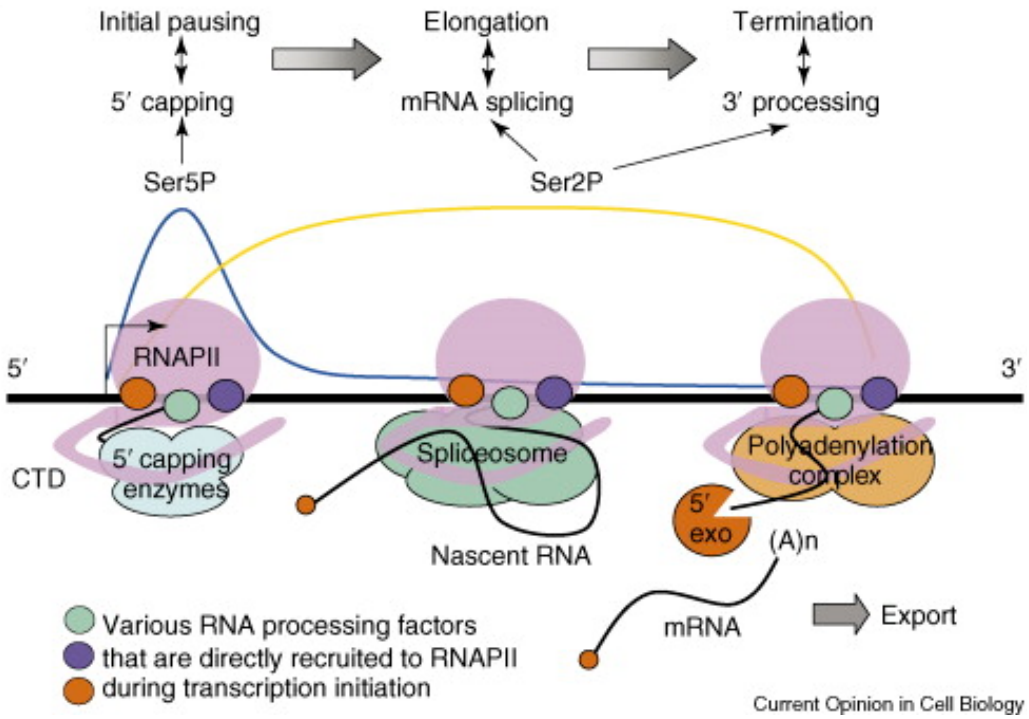

Figure 4. Schéma du couplage de la transcription et de la voie de maturation des pré-ARNm chez la levure. Les enzymes de synthèse de la coiffe en 5' sont recrutées par le biais d'interactions directes avec le domaine carboxy-terminal phosphorylé en Serine 5 (Ser5 CTD phosphoryle) de l'ARN polymérase II (ARNPII). Cette phosphorylation est aussi nécessaire pour le recrutement des facteurs d'épissage, au cours de la transcription. La formation de l'extrémité 3' est fonctionnellement liée à la phase de terminaison de la transcription.

Figure tirée de (Pandit, Wang et al. 2008).

A.III. Couplage spatio-temporelle de la transcription et de la traduction

Le couplage indirect entre la transcription et la traduction est décrit depuis les années 1970 chez les bactéries (Miller, Hamkalo et al. 1970) et chez les archéobactéries. Chez ces dernières, des polysomes directement liées à la double hélice de l'ADN ont pu être visualisée par microscopie électronique chez *Thermococcus kodakaraensis* (Figure 5) (French, Santangelo et al. 2007). En 2010, des études chez *E. coli* ont démontré que la transcription est couplée dans le temps et dans l'espace avec la traduction (Burmann, Schweimer et al. 2010; Proshkin, Rahmouni et al. 2010). Dans la première étude, Nudler et ses collègues ont d'abord étudié l'effet de l'antibiotique chloramphénicol (Cm), un inhibiteur spécifique de la traduction, sur le taux de la transcription. En l'absence de Cm la vitesse de la transcription a été déterminée à 42 nt /s, correspondant à un taux de traduction de 14 aa /s. Toutefois, l'ajout de Cm réduit le taux de transcription à 27 nt /s, correspondant à un taux de traduction de 9 aa /s. Par la suite, les auteurs ont mesuré la vitesse de transcription d'un mutant *rpsL* d'*E. coli* (CH184) dont le taux de traduction est lent. Le phénotype de ce mutant est partiellement corrigé par l'ajout de la streptomycine (Sm). En effet, le taux de transcription plutôt lent (19 nt/s) de CH184 s'est accéléré à 30 nt/s lors de l'addition de Sm, en concordance avec le taux de traduction (dans CH184 a été lent (19 nt/s), mais s'est accéléré à 30 nt/s lors de l'addition de Sm. Pour apporter un soutien supplémentaire à leur conclusion, les auteurs ont comparé le taux de transcription de plusieurs gènes ayant des fréquences différentes des codons rares, ce qui a pour effet de retarder la progression du ribosome. Ainsi, les taux de transcription et de traduction des gènes *rplB* et *tufA* (nombre relativement restreint de codons rares) ont été proportionnels et plus rapides que ceux des gènes *lacZ* et *infB* (fréquence intermédiaire de codons rares), et du gène *srb4* (fréquence élevée de codons rares). Ces résultats suggèrent que l'accélération et la décélération du ribosome affecte la vitesse de l'ARNP (Proshkin, Rahmouni et al. 2010).

Dans une deuxième étude, en utilisant la spectroscopie NMR (résonance magnétique nucléaire), le lien physique de la protéine NusE (10S) de la sous unité 30S du ribosome avec le facteur NusG de l'ARNP a été révélé (Burmann, Schweimer et al. 2010). Un tel mécanisme de coopération entre le ribosome et l'ARNP garantit que le rendement de transcription soit toujours adapté aux besoins de la traduction, qui dépend

elle aussi des conditions de croissance (Burmann, Schweimer et al. 2010). Ce couplage est responsable de la régulation par atténuation de l'expression des gènes (Grundy and Henkin 2006), et de la terminaison précoce de transcription (Pan and Sosnick 2006).

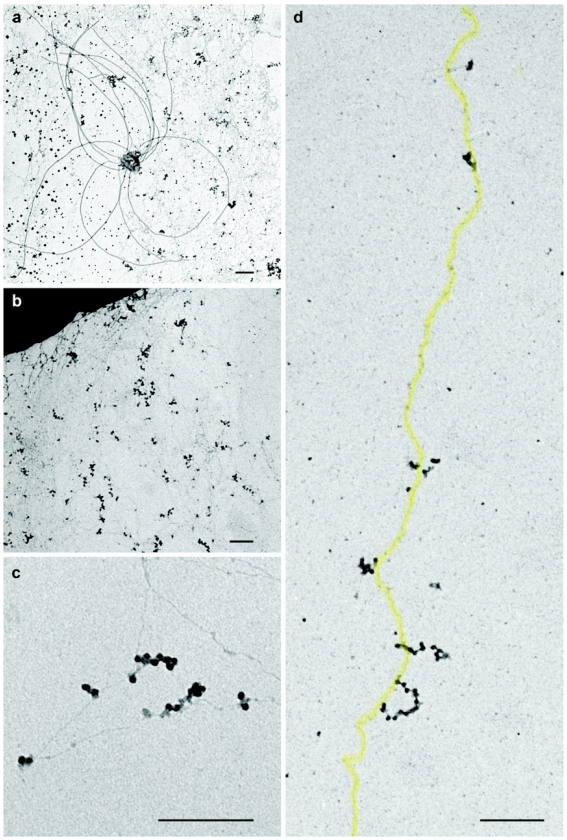

Figure 5. Microscopie électronique des polysomes directement liés à la double hélice d'ADN obtenu à partir du lysat des cellules de l'archéobactérie *Thermococcus kodakaraensis*. (a) lysat des cellules montrant des flagelles et les brins de chromatines, (b, c et d) polysomes attachés aux brins de l'ADN (barre = 0,2 microns). En (d), le brin d'ADN est mis en évidence par un ombrage jaune.
Figure tirée de (French, Santangelo et al. 2007).

A.IV. Intersection des voies métaboliques avec la phosphorylation oxydative

A.IV.1. Diffusion simple versus canalisation des voies métaboliques

La majorité des voies métaboliques est perçue comme un ensemble d'enzymes fonctionnellement séparées dans l'espace, avec des réactions séquentielles connectées par des intermédiaires métaboliques (Pettersson 1991; Wu, Gutfreund et al. 1991). Cette perception classique est pourtant incompatible avec le principe de l'encombrement moléculaire dans les compartiments cellulaires (Ellis 2001; Grunewald, Medalia et al. 2003), qui est principalement dû aux hautes concentrations de protéines (Ellis 2001; Ovadi and Saks 2004; Zhou, Rivas et al. 2008). Par exemple, la concentration des protéines dans la mitochondrie est de 60%, et de 30-40% chez *E. coli* (Figure 6a) (Ovadi and Saks 2004). Ainsi, cet encombrement ne supporte pas la grande vitesse des réactions métaboliques par simple diffusion *in vivo* (Hall and Hoshino 2010). Les auteurs proposent donc l'organisation des enzymes métaboliques en complexes multi-protéiques nommés métabolon (p. ex le cycle de Krebs et la glycolyse) (Winkel 2004), un concept qui reste controversé à l'heure actuelle (Welch 1977; Srere 1987; Winkel 2004).

L'organisation des voies métaboliques en métabolon permettrait d'améliorer l'efficacité catalytique aux sites actifs des enzymes, un mécanisme connu sous le nom de canalisation métabolique (Figure 6b). Cette dernière a pour avantages, (i) d'éviter les contraintes cinétiques qui résultent de la dilution de produits intermédiaires; (ii) d'assurer la conversion rapide des intermédiaires labiles et/ou toxiques, en empêchant leurs diffusions dans la matrice environnante; (iii) d'empêcher les composés qui pourraient avoir un effet inhibiteur sur l'enzyme d'atteindre le site actif; et (iv) de contrôler la coordination des voies métaboliques qui ont des enzymes et/ou produits intermédiaires en communs (Winkel 2004; Jorgensen, Rasmussen et al. 2005). Par contre, les évidences expérimentales en faveur du principe de métabolon sont peu nombreuses (Winkel 2004; Williamson and Sutcliffe 2010). Par exemple, chez les eucaryotes il n'existe aucune évidence de l'association *in vitro* des six enzymes (dont trois multifonctionnelles) catalysant la biosynthèse des purines. Toutefois, en utilisant le marquage fluorescent leur co-localisation *in vivo* est confirmée chez la levure (An, Kumar et al. 2008). D'autre part, en utilisant les marqueurs isotopiques, la canalisation de la plupart (sinon la totalité) des enzymes de la glycolyse a été démontrée chez *Arabidopsis* et chez la pomme de terre. Le

complexe de la glycolyse est formé à la surface de la membrane mitochondriale externe, en réponse à l'expression des protéines d'OXPHOS (Giege, Heazlewood et al. 2003; Graham, Williams et al. 2007).

a **b**

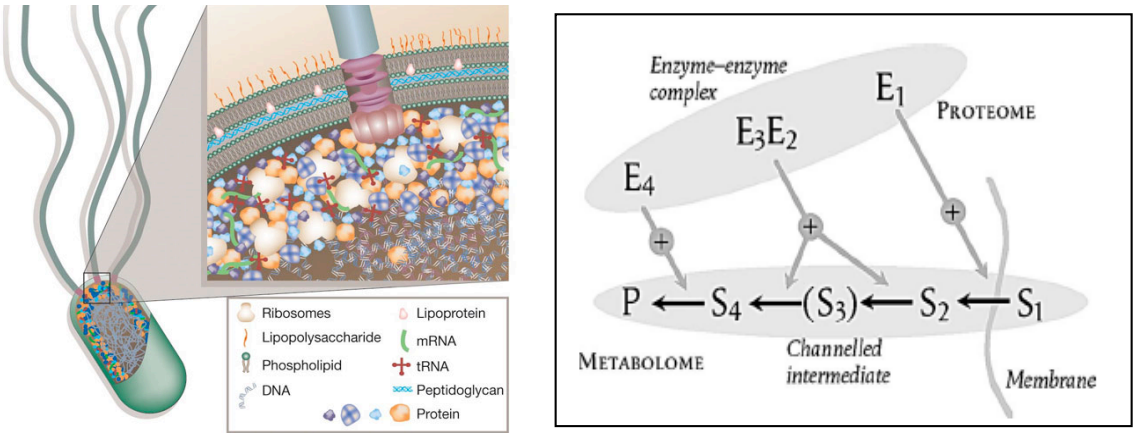

Figure 6. Représentation schématique de (a) l'encombrement moléculaire dans la cellule d'*E. coli* (Dobson 2004) et (b) du principe de la canalisation métabolique (Cornish-Bowden, Cardenas et al. 2004).

Figure 7a tirée de (Dobson 2004)

Figure 7b tirée de (Cornish-Bowden, Cardenas et al. 2004).

A.IV.2. Supercomplexes de la phosphorylation oxydative

L'énergie résultant de l'oxydation d'intermédiaires métaboliques NADH et FADH2 produits lors des réactions cataboliques (p. ex glycolyse et cycle TCA) est utilisée pour générer un gradient de protons entre la matrice et l'espace inter-membranaire. Le transport de ces protons vers la matrice mitochondriale est couplé à la phosphorylation de l'ADP en ATP. On parle alors de la phosphorylation oxydative (OXPHOS). L'OXPHOS est composée d'une centaine de protéines organisées en cinq complexes localisés dans la membrane interne mitochondriale ou la membrane plasmique des bactéries aérobies, auxquels sont associés le coenzyme Q et le cytochrome c qui assurent l'interface entre les complexes. Les complexes I à IV assurent l'oxydation de NADH et FADH2, les complexes I, III et IV génèrent un gradient électrochimique de protons, et le complexe V (ATP synthase) est responsable de la phosphorylation de l'ADP en ATP (Figure 7i). A la suite des données récentes, il est maintenant reconnu que les complexes de l'OXPHOS interagissent physiquement en mégacomplexes de différentes stoechiométries, constituant une sorte de "respirasome" (Figure 7ii) (Dudkina, Heinemeyer et al. 2006; Vonck and Schafer 2009; Wittig and Schagger 2009). Ainsi, en plus de la canalisation de substrats, le respirasome joue un rôle important dans l'assemblage des complexes de l'OXPHOS (p. ex dans les fibroblastes de la souris le complexe IV est nécessaire pour l'assemblage et la stabilité du complexe I (Diaz, Fukui et al. 2006)). Le respirasome peut aussi expliquer que certaines mutations localisées dans une sous unité d'un complexe respiratoire provoquent des défauts secondaires dans d'autres complexes. Ainsi par exemple, chez les mammifères, certaines mutations mitochondriales du cytochrome b affecte l'activité du complexe III et celle du complexe I (Acin-Perez, Bayona-Bafaluy et al. 2004; Vonck and Schafer 2009; Dudkina, Kouril et al. 2010). Ces mégacomplexes représentent donc très probablement l'état fonctionnel de l'OXHPOS (Vonck and Schafer 2009; Dudkina, Kouril et al. 2010).

(i) **(ii)**

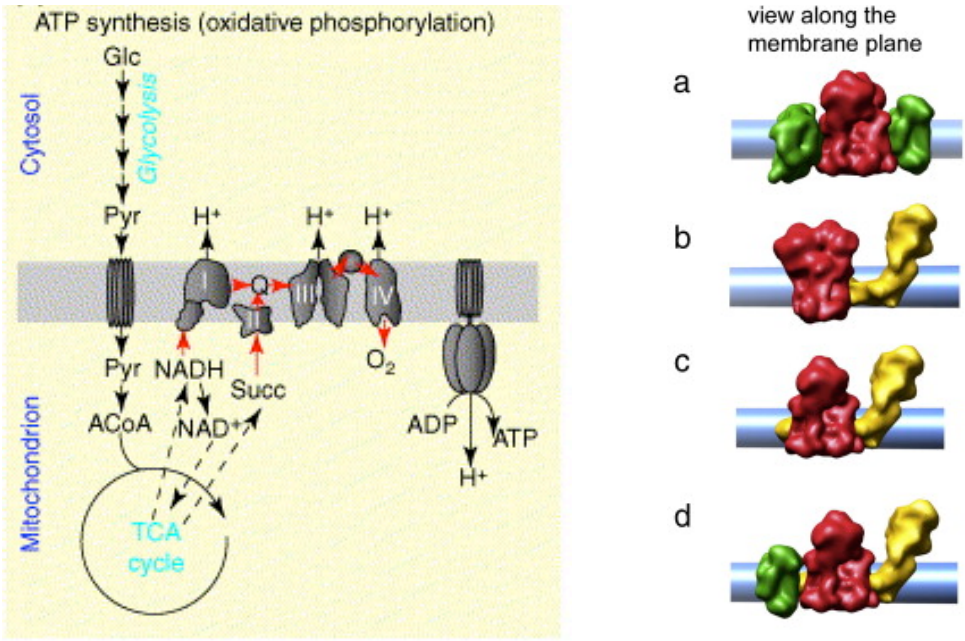

Figure 7. Modèles du lien métabolique entre le cycle TCA et les complexes de la chaîne respiratoire. (i) Schéma des échanges métaboliques entre le cycle TCA et les complexes OXPHOS chez *A. thaliana*. (ii) supercomplexe de la chaîne respiratoire formé par l'association de : (a) deux homodimères du complexe III et deux homodimères du complexe IV de *S. cerevisiae*. (b) complexe I avec deux homodimères du complexe III d'*A. thaliana*. (c) complexe I avec deux homodimères du complexe III de *B. taurus*. (d) complexe I, deux homodimères du complexe III et du complexe IV de *B. taurus*. L'emplacement présumé de la membrane est indiqué en bleu, le complexe I est indiqué en jaune, le complexe III est indiqué en rouge et le complexe IV est indiqué en vert.

Figure tirée de (Vonck and Schafer 2009).

A.IV.3. Évidences d'interactions des protéines métaboliques et de la phosphorylation oxydative

Les évidences de l'association physique entre les protéines de l'OXPHOS et du métabolisme sont peu nombreuses et sont limitées à la succinate déshydrogénase qui est le lien directe entre l'OXPHOS et le cycle TCA, et à la révélation en 2010 d'interaction entre le complexe *bc1* et la malate déshydrogénase (enzyme de cycle TCA) dans la mitochondrie de bœuf (Wang, Yu et al. 2010). Néanmoins, le co-fractionnement de l'isovaleryl-CoA déshydrogénase (biosynthèse des lipides) et du complexe I chez la souris, consolide l'hypothèse de l'association fonctionnelle et structurale entre l'OXPHOS et le métabolisme intermédiaire (principalement le cycle TCA, la glycolyse et l'oxydation des lipides) (Reifschneider, Goto et al. 2006; Wang, Mohsen et al. 2010).

B. Maturation des précurseurs des ARNt (pré-ARNt)

B.I. Maturation en 5' pré-ARNt par la RNase P

La maturation des pré-ARNt est présente chez la majorité des espèces dans les trois domaines de la vie, incluant les mitochondries et les chloroplastes des eucaryotes (Lai, Vioque et al. 2010). Après leur transcription les pré-ARNt subissent plusieurs étapes de maturation aux extrémités 5' et 3' avant l'amino-acétylation par les ARNt-synthétases. La maturation en 5' se fait par la RNase P qui est présente dans le noyau, les mitochondries et les chloroplastes des espèces photosynthétiques (Figure 8) (Lai, Vioque et al. 2010). Exceptions faites de la mitochondrie humaine et de celle d'*Arabidopsis* (et probablement d'autres animaux et plantes) dont l'activité de la RNase P dépend uniquement de protéines (Figure 8) (Holzmann, Frank et al. 2008; Gobert, Gutmann et al. 2010), en général la RNase P est un complexe ribonucléoprotéique et sa sous-unité ARN est responsable de l'activité catalytique (Guerrier-Takada, Gardiner et al. 1983; Cherayil, Krupp et al. 1987; Waugh and Pace 1990; Pannucci, Haas et al. 1999; Kikovska, Svard et al. 2007). Le nombre de protéines associées à la sous-unité ARN varie en fonction des organismes; une seule chez *E. coli*, cinq chez les archéobactéries et chez les eucaryotes, il y en a de neuf à dix dans le noyau, de une à sept dans les mitochondries et les chloroplastes (Figure 8) (Evans, Marquez et al. 2006; Walker and Engelke 2006; Hartmann, Gossringer et al. 2009; Lai, Vioque et al. 2010). Ces protéines ont souvent un rôle de reconnaissance spécifique du substrat de la RNase P (Guerrier-Takada, Gardiner et al. 1983; Pannucci, Haas et al. 1999).

La RNase P possède des substrats autres que les pré-ARNt. Ainsi par exemple, chez *E. coli* et la levure où les fonctions sont les mieux caractérisées, elle est responsable de la terminaison précoce de la transcription (Zangrossi, Briani et al. 2000), de la maturation de l'ARN CI, de l'ARN 4,5S (Peck-Miller and Altman 1991) et des ARNm des opérons *tna* (dégradation du tryptophane), *his* (biosynthèse de l'histidine), *rbs* (transport du D-ribose), *secG* (excrétion de protéines), *lac* (lactose), ainsi que des ORFs b0669 et b0671 (Li and Altman 2003). Chez la levure elle est impliquée dans la maturation des petits ARN nucléolaires (snoRNAs et ncRNA) (Samanta, Tongprasit et al. 2006; Yang and Altman 2007; Coughlin, Pleiss et al. 2008).

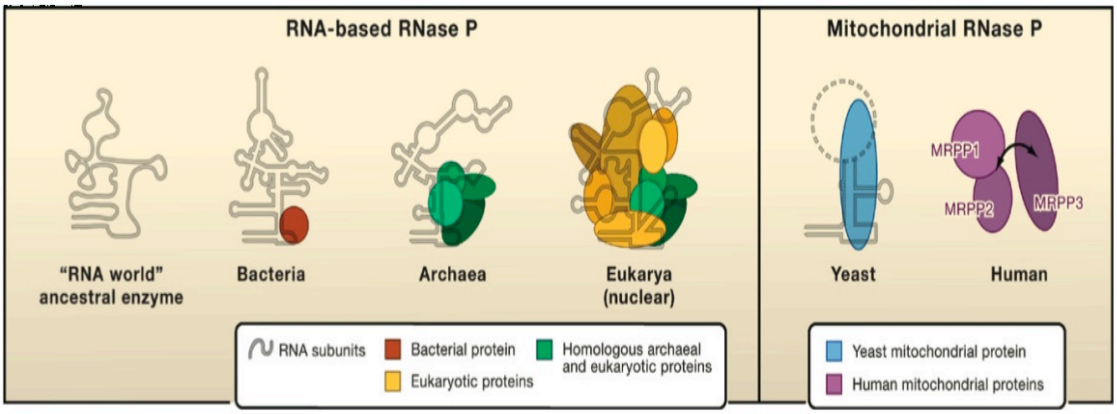

Figure 8. A gauche, schéma représentatif de l'accroissement du nombre de protéines associées à la sous-unité ARN de la RNase P, au cours de l'évolution. A droite, le minimum de protéines nécessaires à l'activité RNase P chez la levure et chez *H. sapiens* dont l'activité de maturation en 5' dépend de trois protéines (Walker and Engelke 2008). Il faut noter que chez la mitochondrie d'*Arabidopsis*, l'activité dépend aussi d'une seule et unique protéine (Holzmann, Frank et al. 2008; Gobert, Gutmann et al. 2010; Lai, Vioque et al. 2010).

Figure tirée de (Walker and Engelke 2008)

B.II. Clivage exonucléotidique et/ou endonucléotidique en 3' pré-ARNt

La génération des ARNt fonctionnels requiert souvent la coupure de la séquence 3'des pré-ARNt, l'épissage des introns, l'édition d'ARN (remplacement et/ou addition de nucléotides) et l'addition successive du motif CCA (Apirion and Miczak 1993; Morl and Marchfelder 2001; Weiner 2004; Xiong and Steitz 2006). Moins élucidée que la maturation en 5' pré-ARNt, le clivage en 3' implique une activité endonucléase et/ou exonucléase selon les espèces étudiées (Apirion and Miczak 1993; Morl and Marchfelder 2001). Ainsi, le mécanisme de la maturation en 3' pré-ARNt est inconnu chez les archéobactéries, mais chez les bactéries il implique plusieurs endo- et exonucléases (Apirion and Miczak 1993; Morl and Marchfelder 2001). Chez *E. coli*, la maturation est initiée pas un clivage impliquant deux endonucléases (RNase III et E), suivie par l'action de six exonucléases (RNases II, BN, D, PH, PNPase et T) (Figure 9) (Li and Deutscher 1996; Morl and Marchfelder 2001).

Dans le noyau, les mitochondries et les chloroplastes des eucaryotes les études biochimiques montrent une activité endonucléase (Castano, Tobian et al. 1985; Morl and Marchfelder 2001) et/ou une activité exonucléase (Garber and Altman 1979; Engelke, Gegenheimer et al. 1985; Mayer, Schiffer et al. 2000)(Papadimitriou and Gross 1996; Wolin and Cedervall 2002). Alors que l'enzyme responsable de l'activité exonucléase est encore inconnue, les études récentes montrent que c'est bien l'endonucléase RNase Z (tRNase Z) (Hartmann, Gossringer et al. 2009) qui est responsable de la maturation en 3' pré-ARNt chez certaines bactéries et les archéobactéries (Hartmann, Gossringer et al. 2009), ainsi que dans le noyau, les mitochondries et les chloroplastes (Mayer, Schiffer et al. 2000; Morl and Marchfelder 2001). La majorité des RNases Z coupent spécifiquement l'extrémité 3' avant l'addition de CCA (Folichon, Arluison et al. 2003; Dubrovsky, Dubrovskaya et al. 2004), et elles sont responsables de la dégradation de plusieurs ARNm chez *E. coli* (Hartmann, Gossringer et al. 2009) et de la maturation d'autres substrats comme l'ARN 5S chez *Haloferax volcanii* (Holzle, Fischer et al. 2008). Alors que l'activité des enzymes impliquées dans la maturation en 3' pré-ARNt est bien caractérisée, l'organisation spatiale ainsi que l'ordre d'action (ex, RNases II, BN, D, PH, PNPase et T *d'E. coli*) sont encore inconnues (Li and Deutscher 1996; Morl and Marchfelder 2001).

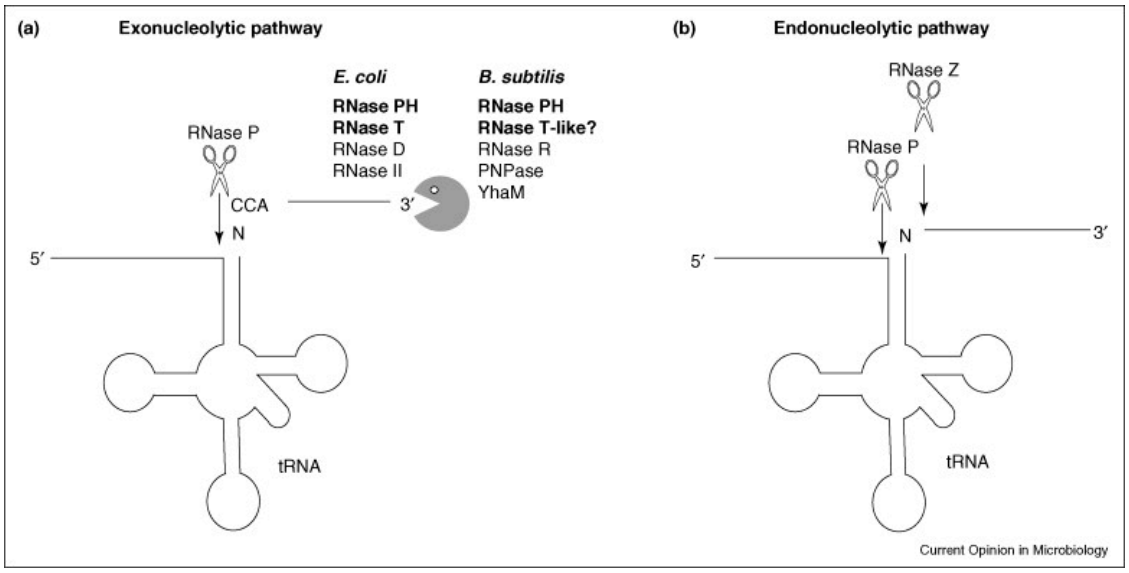

Figure 9. Schéma des voies exonucléotidique (a) et endonucléotidique (b) de la maturation des pré-ARNt chez *E. coli, B*. *subtilis* et chez les espèces dont la RNase Z est impliquée dans l'activité. Les enzymes connues pour être impliquées dans ces deux voies sont indiquées.

Figure tirée de (Condon 2007)

B.III. Évidences de l'association d'enzymes de la maturation des pré-ARNt

Actuellement les quelques évidences qui suggèrent une association des enzymes de la maturation des pré-ARNt proviennent de l'étude d'*E. coli*, *Bacillus subtilis* et de la mitochondrie de la levure (Robertson, Altman et al. 1972; Stark, Kole et al. 1978; Baer and Altman 1985; Morales, Wise et al. 1989; Brown and Pace 1992; Martin 1993). Durant les premières étapes de sa purification, la RNase P d'*E. coli* (constituée de la protéine C5p de 14 kDa et de la sous-unité ARN de 377 nucléotides (Robertson, Altman et al. 1972; Stark, Kole et al. 1978; Baer and Altman 1985; Morales, Wise et al. 1989; Brown and Pace 1992)) a été co-fractionnée avec les activités des enzymes de maturation de l'extrémité 3' pré-ARNt (Robertson, Altman et al. 1972; Stark, Kole et al. 1978). En accord avec ce résultat, l'hypothèse de l'association en complexe a été consolidée par le co-fractionnement de la RNase P mitochondriale de la levure (constituée de la protéine Rpm2p de 119 kDa et de la sous-unité ARN de 427 nucléotides (Morales, Wise et al. 1989)) avec l'activité de la maturation en 3' pré-ARNt (Martin 1993).

B.IV. Intersection de la voie de maturation des pré-ARNt avec celle de la dégradation des ARN et de la biosynthèse des lipides de type II

Indépendamment de la voie de maturation des pré-ARNt, la RNase P et l'(es) enzyme (s) de maturation en 3' sont impliquées dans la maturation, la dégradation et le recyclage des ARNm, des ARNr et des ARNt (Alifano, Rivellini et al. 1994; Carpousis 2007; Mohanty and Kushner 2007). Chez *E. coli* l'endonucléase E et la PNPase (responsables de la maturation en 3') font partie du complexe du RNA dégradosome, qui est constitué en plus de ces deux enzymes, de la protéine DEAH-box (RhlBp) et par des protéines qui sont apparemment sans liens avec le métabolisme des ARN (les chaperonnes DnaK et GroEL, et les protéines métaboliques énolase et polyphosphate kinase (PPK)) (Carpousis 2007). En se basant sur cette double fonction, l'intersection de la voie de maturation des pré-ARNt et celle de la dégradation des ARN a été suggérée chez *E. coli* (Li and Deutscher 1996; Deutscher 2006; Carpousis 2007).

D’autre part, dans le cas de la mitochondrie de levure, le gène RPM2 qui code pour la sous unité protéique de la RNase P est aussi un suppresseur de la délétion de l’allèle isp42-3 (protéine de transport mitochondrial); sa délétion (RPM2) empêche la croissance des cellules avec des substrats fermentescibles (Kassenbrock, Gao et al. 1995). Ceci suppose que notre compréhension de la RNase P est loin d’être complète, surtout avec la révélation en 2008, de l’intersection de la voie de maturation des pré-tRNA avec celle de la biosynthèse des lipides de type II suite à l’accumulation des 5’ pré-ARNt mitochondriaux non matures à cause de la délétion de n’importe quelle enzyme de la voie de FASII (Schonauer, Kastaniotis et al. 2008). Ces données suggèrent que l’association de la RNase P avec des protéines de fonction diverses est forte probable afin d’expliquer son rôle dans des mécanismes apparemment sans lien avec la maturation en 5’ pré-ARNt.

C. Objectifs de cette étude

Plusieurs processus mitochondriaux tels que la réplication, la transcription, la traduction, la phosphorylation oxydative et le transport membranaire sont effectués par des complexes multiprotéiques. Par contre, la voie de maturation des ARN mitochondriaux (p. ex pré-ARNt et ARNr) et le métabolisme sont habituellement traités comme une suite de réactions catalysées par des protéines séparées. Nos deux principaux objectifs dans le présent travail chez la mitochondrie de la levure et du choux-fleur (*B. oleracea*), et chez la bactérie *E. coli* sont :

i) L'étude de l'organisation en complexe de la voie de maturation des pré-ARNt et des voies métaboliques. Les évidences pour un tel complexe sont basées sur la co-purification de ces activités chez plusieurs espèces, mais seulement lors de premières étapes de purification. Il semble que le complexe soit ensuite dissocié. Ainsi par exemple, les protocoles de la purification des activités de la RNase P et de 3' RNase (développés pour la plupart dans les années 80) utilisent de fortes concentrations de sels (p. ex précipitation au sulfate d'ammonium 40%), des détergents (p. ex NP-40, cholate) et plusieurs types de colonnes chromatographiques qui exigent l'élution de l'activité d'intérêt par gradients de sels.

ii) L'étude de l'association physique liant des fonctionnes mitochondriales telles que la réplication, la transcription, la traduction et le métabolisme en supercomplexes multifonctionnels.

L'étude de la mitochondrie offre la possibilité de formuler des conclusions pertinentes et généralisables à travers les eucaryotes et de comparer aux bactéries (les mitochondries résultant de l'endosymbiose avec une α-Protéobactérie (Gray and Doolittle 1982; Lang, Gray et al. 1999)). D'autre part, du point de vue technique, comparativement à l'étude de la cellule au complète, la procédure de purification mitochondriale est assez simple et l'analyse des résultats est moins complexe (en moyenne il y a mille protéines mitochondriales).

CHAPITRE 2. Résultats

Article 1 : Multifunctional matrix supercomplexes in mitochondria and *E. coli*

Rachid Daoud[1], Mohammed Sabar[2] and B. Franz Lang[1, *]

[1]*Département de Biochimie, Centre Robert Cedergren, Université de Montréal, Canada.*

[2] *SIE/ADEREE, Ministère de l'Energie, des Mines des Eaux et de l'Environnement, Agdal-Rabat, Maroc*

[*]Correspondence and requests for materials should be addressed to B.F.L.

Abstract

Metabolic pathways are traditionally perceived as collections of separate enzymes whose reactions are connected *via* freely diffusible intermediates. Yet, *in vivo* pathway kinetics is usually faster than expected from this model, likely because metabolic enzymes are structurally coordinated. Here we provide direct evidence for stable, multifunctional protein supercomplexes in the mitochondrial matrix. In yeast, 14 of 16 purified complexes contain the complete citric acid cycle integrated with amino acid synthesis and ATP synthesis. This core structure combines with varying sets of proteins involved in replication, transcription, translation, RNA processing, etc. Some proteins are of unknown function, and a surprising 132 were previously not known to be mitochondrial. Our finding of stable, higher-order structures that unite cellular processes may explain the poorly understood pleiotropic phenotype of many mitochondrial mutants - as disturbance of supercomplex structure and assembly. Finally we show that supercomplex organization is evolutionary conserved across eukaryotes and bacteria.

According to traditional views, metabolic pathways are pools of individual enzymes (single proteins or small complexes) that freely float in the cell, with sequential enzymatic reaction steps connected *via* diffusible metabolites. Yet, this perception is incompatible with the 'molecular crowding' in most cellular compartments. For example, the protein concentration in the mitochondrial matrix is ~60% (1,2), a concentration incompatible with the high metabolic processivity seen *in vivo* - if based on diffusion principles alone. Therefore, some authors have postulated that metabolic enzymes are organized in large multi-protein complexes termed 'metabolons' (2,3,4,5). These 'molecular machines' would not only improve the kinetics of metabolic reactions by the spatial proximity of reaction partners, but also rationalize observed low concentrations of many (sometimes unstable) reaction intermediates *in vivo*. So far however, there is little direct evidence for protein complexes that include complete metabolic pathways (6,7,8).

The organization of multiple, related functions into supercomplexes is otherwise well known from membrane-bound functions, e.g. oxidative phosphorylation. In yeast mitochondria for instance (e.g., (9)), tightly membrane-bound respiratory chain and ATPase complex components combine among each other, and these associate further with 'soluble' complex components such as cytochrome c, F1 ATPase, and the soluble fraction of succinate dehydrogenase (which is also part of the TCA cycle, i.e., connecting to metabolic pathways). Note however that in the context of a living cell, terms like 'soluble' and 'membrane-bound' are potentially misleading, as these relate to isolation methods in preparative biochemistry that make free use of unphysiological salt concentrations, EDTA and even detergents. In reality, all of these components may link into stable structures under physiological conditions.

Increasing indirect evidence for the organization of metabolic pathways in large protein complexes comes from comprehensive protein-protein interaction (PPI) studies based on two-hybrid and protein complementation assays, and affinity purification of small complexes followed by mass spectrometry (AP-MS) (e.g., (10,11,12,13,14,15,16,17,18)). However, protein complexes inferred by these methods show very little concordance (19, 20), either because of a high number of false positives, or (most probable to our opinion) a major underestimate of cellular interactions. The latter view is consistent with the finding that some otherwise biochemically well-

characterized large complexes and pathway connections are missed (18,19,21), and that protein complexes inferred from PPI and AP-MS studies convincingly interconnect most diverse cellular processes such as translation, transcription, metabolism and regulation, suggesting extensive cross-talk among these processes (11). In other words, cellular functions appear to be not only organized into functional complexes, but these are likely combined into some sort of multifunctional super-structure (15,22,23).

To obtain direct evidence for the physical size and subunit composition of protein complexes in living cells, we developed a method that allows purification of large native protein complexes. We focused on the 'soluble' fraction of the mitochondrial matrix that is separated from highly purified mitochondria after mechanical or hypotonic disruption, without using high salt, EDTA or detergents. For complex separation, we adapted the Blue Native Electrophoresis Gel (BN-PAGE) protocol that was originally developed for detergent-solubilized, membrane-embedded protein complexes (24,25). When using appropriate gel composition, BN-PAGE will separate large protein complexes up to a molecular size of 10 MDa (as confirmed in a recent publication (26), i.e. up to ~300 protein subunits of average size. The subunit composition of electrophoretically separated complexes is analyzed directly by mass spectrometry (i.e., without a second dimension denaturing electrophoresis). This is the most cost-effective and most sensitive approach to protein subunit identification (27, 28). By combining these techniques, we are able to reproducibly purify complexes at concentrations just visible by Coomassie Blue staining, and to reliably identify up to ~230 different proteins per complex. Here we analyze soluble protein complexes that occur in the yeast and plant mitochondrial matrix, as well as in *Escherichia coli* (in order to compare mitochondrial complex organization with that of bacteria, from which mitochondria descend).

EXPERIMENTAL PROCEDURES

Cell culture and mitochondrial isolation

Saccharomyces cerevisiae (BY 4743) was kindly provided by Dr. S. Michnick (Université de Montréal). Yeast GFP (Green Fluorescent Protein) constructs used in this study Aco1-GFP (MATa his3Δ1 leu2Δ0 met15Δ0 ura3Δ0 ACO1-GFP::HIS3), Ilv5-GFP (MATa his3Δ1 leu2Δ0 met15Δ0 ura3Δ0 ILV5-GFP::HIS3) and Rpm2-GFP (MATa his3Δ1 leu2Δ0 met15Δ0 ura3Δ0 RPM2-GFP::HIS3) were kindly provided by Dr. J. Vogel (McGill University). Cells were grown to an optical density of 1.5–2.5 in a medium containing 1% yeast extract, 2% peptone, 3% glycerol and 1% galactose, pH 5.0 (YEPGal), or 5% glucose instead of glycerol/galactose (YEPD). Mitochondrial purification followed previously published procedures with slight modifications (46, 47). Yeast cell walls were removed by digestion with glucanase, spheroplasts were disrupted by osmotic shock, and a crude mitochondrial fraction was isolated by differential centrifugation. Mitochondria were resuspended in "washing buffer" (600 mM sucrose, 1 mM $MgCl_2$, 0.2 mM PMSF, 10 mM MOPS/KOH, pH 7.2) and further purified by centrifugation (60 min at 134, 000 g) through a discontinuous sucrose gradient (concentrations from top to bottom, 25%, 36%, and 60%; 5 mL each). For a second purification step, the mitochondrial band was collected and mixed with about four times its volume of 80% sucrose, layered at the bottom of a discontinuous sucrose gradients, and centrifuged for 120 min at 134, 000 g. Intact mitochondria move upwards ('flotation'), and form a band at the interface between 36% and 60% sucrose. For enhanced purity, this two-step purification of the mitochondria was repeated twice. Purified mitochondria were resuspended in buffer (600 mM sucrose, 0.2 mM PMSF, and 10 mM Tricine/KOH, pH 7.2) and pelleted at 14,000 g for 15 min. Usually, mitochondria were directly processed, but they may also be shock-frozen and kept at -80^0 C until use.

Mitochondria of *Brassica oleracea* were isolated following previously published procedures (47, 48). Briefly, about 1000 g of a cauliflower head (purchased at a local market) was homogenized in a Waring blender with extraction buffer (600 mM mannitol, 20mM Hepes, 3 mM $MgCl_2$, 0.1% (w/v) BSA and 2 mM EDTA, pH 7.8). Mitochondria were purified as outlined above for yeast.

Extraction of soluble matrix proteins

For the extraction of matrix proteins, we adapted a previously published procedure (47, 48). Mitochondria were re-suspended at 10 mg/mL in breaking buffer (600 mM sucrose, 20 mM Hepes/KOH, pH 7.4, 10 mM EDTA), diluted with 9 volumes of buffer (20 mM Hepes/KOH, pH 7.4, 0.5 mM EDTA and 1mM PMSF), and incubated for 30 min on ice. We used three alternative ways for rupturing mitochondria, which only differ in yield but not in banding pattern or protein composition of supercomplexes. The gentlest method is bursting of mitochondria through osmotic shock, by abruptly adding 10 volumes buffer. Alternatively, the mitochondrial suspension is adjusted to a final sucrose concentration of 0.45 M, incubated for 30 min on ice, and then homogenized in a Potter homogenizer for 90 seconds. The third method, for maximum yield of matrix proteins, involves mechanical disruption of mitochondria by shaking with an equal ratio of 125-212 micron and 425-600 micron glass beads (Sigma), in 3 rounds of 20 sec at 4°C. After a clear spin at 12,000 g for 15 min, the supernatant was centrifuged at 100,000 g, for 2 h at 4°C. The pellet containing mitochondrial membranes was discarded, and the supernatant was subjected to a second centrifugation at 120,000 g, for 30 min at 4°C. The matrix protein fraction (supernatant) was mostly used immediately, but may be stored at -80°C after shock-freezing. Protein concentrations were determined with the Bradford protein assay.

Tracking of GFP-tagged marker proteins

Soluble matrix proteins (1.5 mg) isolated from three GFP constructs (Aco1-GFP, Ilv5-GFP and Rpm2-GFP) were separated by ultracentrifugation (16 h at 20,000 g, Beckman SW41 rotor) on discontinuous glycerol gradients (10-15-20-25-30-35-40-45-50-55-60-65-70% glycerol, in a buffer containing 20 mM HEPES-KOH pH 7.9, 50 mM KCl, 1.5 mM $MgCl_2$, and 1 mM DTT). 0.7 mL fractions were collected and analyzed for protein concentration (Bradford protein assay) and relative GFP fluorescence intensity (excitation wavelength at 488 nm, emission at 500–540 nm).

***E. coli* culture and extraction of soluble proteins**

E. coli ML308 was grown on complete medium for 12 hours by shaking (100 rpm) at 37°C. Procedures for extracting *E. coli* soluble proteins were followed as published (49). All operations were carried out at 4°C. Briefly, five grams of *E. coli* were disrupted by grinding with 10 g of alumina in a chilled (-4°C) mortar until a paste is formed. 10 mL of extraction buffer (50 mM Tris-HCl, pH 7.5, 600 mM NH_4Cl, 10 mM $MgCl_2$, 6 mM 2-mercaptoethanol and 1 mM PMSF) was added, together with 10 pg/mL pancreatic DNase. After 30 min at 4°C, the sample was cleared by subsequent centrifugations for 10 min at 15,000 g, and 40 min at 30,000 g. The supernatant was kept on ice until further use.

Blue native gel electrophoresis (BN-PAGE)

Preparation of 4-14% BN-PAGE gels, electrophoresis buffer, and samples followed previously published procedures (24,25,26, 50), except that detergents were omitted (their effect was tested separately in supercomplex stability tests). Approximately 150 µg proteins were loaded per well and electrophoretic separation was performed in a Hoefer (18 x 16 cm) electrophoresis chamber, at 140 V and 9 mA, overnight at 4^0C.

Analysis of supercomplex composition by mass spectrometry

Bands formed in BN-PAGE were cut out from the gel and submitted to liquid chromatography tandem mass spectrometry (LC-MS/MS) analysis (27, 28), provided by a service platform at the Université de Montréal (IRIC) that includes functional annotation by Mascot (51). Details of the procedures are as follows. The gel pieces were digested by trypsin (50 mM ammonium bicarbonate for 8 hours at 37ºC), and peptides were extracted three times with 90% acetonitrile (ACN) in 0.5 M urea. Combined extracts were dried and resuspended in 5% ACN, 0.2% formic acid (FA) prior to mass-spectrometry analyses. Peptides were separated on a 150 µm ID, 10 cm reversed-phase nano-LC column (Jupiter C18, 3 µm, 300 Å, Phenomex) with a loading buffer of water with 0.2% formic acid (FA). Peptide elution was achieved using a gradient of 5%–60% ACN (0.2% FA) in 56 min. The nano-LC column was coupled to an LTQ-Orbitrap mass spectrometer (Thermo Fisher Scientific), and samples were injected in an interleaved

manner. The mass spectrometer was operated in a data-dependent acquisition mode with a 1 s survey scan at 60,000 resolution, followed by three product ion scans (MS/MS) in the ion trap for the most abundant precursors above a threshold of 10,000 counts.

The conventional MS spectra (survey scan) were acquired in profile mode at a resolution of 60,000 at m/z 400. MS/MS spectra were acquired in the ion trap using collision-induced dissociation (CID) only or by combining CID and electron transfer dissociation (ETD) with supplemental activation mode in a decision tree data-dependent fashion for multiply charged ions exceeding a threshold of 10,000 counts. Mass calibration used an internal lock mass (protonated $(Si(CH_3)_2O))_6$; m/z 445.12057) and typically provided mass accuracy within 10 ppm for precursor ion mass measurements.The centroided MS/MS data were merged into single peak-list files and searched with the Mascot search engine v2.0.2 (Mascot 2.3) against the combined forward and reversed NCBI 2006/03/03 database (3.310.354 sequences) to obtain a false discovery rate < 1%. The mass tolerance on precursor and fragment ions was set to ± 0.03 and ± 0.5 Daltons, The threshold score for accepting individual spectra was 25 (Mascot score). The carbamidomethyl (C), deamidation (NG), oxidation (O) and phosphorylation (STY) modification were considered. Peptide clusters were aligned with mascot identification files to assign sequence identity. Expression analyses were performed on proteins identified by at least 2 different peptide sequences across triplicate analyses.

RESULTS

Mitochondrial matrix fraction of yeast contains 16 supercomplexes

To characterize native mitochondrial matrix proteins in yeast (*Saccharomyces cerevisiae*), we prepared highly purified mitochondria (supplementary Fig. S1), gently disrupted the organelles mechanically, and removed membranes (see Methods). To our surprise, the resulting soluble fraction mostly consists of high-molecular-weight protein complexes (migrating far into kinetic glycerol gradients), as seen by tracking three marker proteins tagged by GFP (Aco1p, aconitase, TCA cycle; Ilv5p, isoleucine synthesis; and Rpm2p, a protein subunit of mitochondrial RNase P, tRNA processing; Fig. 1A). To separate complexes into distinct bands we applied BN-PAGE, with all steps performed in the absence of detergents in order to preserve native structures.

Yeast mitochondrial matrix proteins separate into at least 16 discrete and reproducible bands (Fig. 1B) referred to in the following as supercomplexes SC1-SC16. To ensure homogeneity of the isolated complexes (i.e., that bands contain only single structural units), eight of the 16 supercomplexes were re-purified on gels (with a polyacrylamide concentration gradient close to their migration in the first gel; not shown). Only singly bands were identified, and no significant difference in protein composition was observed by mass spectrometry. In addition, the homogeneity of complexes SC3 and SC4 are demonstrated by electron microscopy (supplementary Fig. S1).

Mass spectrometry (LC-MS-MS) identified ~60 to 230 proteins per supercomplex (confirmed by four independent LC-MS-MS analyses), adding up to a total of ~555 distinct mitochondrial matrix proteins (Supplementary Excel data 1). Of these, ~423 were previously recognized as mitochondrial according to authoritative compilations ((29) and references therein). 65 of the extra proteins are currently annotated as cytoplasmic and 21 as nucleolar components, while 13 are of unknown subcellular localization (Figure 2A, Supplementary Table S1). Interestingly, many of the respective extra genes cause mitochondrial defects when deleted (e.g., EGD2 and GLN4 (30,31)), which is consistent with their mitochondrial location. Three lines of evidence confirm that the extra proteins are truly inside mitochondria. First, meticulously purified mitochondria were used in our experiments (supplementary Fig. S2). Second, the membrane fraction that is likely the most important source of contamination (non-mitochondrial proteins attached to the outer

mitochondrial membrane) was removed immediately after disruption of mitochondria. Third, the extra proteins are integral parts of electrophoretically distinct supercomplexes that contain recognized mitochondrial proteins to a large majority; these super-structures remain stable under various dissociating conditions (see below).

Apart from demonstrating that mitochondrial matrix proteins are organized into large soluble complexes, our procedure provides a powerful new means for the confident identification of organellar proteins. We posit that the total number of previously unrecognized yeast mitochondrial proteins is even higher than the determined 131, as we disregard membrane-bound proteins.

Mitochondrial matrix supercomplexes in yeast are stable and native

Supercomplexes do not result from unspecific protein aggregation, which would rather result in a background smear instead of discrete bands. There is also no evidence for a gradual aggregation of complexes into superstructures, as the electrophoretic separation pattern is perfectly reproducible under various experimental conditions - likely because the electrophoresis buffer together with the charge-conferring Coomassie Blue stain are mildly dissociating. Also temperatures up to 60°C leave the number, size, and protein composition of supercomplexes virtually unchanged, as do repeated cycles of freezing and thawing (except for slightly lowering the intensity of SC3 and SC8). Only heating beyond 60°C followed by cooling results in fortuitous aggregation (see the indistinct smear pattern in BN-PAGE; supplementary Fig. S3). Mitochondrial supercomplexes remain further intact after EDTA treatment, which may otherwise dissociate complexes that are stabilized by bivalent cations (e.g., ribosomal subunits). We further ruled out unspecific protein aggregation mediated by DNA and RNA (liberated during the preparation process) that may cross-link proteins as DNase and RNase treatments did not change the electrophoretic band pattern (Fig. 1B). Finally, the mitochondrial supercomplex pattern is surprisingly resistant to relatively high concentrations of detergent (2% digitonin or 2% Triton 100X; Fig. 1B). Taken together, these experiments provide convincing evidence that supercomplexes are stable, and not the result of fortuitous aggregation.

Protein composition of mitochondrial supercomplexes

Proteomic analysis revealed that all 16 characterized yeast supercomplexes comprise multiple functions, with metabolism and energy production contributing most to a common core structure. 14 supercomplexes contain complete sets of TCA cycle, amino acid biosynthesis enzymes (serine, glycine, valine and aspartate), and soluble moieties of oxidative phosphorylation and electron transport including five subunits of F1 ATP synthase; one subunit of succinate dehydrogenase (Sdh1p), and two matrix-exposed proteins of the cytochrome bc_1 complex (Cor1p, Cor2p). Additional core components are two chaperons (Hsp60p, Hsp70p), a protein involved in protein translocation across mitochondrial membranes (Ssc1p), superoxide dismutase (trapping radicals), and the mitochondrial translation factor Tef2p (Fig. 2B, Table 1; supplementary Fig. S4 and Excel data 1). The 16 supercomplexes differ by the presence of a variety of additional components, some constituting complete and others incomplete pathways and functions (Fig. 2B, Table 1; supplementary Fig. S4 and Excel data 1). These include fatty acid biosynthesis, tRNA synthetases (up to a total of 22), ten translation factors, aminopeptidases, RNA processing enzymes, the protein and RNA subunits of RNase P, and 175 ribosomal proteins (of which only 163 are currently considered of mitochondrial localization, according to (29)). The majority of ribosomal proteins are in five supercomplexes (a total of ~100 in SC2, SC13-SC16), but none represents a complete ribosome (which according to literature are membrane-bound in mitochondria (32), therefore removed during purification of matrix proteins), and some of these also include eight or more aminoacyl-tRNA synthetases (SC6, SC7, SC10, SC16). According to the BioGRID (www.thebiogrid.org) database, a high number of the physical protein-protein interactions were revealed among the proteins of these supercomplexes For example, 1997, 884, 2133 and 2768 interactions are listed for SC2, SC4, SC13 and SC15 respectively, in support of their organization in large structural units.

The composition of the 16 examined supercomplexes overlaps conspicuously (Fig. 2B, supplementary Table S2). This may be interpreted in two non-exclusive ways: (i) the mitochondrial matrix is organized in a single gigantic hyper-complex that also links with membrane components, and breaks up into the observed, distinct supercomplexes through experimental manipulation (rupture of mitochondria, dilution of the mitochondrial

extract, mildly dissociating electrophoresis buffer and Coomassie Blue). The presence of a large number of ribosomal proteins in a few supercomplexes is consistent with this view. Alternatively, (ii) supercomplexes reflect the *in vivo* organization principle in which certain, central pathway components form a central core (i.e., the TCA cycle together with other components such as chaperones, Tef2p, etc; see listing above), to which other pathway components may attach in a modular way.

Cross-talk among distinct biological processes

We showed that supercomplexes combine proteins of several distinct biological functions as different as translation, metabolism, transcription and RNA processing. That for instance the mitochondrial translation apparatus is indeed physically associated with metabolic functions is in agreement with data from tag-purified yeast mitochondrial ribosomes (33) and yeast protein-protein interactions documented in the Biogrid Database (www.thebiogrid.org). According to the Biogrid compilation, physical associations between ribosomal proteins and the TCA cycle are restricted to three functionally connected enzymes, aconitase, 2-ketoglutarate and isocitrate dehydrogenase (Fig. 3).

Among the 16 supercomplexes, two are of particular interest. SC13 contains mitochondrial RNA polymerase (Rpo41p and Mtf1p) together with enzymes involved in nucleotide biosynthesis (UTP, CTP, deoxy-ATP and deoxy-GTP). In addition, SC13 has 20 out of the ~22 proteins that make up yeast mitochondrial nucleoids (34). Nucleoids are involved in mtDNA maintenance, dense DNA packaging, and control of segregation during organelle division (35). According to our data, SC13 is the only supercomplex to contain substantial amounts of DNA (80% of the amount present in the matrix fraction). Interestingly, SC13 contains the catalytic subunit of DNA polymerase (MIP1), but also two previously postulated yet elusive functions of mitochondrial replication: a primase (Pri2p) and ribonuclease H1 (Rnh1p, degrading Okazaki fragments). This is the first report to demonstrate that nucleoids are soluble in the absence of detergents, and that they contain a complete DNA replication machinery. The second supercomplex of particular interest is SC3, which contains nine exo- and endonucleases including RNase P (5` pre-tRNA processing (36)), and RNase Z (3' tRNA processing, 35S rRNA processing and

mitochondrial biogenesis (37)). We confirmed in an *in vitro* assay that this supercomplex accurately processes 5' and 3' termini of tRNA precursors (details to be published elsewhere).

Finally, glycolysis has been traditionally placed in the cytoplasm of the eukaryotic cell, separate from the TCA cycle, but according to more recent data at least part of glycolysis is (also) located in mitochondria (29). For yeast, a recent report identifies three glycolytic enzymes (enolase, aldolase, and GAPDH; converting C-3 intermediates) contained in a small detergent-purified mitochondrial protein complex that also includes two TCA cycle enzymes (Cit1p and Mdh1p), two F1 ATPase subunits, and six other proteins (7). In fact, four of the here described supercomplexes (SC3, SC4, SC7 and SC9) have all six C3-converting glycolytic enzymes (including several isoforms; Fig 2B, Table 1, supplementary Fig. S4 and Excel data 1). Our results imply that only the upstream half of glycolytic enzymes converting C-6 intermediates is exclusively cytoplasmic, although a potential physical link with mitochondrial membranes remains to be investigated.

Mitochondrial supercomplex pattern of glucose-repressed yeast

Glucose repression is known to correlate with widespread change of fundamental cellular processes. Whereas the glycolytic pathway is induced other functions are suppressed, including mitochondrial protein and DNA synthesis, respiratory chain and oxidative phosphorylation, and the use of alternative carbon sources (e.g. glycerol, galactose)(38).We reasoned that major changes in mitochondrial metabolism such as glucose repression should lead to a different mitochondrial supercomplex pattern and core composition. Therefore, we analyzed cells grown on high (5%) glucose.

The supercomplex pattern of glucose-repressed cells is not only completely different from that grown on galactose/glycerol (Fig. 4A), but the protein composition perfectly correlates with known regulatory changes under glucose repression (e.g., SC2-glucose; Fig. 4B, supplementary Excel data 2). For instance, the two most prominent complexes SC1-glucose (107 proteins) and SC2-glucose (127 proteins) have both an incomplete TCA cycle with only five enzymes (PDH complex, Cit1p, Aco1p, Idh1p, Idh2p and Idp1p). These are required for linking glycolysis, amino acid and fatty acid synthesis, and ethanol metabolism. Soluble moieties of oxidative phosphorylation and electron transport

are missing (F1-ATPase, Sdh1p). On the other hand, the C3-converting glycolytic pathway (all components, including several isoforms) is present, so are amino acid biosynthesis (leucine, valine, aspartate, glutamate, ornithine, citruline, serine and glycine), acetate metabolism, and fatty acid biosynthesis (Fig. 4B, supplementary Excel data 2).

That this type of complex organization may have far-reaching functional and regulatory implications is illustrated by the following example. A yeast gene deletion of a component of the mitochondrial fatty acid type II biosynthetic pathway (mutant strain oar1Δ; 3-Oxoacyl-(acyl-carrier-protein) reductase) has both, a defect in fatty acid synthesis and in 5′ processing of mitochondrial tRNAs (39). The authors have tested if this complex phenotype is due to a lack of protein modification (i.e., a regulatory defect), but have not found evidence for this hypothesis. According to our findings (details to be published elsewhere), this mutant no longer has supercomplex SC3, containing Oar1p and various components of RNase P (5' tRNA processing). The pleiotropic mutant phenotype is therefore best explained by a structural (assembly) defect *specifically* in one of the mitochondrial complexes.

Supercomplexes in plant mitochondria and in *E. coli*

Our findings in yeast evoke two questions: is supercomplex organization of mitochondrial functions evolutionary conserved throughout eukaryotes? Are such superstructures also present in bacteria from which mitochondria descend? To address these issues, we analyzed non-yeast fungi (*Neurospora crassa* and *Rhizopus oryzae*), an animal (*Bos taurus*), plant (*Brassica oleracea*), and *E. coli*. Yeast-like supercomplexes were found in all taxa studied. While the composition of supercomplexes in non-yeast fungi (e.g., *Neurospora crassa*; supplementary Fig. S5 and Excel data 3) and animals closely resemble yeast. Plants and *E. coli* feature more recognizable differences, as detailed below.

B. oleracea (cauliflower, a very close relative of *A. thaliana* with essentially identical protein sequences) has at least 24 mitochondrial supercomplexes (Fig. 5A) of which 17 most prominent were analyzed. In each supercomplex we identified approximately 100 to 180 different proteins, more than 740 in total. All biological functions observed in yeast

supercomplexes are also found in *Brassica* (Supplementary Excel data 4). Additional components include plant-specific enzymes involved in the biosynthesis of sugars and secondary metabolites, proteins of the lectin family (plant defense, among other functions), and 14 pentatricopeptide repeat proteins (PPR; members of this large protein family are involved in mitochondrial RNA editing (40) among a few other functions). As in yeast, we find a large number of proteins that were previously not known to be located in mitochondria and 72 of unknown function. Two particularly interesting supercomplexes (CF6 and CF12) contain in addition to DNA gyrase (both A and B subunits) several proteins required for genome maintenance, and two types of DNA polymerase subunits, the catalytic subunit of DNA polymerase epsilon (*POLE1Bp*; At2g27120) (41) and a TEB protein with helicase and DNA polymerase domains (42) (At4G32700, see supplementary Excel data 4). Our findings provide a first glimpse at the elusive plant mitochondrial replication apparatus (41, 42). It is possible that additional polymerase subunits are present in the remaining seven yet uncharacterized complexes.

In *E. coli*, we distinguish 25 supercomplexes (E1-25; Fig. 5B and 5C), from which we analyzed the 22 most prominent ones. In each supercomplex, we identify 70 to 200 distinct proteins. As in yeast mitochondria, vital metabolic processes and energy production (TCA cycle, lipid and amino acid) constitute common core functions (Supplementary Excel data 5), and two supercomplexes (E19 and E22) contain most (41) of the 56 bacterial ribosomal proteins (43). Yet, unlike mitochondria, three of the *E. coli* supercomplexes (E7, E16 and E18) physically link the complete glycolytic pathway (i.e., the C-3 plus C-6 converting enzymes) with the TCA cycle. In addition, five enzymes of the pentose phosphate pathway are present together with the TCA cycle and glycolysis (E16, E18). We note that despite the substantial evolutionary distance, multifunctional supercomplex organization in the matrix of mitochondria and in *E. coli* is strikingly similar.

DISCUSSION

Our findings provide new insights into the organization and biogenesis of cellular functions, in mitochondria and in bacteria. It is known that processes such as transcription, translation and intron splicing require a multitude of proteins (plus a few non-protein components) organized in large 'molecular machines' (44). Here we extend this principle to metabolic pathways (metabolons), and show that metabolism is physically interlinked (in supercomplexes) with translation, replication, transcription and RNA processing, etc. Further, the supercomplexes described here also contain a variety of helper proteins, in support of earlier reports that describe chaperons as a structural unit of complexes whose assembly they assist (e.g., (45)). In principle, this concept applies to all supercomplex components, i.e. they have to be selected for their known function as well as for structural interactions with one or more supercomplex neighbours.

Finally, our findings offer a new testable hypothesis on the nature of pleiotropy. We postulate that a number of pleiotropic effects may be caused by single mutations that perturb supercomplex structure or assembly (as in mutants defective in mitochondrial fatty acid synthesis), thus triggering cascades of seemingly unrelated impaired biological functions, which in human manifests as complex disease states.

REFERENCES

1. Scalettar, B.A., Abney, J.R., and Hackenbrock, C.R. (1991). Dynamics, structure, and function are coupled in the mitochondrial matrix. Proc Natl Acad Sci U S A *88*, 8057-8061.
2. Ovadi, J., and Saks, V. (2004). On the origin of intracellular compartmentation and organized metabolic systems. Mol Cell Biochem *256-257*, 5-12.
3. Winkel, B.S. (2004). Metabolic channeling in plants. Annu Rev Plant Biol *55*, 85-107.
4. Srere, P.A., and Ovadi, J. (1990). Enzyme-enzyme interactions and their metabolic role. FEBS Lett *268*, 360-364.
5. Ovadi, J., and Srere, P.A. (2000). Macromolecular compartmentation and channeling. Int Rev Cytol *192*, 255-280.
6. Narayanaswamy, R., Levy, M., Tsechansky, M., Stovall, G.M., O'Connell, J.D., Mirrielees, J., Ellington, A.D., and Marcotte, E.M. (2009). Widespread reorganization of metabolic enzymes into reversible assemblies upon nutrient starvation. Proc Natl Acad Sci U S A *106*, 10147-10152.
7. Brandina, I., Graham, J., Lemaitre-Guillier, C., Entelis, N., Krasheninnikov, I., Sweetlove, L., Tarassov, I., and Martin, R.P. (2006). Enolase takes part in a macromolecular complex associated to mitochondria in yeast. Biochim Biophys Acta *1757*, 1217-1228.
8. Grandier-Vazeille, X., Bathany, K., Chaignepain, S., Camougrand, N., Manon, S., and Schmitter, J.M. (2001). Yeast mitochondrial dehydrogenases are associated in a supramolecular complex. Biochemistry *40*, 9758-9769.
9. Heinemeyer, J., Braun, H.P., Boekema, E.J., and Kouril, R. (2007). A structural model of the cytochrome C reductase/oxidase supercomplex from yeast mitochondria. J Biol Chem *282*, 12240-12248.
10. Li, S., Armstrong, C.M., Bertin, N., Ge, H., Milstein, S., Boxem, M., Vidalain, P.O., Han, J.D., Chesneau, A., Hao, T., et al. (2004). A map of the interactome network of the metazoan C. elegans. Science *303*, 540-543.
11. Bouwmeester, T., Bauch, A., Ruffner, H., Angrand, P.O., Bergamini, G., Croughton, K., Cruciat, C., Eberhard, D., Gagneur, J., Ghidelli, S., et al. (2004). A

physical and functional map of the human TNF-alpha/NF-kappa B signal transduction pathway. Nat Cell Biol *6*, 97-105.

12. Gavin, A.C., Aloy, P., Grandi, P., Krause, R., Boesche, M., Marzioch, M., Rau, C., Jensen, L.J., Bastuck, S., Dumpelfeld, B., et al. (2006). Proteome survey reveals modularity of the yeast cell machinery. Nature *440*, 631-636.
13. Gavin, A.C., Bosche, M., Krause, R., Grandi, P., Marzioch, M., Bauer, A., Schultz, J., Rick, J.M., Michon, A.M., Cruciat, C.M., et al. (2002). Functional organization of the yeast proteome by systematic analysis of protein complexes. Nature *415*, 141-147.
14. Gavin, A.C., and Superti-Furga, G. (2003). Protein complexes and proteome organization from yeast to man. Curr Opin Chem Biol *7*, 21-27.
15. Kuhner, S., van Noort, V., Betts, M.J., Leo-Macias, A., Batisse, C., Rode, M., Yamada, T., Maier, T., Bader, S., Beltran-Alvarez, P., et al. (2009). Proteome organization in a genome-reduced bacterium. Science *326*, 1235-1240.
16. Butland, G., Peregrin-Alvarez, J.M., Li, J., Yang, W., Yang, X., Canadien, V., Starostine, A., Richards, D., Beattie, B., Krogan, N., et al. (2005). Interaction network containing conserved and essential protein complexes in Escherichia coli. Nature *433*, 531-537.
17. Krogan, N.J., Cagney, G., Yu, H., Zhong, G., Guo, X., Ignatchenko, A., Li, J., Pu, S., Datta, N., Tikuisis, A.P., et al. (2006). Global landscape of protein complexes in the yeast Saccharomyces cerevisiae. Nature *440*, 637-643.
18. Goll, J., and Uetz, P. (2006). The elusive yeast interactome. Genome Biol *7*, 223.
19. Wodak, S.J., Pu, S., Vlasblom, J., and Seraphin, B. (2009). Challenges and rewards of interaction proteomics. Mol Cell Proteomics *8*, 3-18.
20. Pu, S., Vlasblom, J., Emili, A., Greenblatt, J., and Wodak, S.J. (2007). Identifying functional modules in the physical interactome of Saccharomyces cerevisiae. Proteomics *7*, 944-960.
21. Shoemaker, B.A., and Panchenko, A.R. (2007). Deciphering protein-protein interactions. Part I. Experimental techniques and databases. PLoS Comput Biol *3*, e42.

22. Proshkin, S., Rahmouni, A.R., Mironov, A., and Nudler, E. (2010). Cooperation between translating ribosomes and RNA polymerase in transcription elongation. Science *328*, 504-508.

23. Burmann, B.M., Schweimer, K., Luo, X., Wahl, M.C., Stitt, B.L., Gottesman, M.E., and Rosch, P. (2010). A NusE:NusG complex links transcription and translation. Science *328*, 501-504.

24. Schagger, H., and von Jagow, G. (1991). Blue native electrophoresis for isolation of membrane protein complexes in enzymatically active form. Anal Biochem *199*, 223-231.

25. Wittig, I., Braun, H.P., and Schagger, H. (2006). Blue native PAGE. Nat Protoc *1*, 418-428.

26. Strecker, V., Wumaier, Z., Wittig, I., and Schagger, H. (2010). Large pore gels to separate mega protein complexes larger than 10 MDa by blue native electrophoresis: Isolation of putative respiratory strings or patches. Proteomics.

27. Wessels, H.J., Vogel, R.O., van den Heuvel, L., Smeitink, J.A., Rodenburg, R.J., Nijtmans, L.G., and Farhoud, M.H. (2009). LC-MS/MS as an alternative for SDS-PAGE in blue native analysis of protein complexes. Proteomics *9*, 4221-4228.

28. Fandino, A.S., Rais, I., Vollmer, M., Elgass, H., Schagger, H., and Karas, M. (2005). LC-nanospray-MS/MS analysis of hydrophobic proteins from membrane protein complexes isolated by blue-native electrophoresis. J Mass Spectrom *40*, 1223-1231.

29. Smith, A.C., and Robinson, A.J. (2009). MitoMiner, an integrated database for the storage and analysis of mitochondrial proteomics data. Mol Cell Proteomics *8*, 1324-1337.

30. George, R., Beddoe, T., Landl, K., and Lithgow, T. (1998). The yeast nascent polypeptide-associated complex initiates protein targeting to mitochondria in vivo. Proc Natl Acad Sci U S A *95*, 2296-2301.

31. Ludmerer, S.W., and Schimmel, P. (1985). Cloning of GLN4: an essential gene that encodes glutaminyl-tRNA synthetase in Saccharomyces cerevisiae. J Bacteriol *163*, 763-768.

32. Fox, T.D. (1996). Translational control of endogenous and recoded nuclear genes in yeast mitochondria: regulation and membrane targeting. Experientia *52*, 1130-1135.

33. Gan, X., Kitakawa, M., Yoshino, K., Oshiro, N., Yonezawa, K., and Isono, K. (2002). Tag-mediated isolation of yeast mitochondrial ribosome and mass spectrometric identification of its new components. Eur J Biochem *269*, 5203-5214.

34. Chen, X.J., Wang, X., Kaufman, B.A., and Butow, R.A. (2005). Aconitase couples metabolic regulation to mitochondrial DNA maintenance. Science *307*, 714-717.

35. Kuroiwa, T., Nishida, K., Yoshida, Y., Fujiwara, T., Mori, T., Kuroiwa, H., and Misumi, O. (2006). Structure, function and evolution of the mitochondrial division apparatus. Biochim Biophys Acta *1763*, 510-521.

36. Morales, M.J., Dang, Y.L., Lou, Y.C., Sulo, P., and Martin, N.C. (1992). A 105-kDa protein is required for yeast mitochondrial RNase P activity. Proc Natl Acad Sci U S A *89*, 9875-9879.

37. Vogel, A., Schilling, O., Spath, B., and Marchfelder, A. (2005). The tRNase Z family of proteins: physiological functions, substrate specificity and structural properties. Biol Chem *386*, 1253-1264.

38. Kolkman, A., Olsthoorn, M.M., Heeremans, C.E., Heck, A.J., and Slijper, M. (2005). Comparative proteome analysis of Saccharomyces cerevisiae grown in chemostat cultures limited for glucose or ethanol. Mol Cell Proteomics *4*, 1-11.

39. Schonauer, M.S., Kastaniotis, A.J., Hiltunen, J.K., and Dieckmann, C.L. (2008). Intersection of RNA processing and the type II fatty acid synthesis pathway in yeast mitochondria. Mol Cell Biol *28*, 6646-6657.

40. Okuda, K., Chateigner-Boutin, A.L., Nakamura, T., Delannoy, E., Sugita, M., Myouga, F., Motohashi, R., Shinozaki, K., Small, I., and Shikanai, T. (2009). Pentatricopeptide repeat proteins with the DYW motif have distinct molecular functions in RNA editing and RNA cleavage in Arabidopsis chloroplasts. Plant Cell *21*, 146-156.

41. Ronceret, A., Guilleminot, J., Lincker, F., Gadea-Vacas, J., Delorme, V., Bechtold, N., Pelletier, G., Delseny, M., Chaboute, M.E., and Devic, M. (2005). Genetic analysis of two Arabidopsis DNA polymerase epsilon subunits during early embryogenesis. Plant J *44*, 223-236.

42. Inagaki, S., Suzuki, T., Ohto, M.A., Urawa, H., Horiuchi, T., Nakamura, K., and Morikami, A. (2006). Arabidopsis TEBICHI, with helicase and DNA polymerase domains, is required for regulated cell division and differentiation in meristems. Plant Cell *18*, 879-892.

43. Arnold, R.J., and Reilly, J.P. (1999). Observation of Escherichia coli ribosomal proteins and their posttranslational modifications by mass spectrometry. Anal Biochem *269*, 105-112.

44. Alberts, B. (1998). The cell as a collection of protein machines: preparing the next generation of molecular biologists. Cell *92*, 291-294.

45. Aloy, P., Bottcher, B., Ceulemans, H., Leutwein, C., Mellwig, C., Fischer, S., Gavin, A.C., Bork, P., Superti-Furga, G., Serrano, L., et al. (2004). Structure-based assembly of protein complexes in yeast. Science *303*, 2026-2029.

46. Sims, G.M. (1975). Letter: Assay of alkaline phosphatase. Am J Med Technol *41*, 32.

47. Zahedi, R.P., Sickmann, A., Boehm, A.M., Winkler, C., Zufall, N., Schonfisch, B., Guiard, B., Pfanner, N., and Meisinger, C. (2006). Proteomic analysis of the yeast mitochondrial outer membrane reveals accumulation of a subclass of preproteins. Mol Biol Cell *17*, 1436-1450.

48. Meisinger, C., Sommer, T., and Pfanner, N. (2000). Purification of Saccharomcyes cerevisiae mitochondria devoid of microsomal and cytosolic contaminations. Anal Biochem *287*, 339-342.

49. Robertson, H.D., Altman, S., and Smith, J.D. (1972). Purification and properties of a specific Escherichia coli ribonuclease which cleaves a tyrosine transfer ribonucleic acid presursor. J Biol Chem *247*, 5243-5251.

50. Bentlage, H.A., Janssen, A.J., Chomyn, A., Attardi, G., Walker, J.E., Schagger, H., Sengers, R.C., and Trijbels, F.J. (1995). Multiple deficiencies of mitochondrial DNA- and nuclear-encoded subunits of respiratory NADH

dehydrogenase detected with peptide- and subunit-specific antibodies in mitochondrial myopathies. Biochim Biophys Acta *1234*, 63-73.

51. Perkins, D.N., Pappin, D.J., Creasy, D.M., and Cottrell, J.S. (1999). Probability-based protein identification by searching sequence databases using mass spectrometry data. Electrophoresis *20*, 3551-3567.

Acknowledgements

We thank Gertraud Burger and Emmanuel Levy (Université de Montréal) for valuable comments on the manuscript, Stephen Michnick for discussions, and Natacha Beck and Pierre Rioux (Université de Montréal) for bioinformatics support. This research was funded by the Canadian Research Chair Program and the National Science and Engineering Research Council (NSERC) of Canada.

Author contributions

Planning and discussion of experiments were carried out by all authors, RD performed experiments, MS provided an initiation to the use of BN-PAGE. RD and BFL wrote, and all authors reviewed the manuscript.

Competing financial interests

The authors declare no competing financial interests.

Figure Legends

Figure 1. Glycerol gradient fractionation, electrophoretic separation and stability of yeast mitochondrial matrix supercomplexes.

A, Relative GFP fluorescence of the GFP fusion proteins (GFP-Aco1p, GFP-Ilv5p and GFP-Rpm2p) were tracked on discontinuous 10-70% glycerol gradients.

B, Supercomplexes were separated on linear BN-PAGE. Untreated, and treated for 30 min with digitonin, DNase, RNase, Triton X100, or EDTA, prior to supercomplex separation

Figure 2. Proteins localization and composition of soluble yeast mitochondrial supercomplexes.

A, Cellular localization of the identified yeast mitochondrial proteins according to the SGD data (http://www.yeastgenome.org/) and to Smith, A. C. and Robinson, A. J., Mol Cell Proteomics 8 (6), 1324 (2009).

B, SC1 - SC16, supercomplex 1 to 16. The protein distribution of supercomplexes is classified by functional group. Rectangles represent distinct proteins (isoforms are counted only once). Ribosomal proteins are not represented in this figure.

Figure 3. Cross-talk of biological processes according to protein-protein interaction data. Schematic illustration for the crosstalk between the TCA cycle and ribosomal proteins, based on published protein-protein interactions (compiled in the Biogrid Database; www.thebiogrid.org). Only the (arguable more reliable) tag-based interactions were used for building this graph, not two-hybrid and genetic interactions. All proteins shown here to interact with the TCA cycle are also found in supercomplexes identified by us.

Figure 4. M**itochondrial supercomplexes in glucose-repressed yeast cells.**

A, supercomplexes were separated on linear 4%-12% BN-PAGE. Detergent/protein ratios (g/g) and enzyme and EDTA concentrations are indicated. The two most prominent bands are SC2- and SC3-glucose; SC1-glucose is a clearly distinct band with reproducible protein composition (see supplementary Excel data 2) that is however barely visible in this figure.

B, Comparison of metabolic pathways between galactose- (SC3-galactose) and glucose-grown cells (Sc2-glucose). Black, shared pathways components; blue, specific for galactose; red, specific for glucose. Full protein names and detailed functions are listed in supplementary Excel data 1 and 2.

Figure 5. Electrophoretic separation of supercomplexes from *Brassica oleracea* mitochondria and *E. coli*.

A, *B. oleracea* mitochondrial supercomplexes; untreated and treated for 30 min with digitonin, DNase and RNase, or heated at the indicated temperature prior to supercomplex separation.

B, *E. coli* supercomplexes; untreated and incubated for 5 min at various temperatures.

C, *E. coli* supercomplexes, treated for 30 min with detergents, DNase, RNase or EDTA prior to separation. Detergent/protein ratios (g/g), enzyme, and EDTA concentrations are indicated.

Tables

Table 1: Protein composition of soluble yeast mitochondrial supercomplexes. Protein identification by Mascot. Names and detailed functions of individual proteins are listed in supplementary Excel data 1 (Supplementary information).

Figures

Figure 1

A

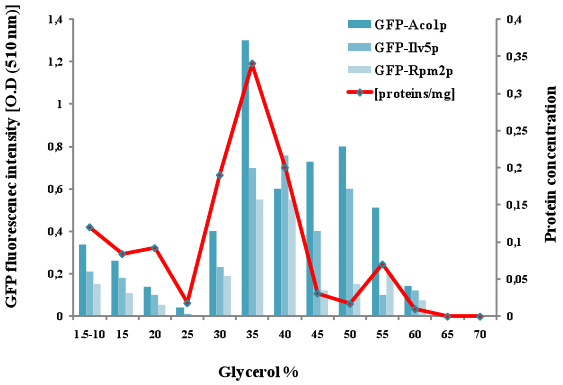

B

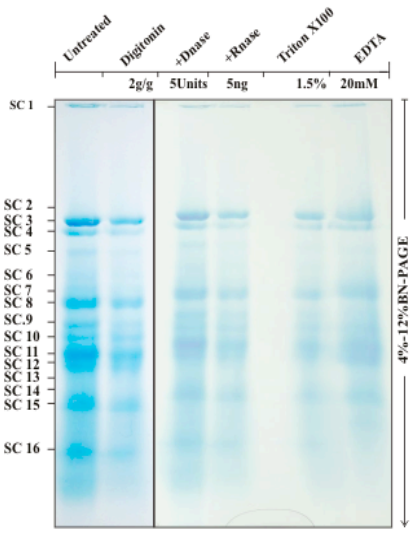

Figure 2

A

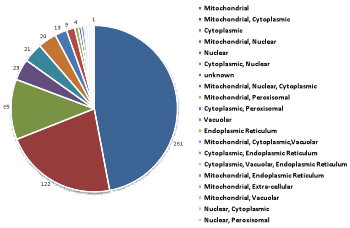
Mitochondrial
Mitochondrial, Cytoplasmic
Cytoplasmic
Mitochondrial, Nuclear
Nuclear
Cytoplasmic, Nuclear
unknown
Mitochondrial, Nuclear, Cytoplasmic
Mitochondrial, Peroxisomal
Cytoplasmic, Peroxisomal
Vacuolar
Endoplasmic Reticulum
Mitochondrial, Cytoplasmic,Vacuolar
Cytoplasmic, Endoplasmic Reticulum
Cytoplasmic, Vacuolar, Endoplasmic Reticulum
Mitochondrial, Endoplasmic Reticulum
Mitochondrial, Extra-cellular
Mitochondrial, Vacuolar
Nuclear, Cytoplasmic
Nuclear, Peroxisomal

B

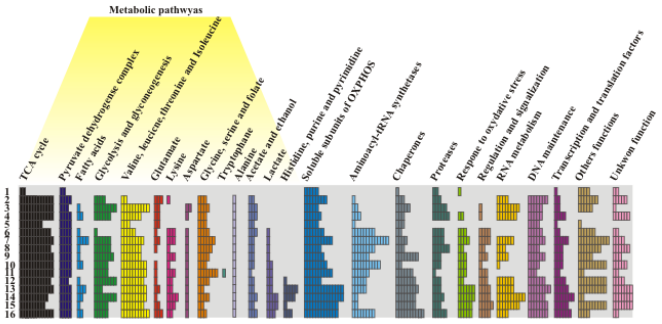
Metabolic pathwyas
TCA cycle
Pyruvate dehydrogenase complex
Fatty acids
Glycolysis and gluconeogenesis
Valine, leucine, threonine and isoleucine
Glutamate
Lysine
Aspartate
Glycine, serine and folate
Tryptophane
Alanine
Acetate and ethanol
Lactate
Histidine, purine and pyrimidine
Soluble subunits of OXPHOS
Aminoacyl-tRNA synthetases
Chaperones
Proteases
Response to oxydative stress
Regulation and signalization
RNA metabolism
DNA maintenance
Transcription and translation factors
Others functions
Unkwon function

Figure 3

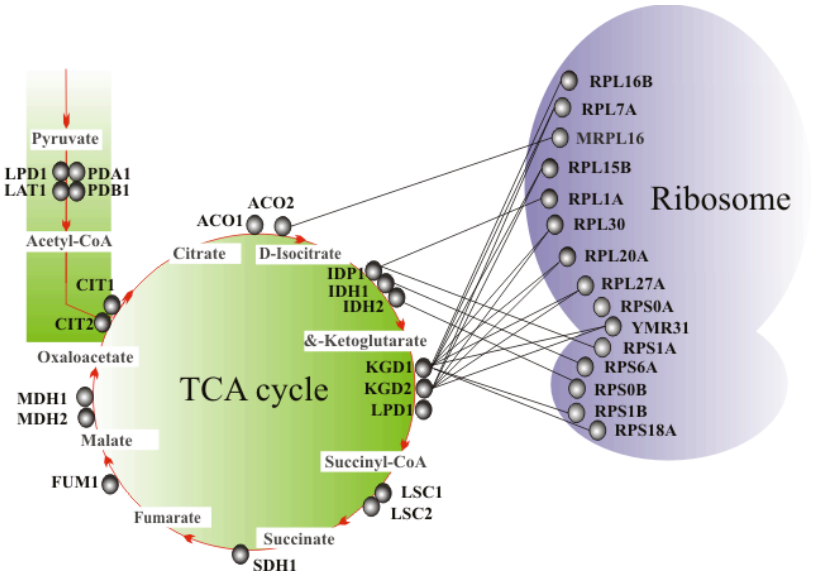
Pyruvate
LPD1
PDA1
LAT1
PDB1
Acetyl-CoA
CIT1
CIT2
Oxaloacetate
MDH1
MDH2
Malate
FUM1
Fumarate
Succinate
SDH1
Citrate
ACO2
ACO1
D-Isocitrate
IDP1
IDH1
IDH2
&-Ketoglutarate
KGD1
KGD2
LPD1
Succinyl-CoA
LSC1
LSC2
TCA cycle
Ribosome
RPL16B
RPL7A
MRPL16
RPL15B
RPL1A
RPL30
RPL20A
RPL27A
RPS0A
YMR31
RPS1A
RPS6A
RPS0B
RPS1B
RPS18A

Figure 4

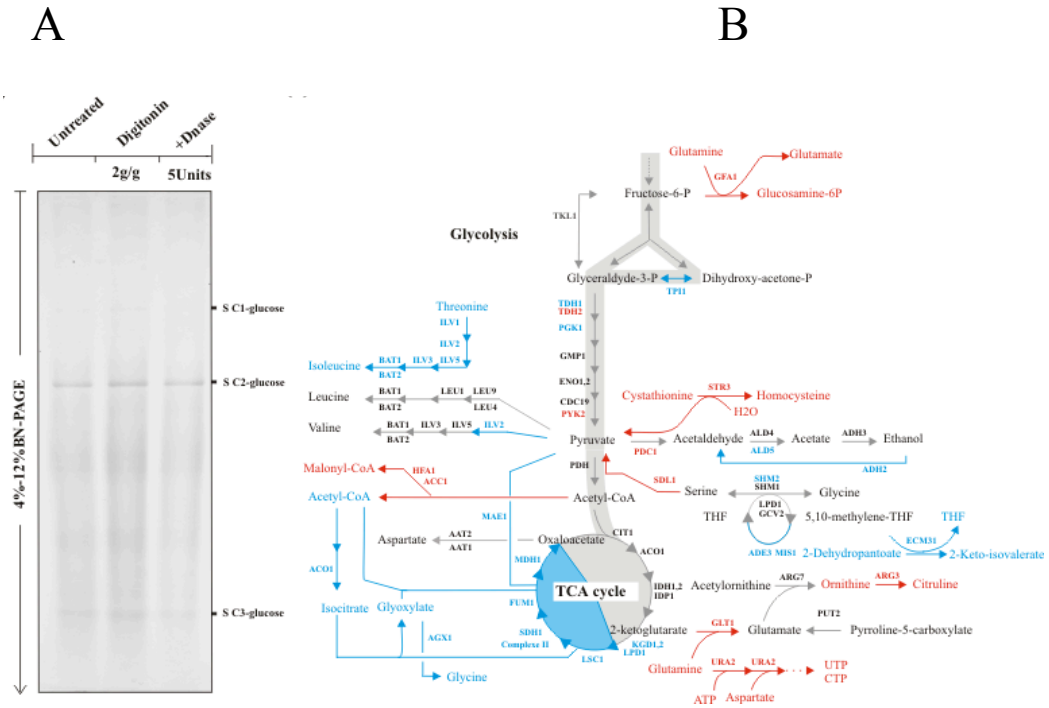
A
B
Untreated
Digitonin
+Dnase
2g/g
5Units
4%-12%BN-PAGE
S C1-glucose
S C2-glucose
S C3-glucose
Glycolysis
Glutamine
Glutamate
GFA1
Glucosamine-6P
Fructose-6-P
TKL1
Glyceraldyde-3-P
Dihydroxy-acetone-P
TPI1
TDH1
TDH2
PGK1
GMP1
ENO1,2
CDC19
PYK2
Pyruvate
Threonine
ILV1
ILV2
Isoleucine
BAT1
BAT2
ILV3
ILV5
Leucine
LEU1
LEU9
LEU4
Valine
ILV5
Cystathionine
STR3
Homocysteine
H2O
PDC1
Acetaldehyde
ALD4
ALD5
Acetate
ADH3
ADH2
Ethanol
PDH
SDL1
Serine
SHM2
SHM1
Glycine
THF
LPD1
GCV2
5,10-methylene-THF
Malonyl-CoA
HFA1
ACC1
Acetyl-CoA
MAE1
Aspartate
AAT2
AAT1
Oxaloacetate
CIT1
ACO1
MDH1
ADE3
MIS1
2-Dehydropantoate
ECM31
2-Keto-isovalerate
TCA cycle
IDH1,2
IDP1
Acetylornithine
ARG7
Ornithine
ARG3
Citruline
Isocitrate
Glyoxylate
FUM1
AGX1
SDH1
Complex II
2-ketoglutarate
KGD1,2
LPD1
LSC1
GLT1
Glutamate
PUT2
Pyrroline-5-carboxylate
Glutamine
URA2
URA2
UTP
CTP
ATP
Aspartate
Glycine

Figure 5

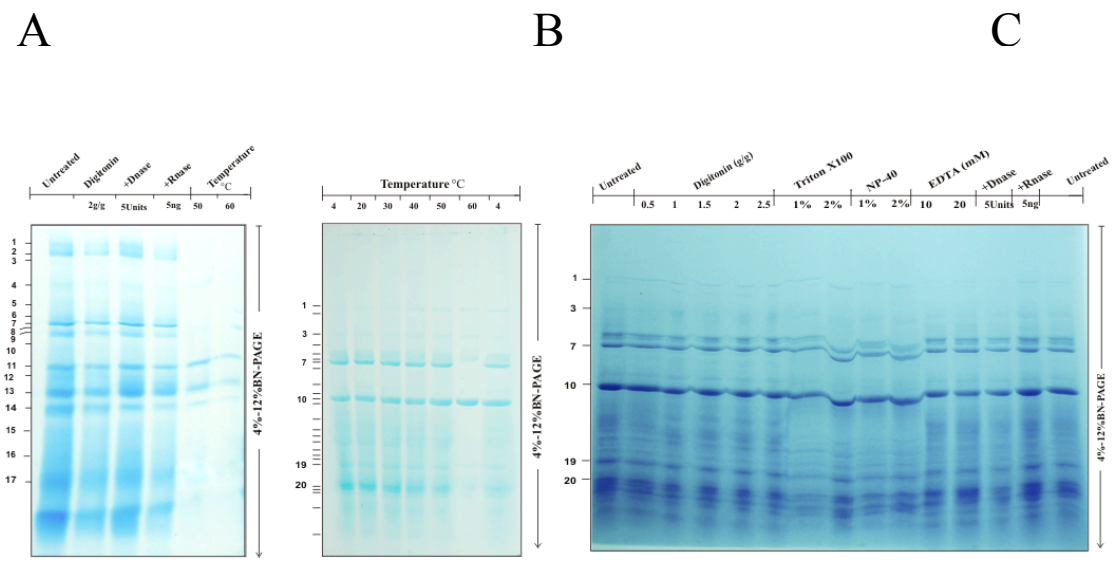
A
B
C
Untreated
Digitonin
+Dnase
+Rnase
Temperature °C
2g/g
5Units
5ng
50
60
4%-12%BN-PAGE
Temperature °C
4
20
30
40
50
60
4
Untreated
Digitonin (g/g)
Triton X100
NP-40
EDTA (mM)
+Dnase
+Rnase
Untreated
0.5
1
1.5
2
2.5
1%
2%
1%
2%
10
20
5Units
5ng

Table :

	Supercomplexes															
Biological Functions	**SC1**	**SC2**	**SC3**	**SC4**	**SC5**	**SC6**	**SC7**	**SC8**	**SC9**	**SC10**	**SC11**	**SC12**	**SC13**	**SC14**	**SC15**	**SC16**
Tricarboxylic acid cycle	2	12 (1)	12 (1)	12 (3)	8 (2)	11 (2)	12 (4)	11 (2)	12 (3)	12 (4)	12 (5)	11 (5)	12 (3)	11 (2)	12 (1)	12 (3)
Pyruvate dehydrogenase complex	3	3	3	3	3	3	3	3	3	3	3	2	3	3	3	3
Common amino acid pathways constituting the core	1	6	6 (2)	6 (1)	3	6 (2)	6 (2)	6 (1)	6 (1)	6 (3)	6 (2)	6 (2)	6 (2)	6 (1)	6 (1)	6 (1)
Other amino acid, choline and pyrimidine pathways	5	6	15 (2)	10 (1)	9	15 (1)	19 (2)	10 (1)	13 (1)	12 (1)	14 (3)	14 (3)	22 (2)	16 (2)	20 (1)	16 (1)
Acetate and ethanol metabolism	1	2 (1)	2 (2)	3 (2)	2 (1)	3 (3)	2 (2)	2 (4)	2 (3)	2 (2)	1	2 (2)	1	3 (2)	1 (2)	2 (2)
Fatty acid metabolism	0	1	1	2	0	1	4	1	1	2	0	1	3	2	1	2
Common solubles subunits of the oxidative phosphorylation complexes constituting the core	3	8	8	8	5	8	8	8	8	8	8	8	8	8	8	8
Solubles subunits of the oxidative phosphorylation complexes	2	1	0	0	0	2	4	0	4	2	3	3	7	7	6	6
Ribosomal proteins	25	92	35	49	25	44	52	29	33	24	9	33	86	101	102	100
Translational elongation factor	1	2	2	4	1	2	5	3	3	3	2	4	5	7	5	6
Aminoacyl-tRNA synthetases	0	1	2	3	1	8	13	8	6	10	6	5	5	2	2	8
Chaperones	1	3	5	3	3	2	4	3	8	2	6	7	10	7	7	9
Aminopeptidases	2	3	5	6	0	4	4	6	3	3	1	3	3	4	3	5
Proteins of detoxification and cell death	1	0	0	2	0	3	4	2	3	3	3	2	6	6	5	5
Regulation and signalization	0	0	1	1	0	4	4	2	3	1	3	3	4	4	5	4
Proteins of RNA processing	0	4	9	7	0	0	6	3	4	1	0	6	6	10	8	4
Proteins of genome maintenance	2	6	6	5	4	5	6	4	6	4	3	6	8	6	7	7
Proteins of unknown function	2	5	1	5	0	2	4	6	3	5	2	4	7	7	7	2
Glycolysis and gluconeogenesis	1	4	7	8	0	7	8 (1)	7	7	4	5	5	3	5	4	4
Other functions	4	7	5	0	1	6	11	8	5	10	2	10	10	2	10	4
Total number of proteins	**54**	**167**	**130**	**143**	**69**	**145**	**188**	**128**	**138**	**127**	**100**	**144**	**222**	**226**	**227**	**223**

SC1 - SC16, supercomplex 1 to 16; see also Fig. 2a,c. Numbers refer to distinct proteins (based on four independent proteomic analyses), which are regrouped according to function. The inferred molecular mass of supercomplexes is ~2-10 MDa (assuming equal subunit stoichiometry). Except SC1 and SC5, all supercomplexes contain a complete set of proteins constituting the TCA cycle plus a variable number of isozymes (number in parentheses). Because two types of isocitrate dehydrogenase exist, one made up of two subunits (Idh1p and Idh2p) and an alternative with only one subunit (Idp1p), a complete, functional TCA cycle requires either 11 or 12 proteins.

Supplementary information

Supplementary Figure S1. Ultrapure yeast mitochondria separated with sucrose-density gradient and flotation, detailed of the procedure is listed in Methods.

Supplementary Figure S2. Negative staining for high-resolution electron microscopy of the supercomplexes SC3 and SC4.

Supplementary Figure S3. Stability of soluble yeast mitochondrial supercomplexes. Supercomplexes were separated on linear BN-PAGE. Incubated for 5 min at indicated temperatures, prior to supercomplex separation.

Supplementary Figure S4. Metabolic pathway schemata of yeast supercomplexes SC1-SC16. Intermediate products are in black and enzymes in green; detailed protein functions are listed in Supplementary Excel data 1.

Supplementary Figure S5. Electrophoretic separation and stability of *Neurospora crassa* mitochondrial supercomplexes. Supercomplexes were separated on linear BN-PAGE. NC1 - NC12, supercomplexes 1 to 12.

Supplementary Table S1. Cellular localization of the identified yeast mitochondrial proteins according to SGD (http://www.yeastgenome.org/) and Smith, A. C. and Robinson, A. J., Mol Cell Proteomics 8 (6), 1324 (2009).

Supplementary Table S2. Number of shared proteins between yeast supercomplexes SC1-SC16.

Excel data 1. Protein composition of yeast mitochondrial supercomplexes. For the electrophoretic separation pattern see Fig. 1B. First column, protein ID; second column, protein function; third column, protein name; fourth column, subcellular localization according to the SGD database (http://www.yeastgenome.org/) and ([28] and references therein).

Excel data 2. Protein composition of mitochondrial supercomplexes from glucose-repressed yeast. The two analyzed supercomplexes are SC1-glucose and SC2-glucose. For the electrophoretic separation pattern see Fig. 4A. First column, protein ID; second column, protein name.

Excel data 3. Protein composition of *Neurospora crassa* mitochondrial supercomplexes. For the electrophoretic separation pattern of NC1 - NC12 see Fig. S5. First column, protein ID; second column, protein name.

Excel data 4. Protein composition of *Brassica oleracea* mitochondrial supercomplexes. For the electrophoretic separation pattern of BC1 - BC17 see Fig. 5A. First column, protein ID; second column, protein function; third column, protein name.

Excel data 5. Protein composition of *E. coli* supercomplexes. For the electrophoretic separation pattern of EC1 – EC24 see Fig. 5B. First column, protein ID; second column, protein function; third column, protein name.

Supplementary Figure S1

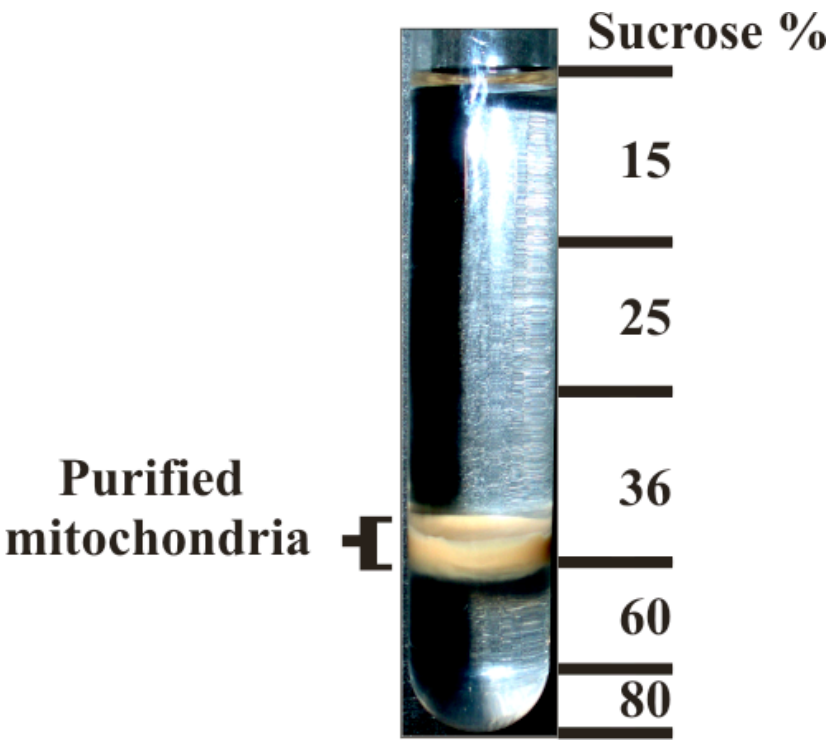

Supplementary Figure S2

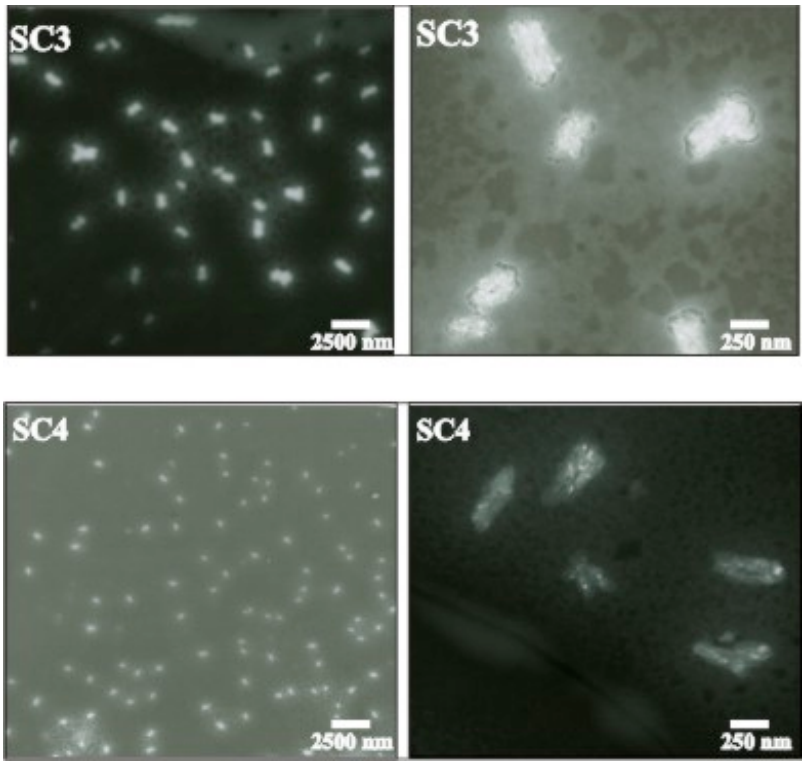

Supplementary Figure S3

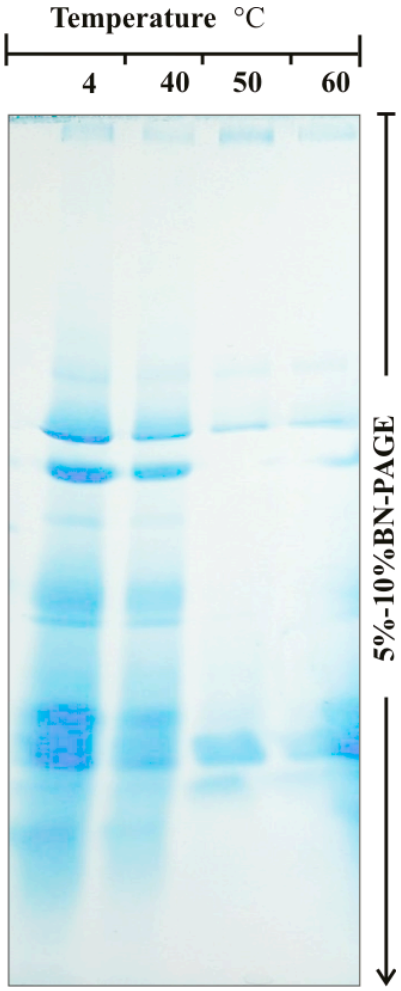

Supplementary Figure S4

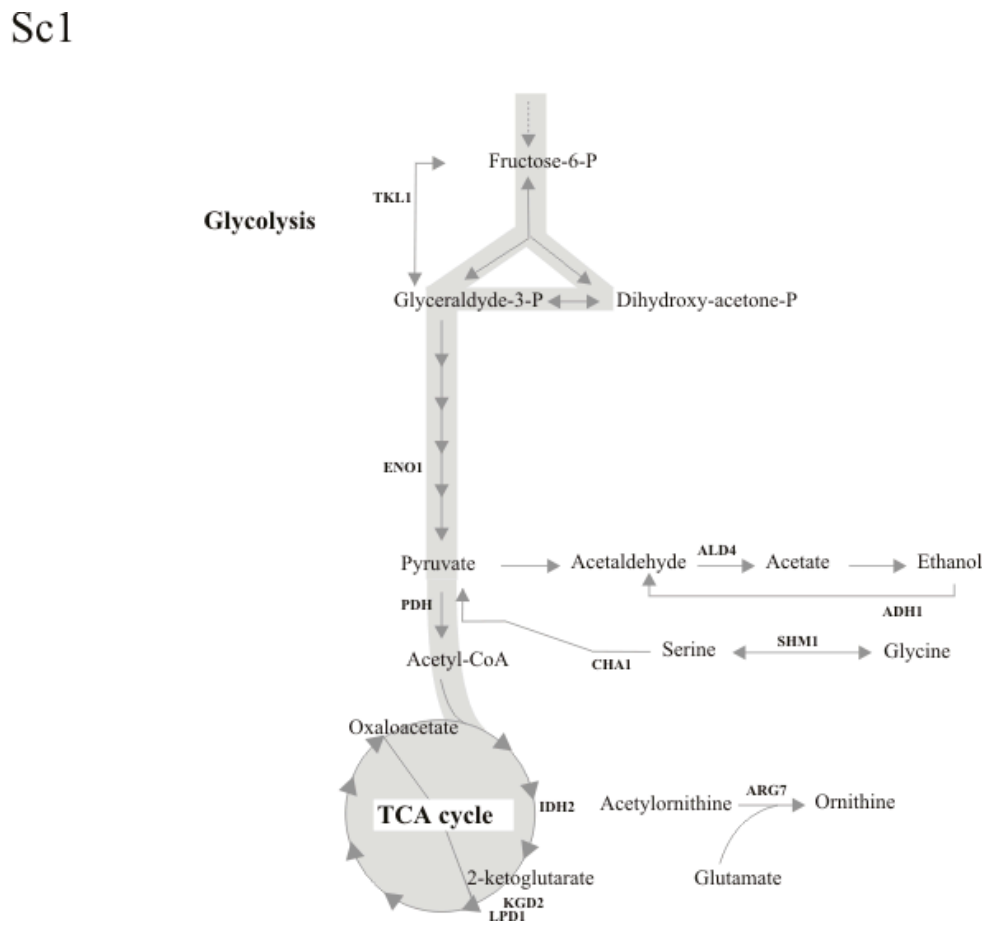

Sc2

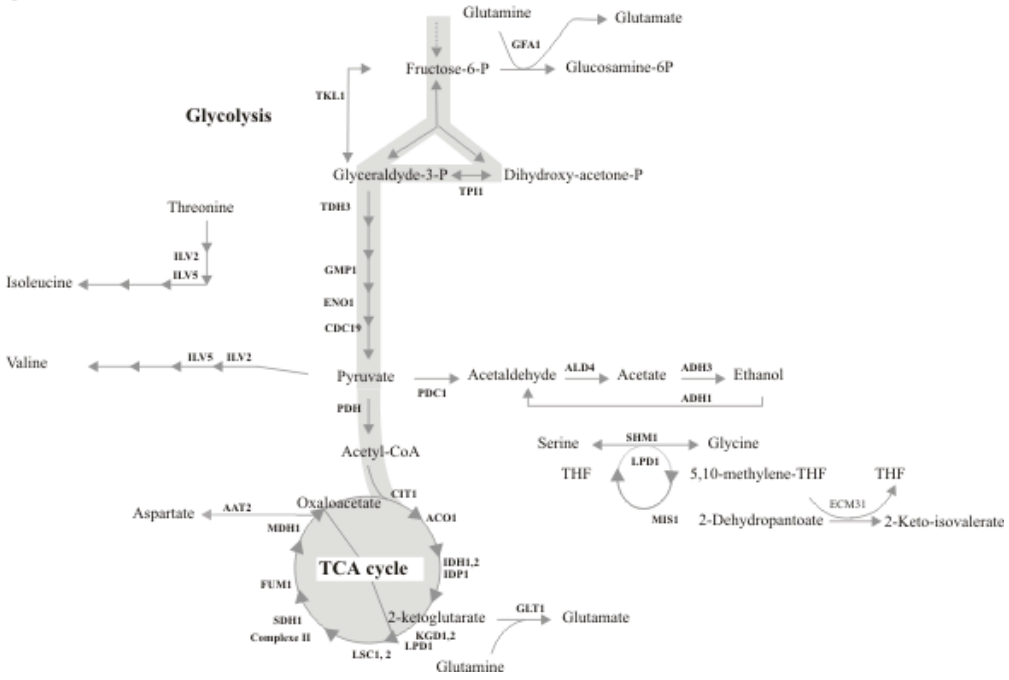
Glutamine
Glutamate
GFA1
Fructose-6-P
Glucosamine-6P
TKL1
Glycolysis
Glyceraldyde-3-P
Dihydroxy-acetone-P
TPI1
Threonine
TDH3
ILV2
ILV5
Isoleucine
GMP1
ENO1
CDC19
Valine
ILV5
ILV2
Pyruvate
PDC1
Acetaldehyde
ALD4
Acetate
ADH3
Ethanol
ADH1
PDH
Acetyl-CoA
Serine
SHM1
Glycine
THF
LPD1
5,10-methylene-THF
THF
ECM31
MIS1
2-Dehydropantoate
2-Keto-isovalerate
CIT1
Aspartate
AAT2
Oxaloacetate
ACO1
MDH1
TCA cycle
IDH1,2
IDP1
FUM1
SDH1
Complexe II
2-ketoglutarate
GLT1
Glutamate
KGD1,2
LPD1
LSC1, 2
Glutamine

Sc3

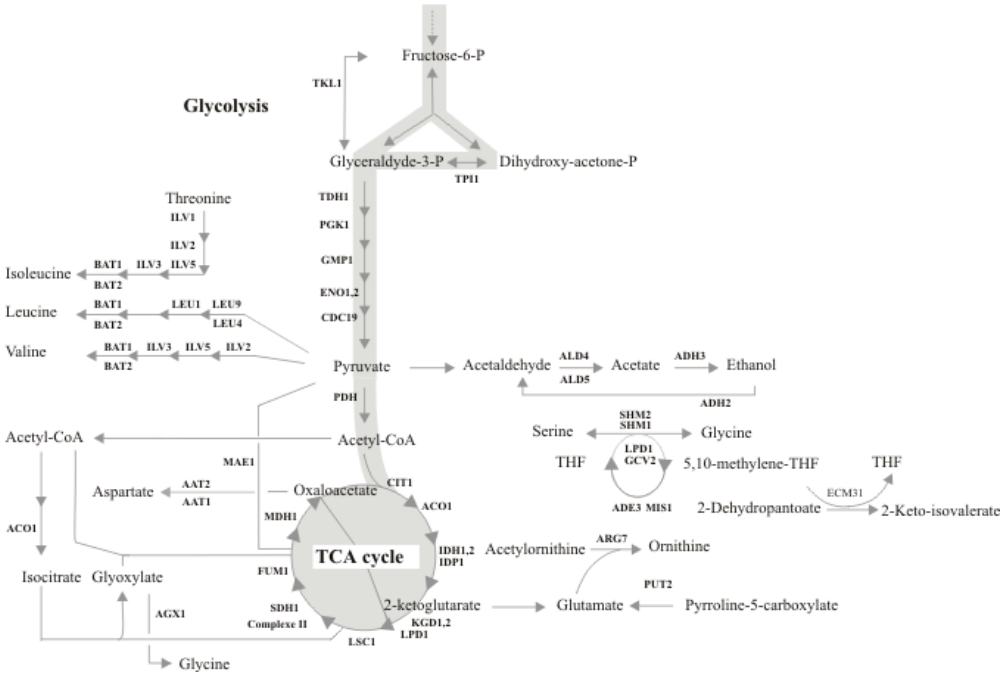
Glycolysis
Fructose-6-P
TKL1
Glyceraldyde-3-P
Dihydroxy-acetone-P
TPI1
TDH1
PGK1
GMP1
ENO1,2
CDC19
Pyruvate
Acetaldehyde
ALD4
ALD5
Acetate
ADH3
Ethanol
ADH2
PDH
Acetyl-CoA
Acetyl-CoA
Threonine
ILV1
ILV2
Isoleucine
BAT1
BAT2
ILV3
ILV5
Leucine
LEU1
LEU9
LEU4
Valine
ILV5
ILV2
Serine
SHM2
SHM1
Glycine
THF
LPD1
GCV2
5,10-methylene-THF
THF
ECM31
2-Dehydropantoate
2-Keto-isovalerate
ADE3
MIS1
MAE1
Aspartate
AAT2
AAT1
Oxaloacetate
CIT1
ACO1
MDH1
TCA cycle
IDH1,2
IDP1
Acetylornithine
ARG7
Ornithine
PUT2
Pyrroline-5-carboxylate
Glutamate
2-ketoglutarate
KGD1,2
LPD1
LSC1
SDH1
Complexe II
FUM1
Isocitrate
Glyoxylate
AGX1
Glycine

Sc4

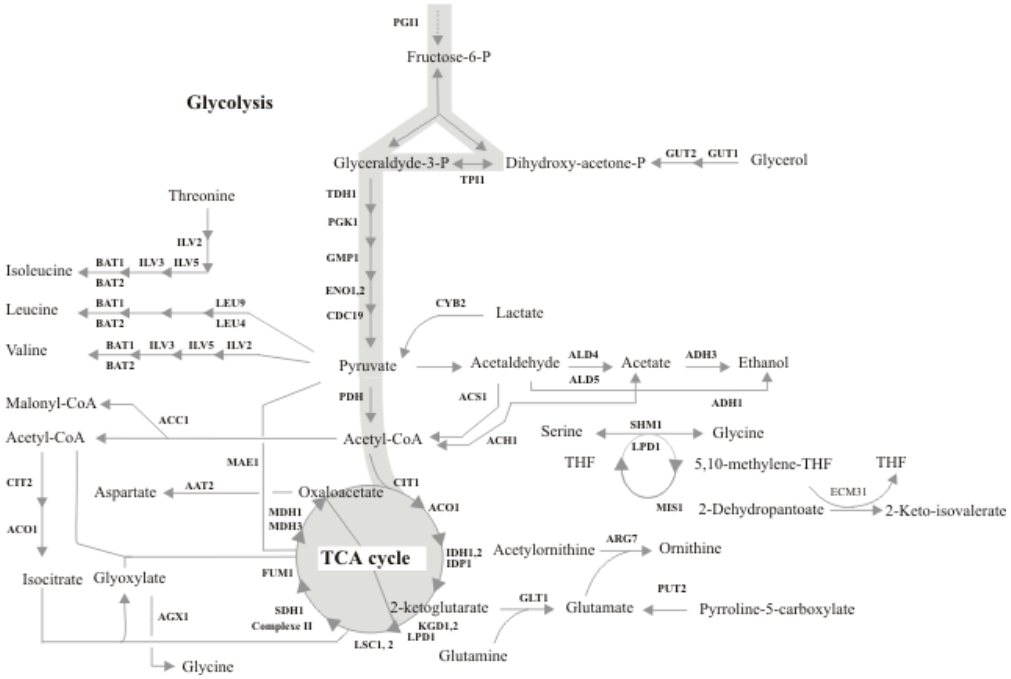
PGI1
Fructose-6-P
Glycolysis
Glyceraldyde-3-P
Dihydroxy-acetone-P
GUT2
GUT1
Glycerol
TPI1
Threonine
TDH1
PGK1
ILV2
GMP1
Isoleucine
BAT1
ILV3
ILV5
BAT2
ENO1,2
Leucine
BAT1
LEU9
CDC19
CYB2
Lactate
BAT2
LEU4
Valine
BAT1
ILV3
ILV5
ILV2
Pyruvate
Acetaldehyde
ALD4
Acetate
ADH3
Ethanol
BAT2
ALD5
ADH1
PDH
ACS1
Malonyl-CoA
ACC1
Acetyl-CoA
Acetyl-CoA
ACH1
Serine
SHM1
Glycine
LPD1
THF
5,10-methylene-THF
THF
MAE1
CIT2
Aspartate
AAT2
Oxaloacetate
CIT1
ECM31
MIS1
2-Dehydropantoate
2-Keto-isovalerate
MDH1
MDH3
ACO1
ACO1
TCA cycle
IDH1,2
IDP1
Acetylornithine
ARG7
Ornithine
Isocitrate
Glyoxylate
FUM1
PUT2
SDH1
Complexe II
2-ketoglutarate
GLT1
Glutamate
Pyrroline-5-carboxylate
AGX1
KGD1,2
LPD1
LSC1, 2
Glutamine
Glycine

Sc5

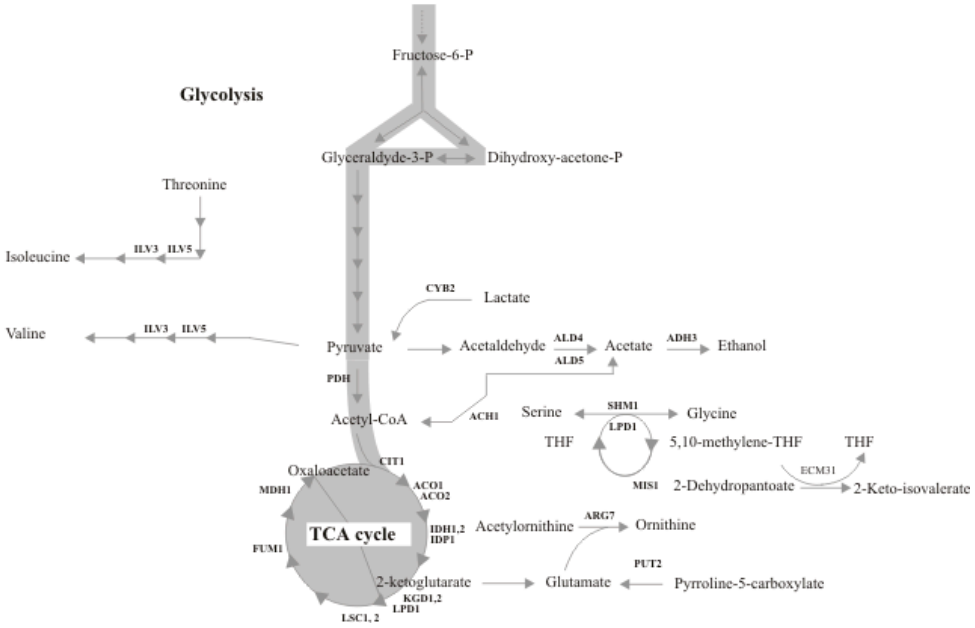
Glycolysis
Fructose-6-P
Glyceraldyde-3-P
Dihydroxy-acetone-P
Threonine
Isoleucine
ILV3
ILV5
Valine
CYB2
Lactate
Pyruvate
Acetaldehyde
ALD4
ALD5
Acetate
ADH3
Ethanol
PDH
Acetyl-CoA
ACH1
Serine
SHM1
LPD1
Glycine
THF
5,10-methylene-THF
THF
ECM31
MIS1
2-Dehydropantoate
2-Keto-isovalerate
CIT1
Oxaloacetate
MDH1
ACO1
ACO2
TCA cycle
IDH1,2
IDP1
FUM1
Acetylornithine
ARG7
Ornithine
PUT2
2-ketoglutarate
Glutamate
Pyrroline-5-carboxylate
KGD1,2
LPD1
LSC1, 2

Sc6

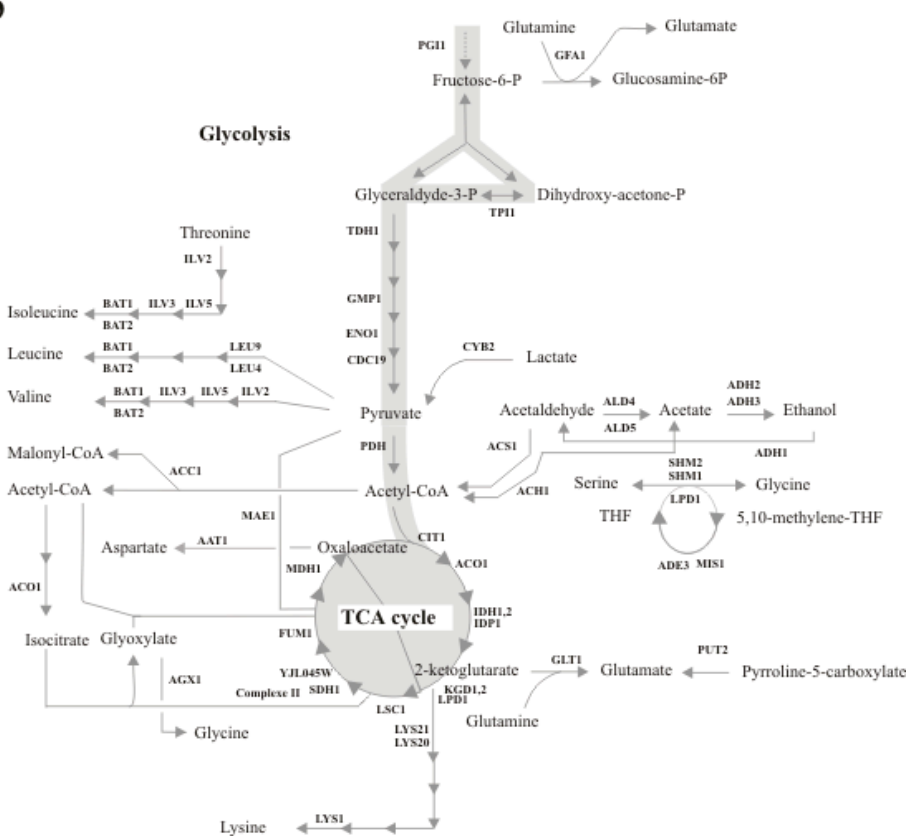
Glycolysis
Glutamine
Glutamate
GFA1
PGI1
Fructose-6-P
Glucosamine-6P
Glyceraldyde-3-P
Dihydroxy-acetone-P
TPI1
TDH1
Threonine
ILV2
Isoleucine
BAT1
ILV3
ILV5
BAT2
GMP1
ENO1
Leucine
LEU9
LEU4
CDC19
CYB2
Lactate
Valine
ILV2
Pyruvate
Acetaldehyde
ALD4
ALD5
Acetate
ADH2
ADH3
Ethanol
ADH1
PDH
ACS1
Malonyl-CoA
ACC1
Acetyl-CoA
ACH1
SHM2
SHM1
Serine
Glycine
LPD1
THF
5,10-methylene-THF
ADE3
MIS1
MAE1
CIT1
Aspartate
AAT1
Oxaloacetate
MDH1
ACO1
TCA cycle
IDH1,2
IDP1
FUM1
Isocitrate
Glyoxylate
AGX1
YJL045W
Complexe II
SDH1
2-ketoglutarate
KGD1,2
LPD1
LSC1
GLT1
Glutamate
PUT2
Pyrroline-5-carboxylate
Glutamine
Glycine
LYS21
LYS20
Lysine
LYS1

Sc7

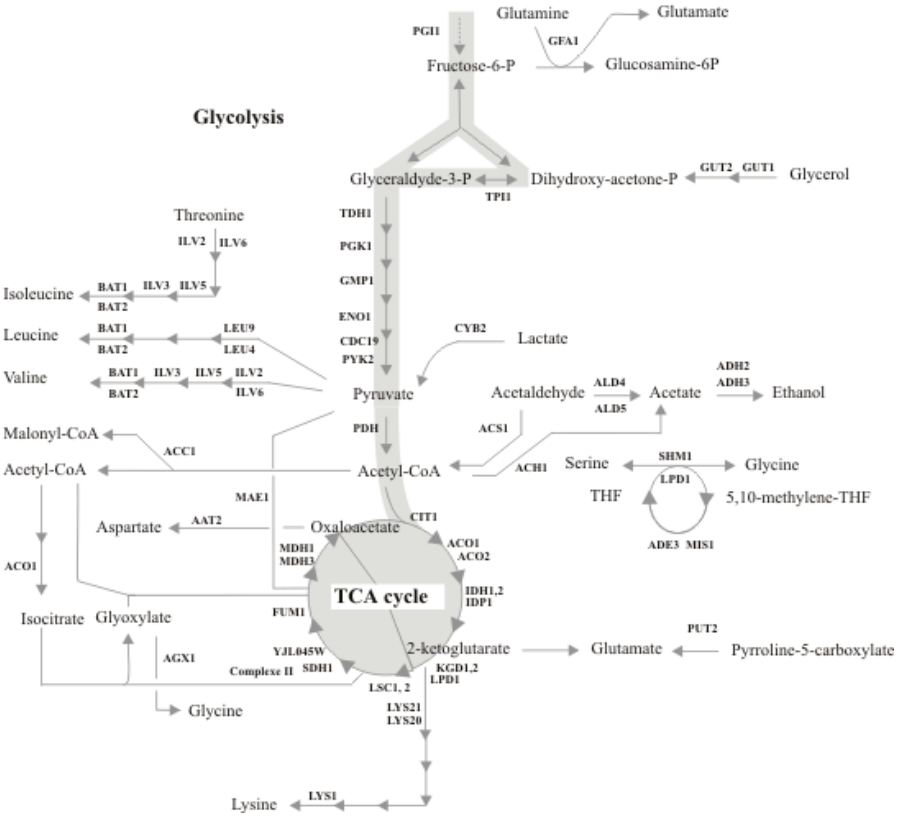
Glycolysis
Glutamine
Glutamate
GFA1
PGI1
Fructose-6-P
Glucosamine-6P
Glyceraldyde-3-P
Dihydroxy-acetone-P
TPI1
GUT2
GUT1
Glycerol
TDH1
PGK1
GMP1
ENO1
CDC19
PYK2
Threonine
ILV2
ILV6
Isoleucine
BAT1
BAT2
ILV3
ILV5
Leucine
LEU9
LEU4
Valine
CYB2
Lactate
Pyruvate
Acetaldehyde
ALD4
ALD5
Acetate
ADH2
ADH3
Ethanol
PDH
ACS1
ACH1
Malonyl-CoA
ACC1
Acetyl-CoA
Serine
SHM1
LPD1
Glycine
THF
5,10-methylene-THF
ADE3
MIS1
MAE1
Aspartate
AAT2
Oxaloacetate
CIT1
ACO1
ACO2
MDH1
MDH3
TCA cycle
IDH1,2
IDP1
FUM1
Isocitrate
Glyoxylate
AGX1
YJL045W
Complexe II
SDH1
2-ketoglutarate
KGD1,2
LPD1
LSC1, 2
PUT2
Pyrroline-5-carboxylate
Glycine
LYS21
LYS20
Lysine
LYS1

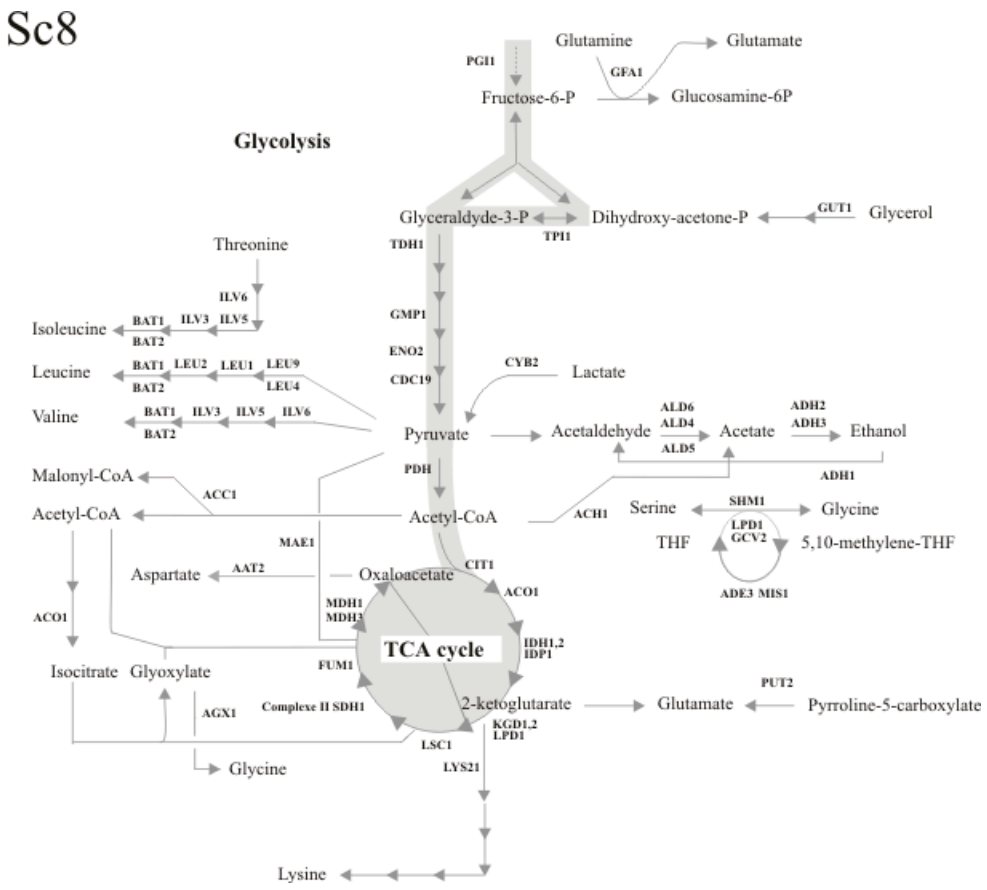
Sc8
Glycolysis
Glutamine
Glutamate
PGI1
GFA1
Fructose-6-P
Glucosamine-6P
Glyceraldyde-3-P
Dihydroxy-acetone-P
GUT1
Glycerol
TPI1
TDH1
Threonine
ILV6
Isoleucine
BAT1
ILV3
ILV5
BAT2
GMP1
ENO2
Leucine
LEU2
LEU1
LEU9
LEU4
CDC19
CYB2
Lactate
Valine
ILV6
Pyruvate
Acetaldehyde
ALD6
ALD4
ALD5
Acetate
ADH2
ADH3
Ethanol
ADH1
PDH
Malonyl-CoA
ACC1
Acetyl-CoA
ACH1
Serine
SHM1
Glycine
LPD1
GCV2
THF
5,10-methylene-THF
ADE3
MIS1
MAE1
Aspartate
AAT2
Oxaloacetate
CIT1
ACO1
MDH1
MDH3
TCA cycle
IDH1,2
IDP1
FUM1
Isocitrate
Glyoxylate
AGX1
Complexe II SDH1
2-ketoglutarate
PUT2
Glutamate
Pyrroline-5-carboxylate
KGD1,2
LPD1
LSC1
LYS21
Glycine
Lysine

Sc9

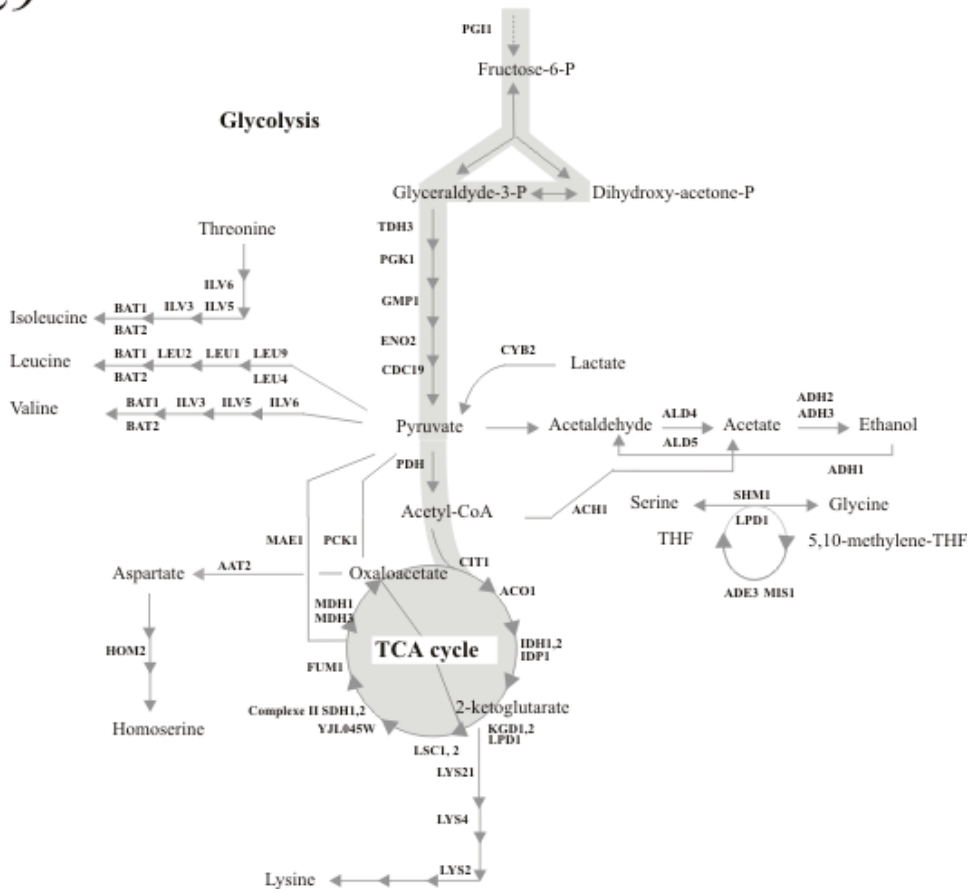
PGI1
Fructose-6-P
Glycolysis
Glyceraldyde-3-P
Dihydroxy-acetone-P
Threonine
TDH3
PGK1
GMP1
ENO2
CDC19
ILV6
BAT1
ILV3
ILV5
BAT2
Isoleucine
Leucine
LEU2
LEU1
LEU9
LEU4
Valine
ILV6
CYB2
Lactate
Pyruvate
Acetaldehyde
ALD4
ALD5
Acetate
ADH2
ADH3
Ethanol
ADH1
PDH
Acetyl-CoA
ACH1
Serine
SHM1
Glycine
LPD1
THF
5,10-methylene-THF
ADE3
MIS1
MAE1
PCK1
CIT1
Aspartate
AAT2
Oxaloacetate
ACO1
MDH1
MDH3
TCA cycle
IDH1,2
IDP1
HOM2
FUM1
Complexe II SDH1,2
YJL045W
2-ketoglutarate
KGD1,2
LPD1
LSC1, 2
Homoserine
LYS21
LYS4
LYS2
Lysine

Sc10

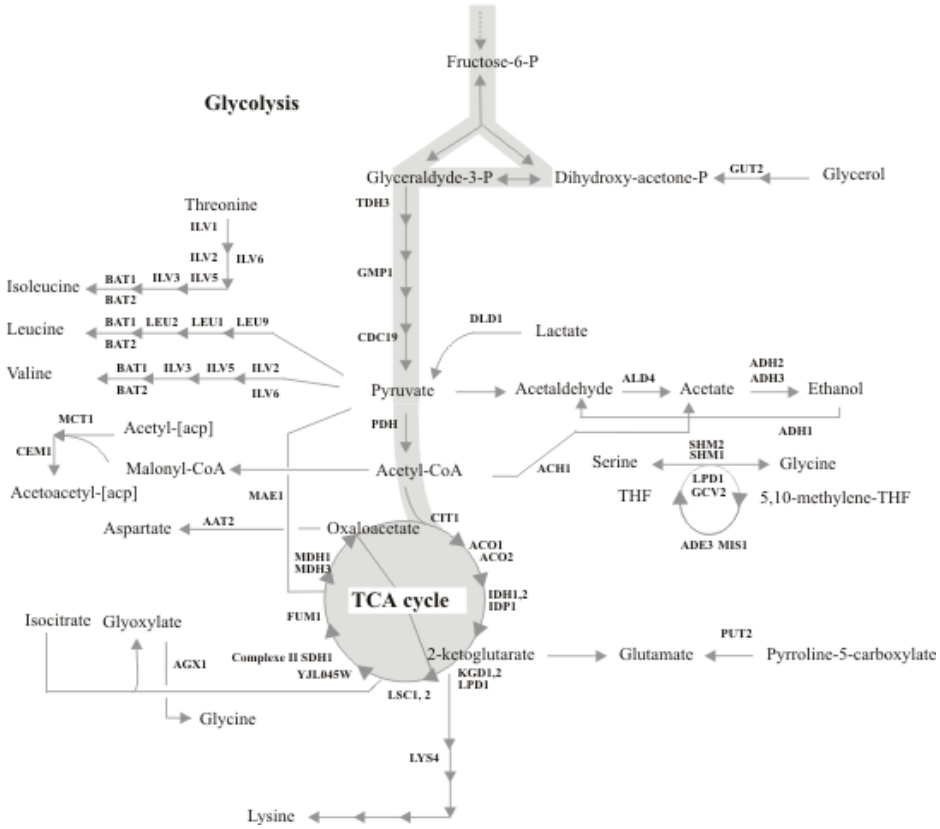
Glycolysis
Fructose-6-P
Glyceraldyde-3-P
Dihydroxy-acetone-P
GUT2
Glycerol
TDH3
GMP1
CDC19
DLD1
Lactate
Pyruvate
Acetaldehyde
ALD4
Acetate
ADH2
ADH3
Ethanol
ADH1
PDH
ACH1
Acetyl-CoA
Malonyl-CoA
MCT1
Acetyl-[acp]
CEM1
Acetoacetyl-[acp]
MAE1
Serine
SHM2
SHM1
Glycine
THF
LPD1
GCV2
5,10-methylene-THF
ADE3
MIS1
Aspartate
AAT2
Oxaloacetate
CIT1
ACO1
ACO2
MDH1
MDH3
TCA cycle
IDH1,2
IDP1
FUM1
Isocitrate
Glyoxylate
AGX1
Complexe II SDH1
YJL045W
2-ketoglutarate
KGD1,2
LPD1
LSC1, 2
Glutamate
PUT2
Pyrroline-5-carboxylate
Glycine
LYS4
Lysine
Threonine
ILV1
ILV2
ILV6
Isoleucine
BAT1
ILV3
ILV5
BAT2
Leucine
LEU2
LEU1
LEU9
Valine

Sc11

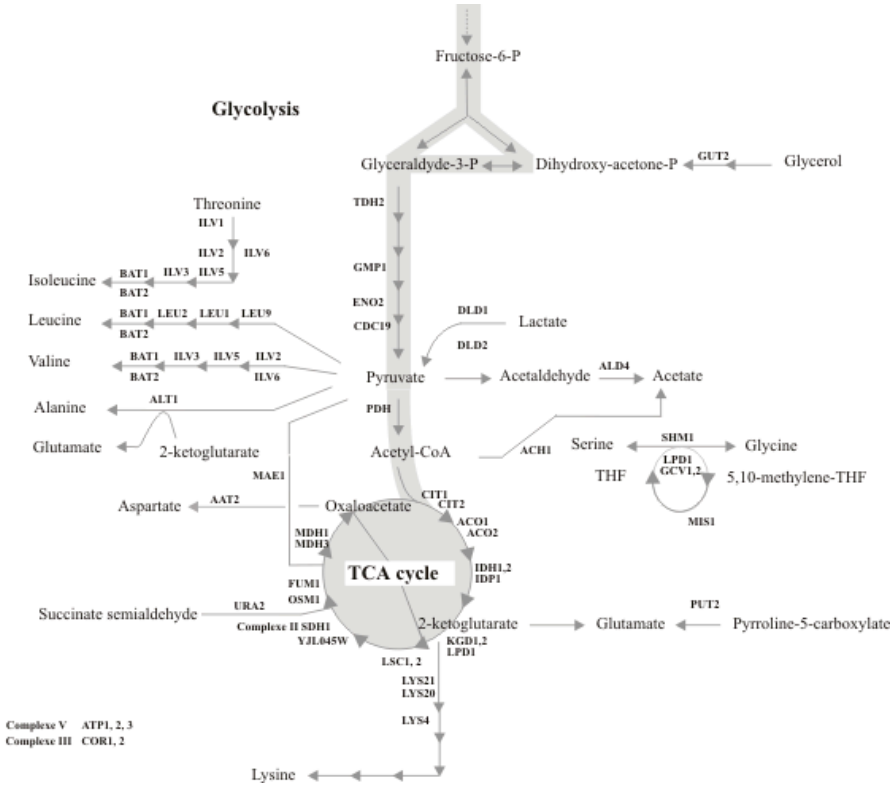
Glycolysis
Fructose-6-P
Glyceraldyde-3-P
Dihydroxy-acetone-P
GUT2
Glycerol
TDH2
GMP1
ENO2
CDC19
DLD1
DLD2
Lactate
Pyruvate
Acetaldehyde
ALD4
Acetate
PDH
Acetyl-CoA
ACH1
Threonine
ILV1
ILV2
ILV6
Isoleucine
BAT1
ILV3
ILV5
BAT2
Leucine
LEU2
LEU1
LEU9
Valine
Alanine
ALT1
Glutamate
2-ketoglutarate
Serine
SHM1
Glycine
THF
LPD1
GCV1,2
5,10-methylene-THF
MIS1
MAE1
Aspartate
AAT2
Oxaloacetate
CIT1
CIT2
ACO1
ACO2
MDH1
MDH3
TCA cycle
IDH1,2
IDP1
FUM1
OSM1
URA2
Succinate semialdehyde
Complexe II SDH1
YJL045W
2-ketoglutarate
KGD1,2
LPD1
LSC1, 2
Glutamate
PUT2
Pyrroline-5-carboxylate
LYS21
LYS20
LYS4
Lysine
Complexe V ATP1, 2, 3
Complexe III COR1, 2

Sc12

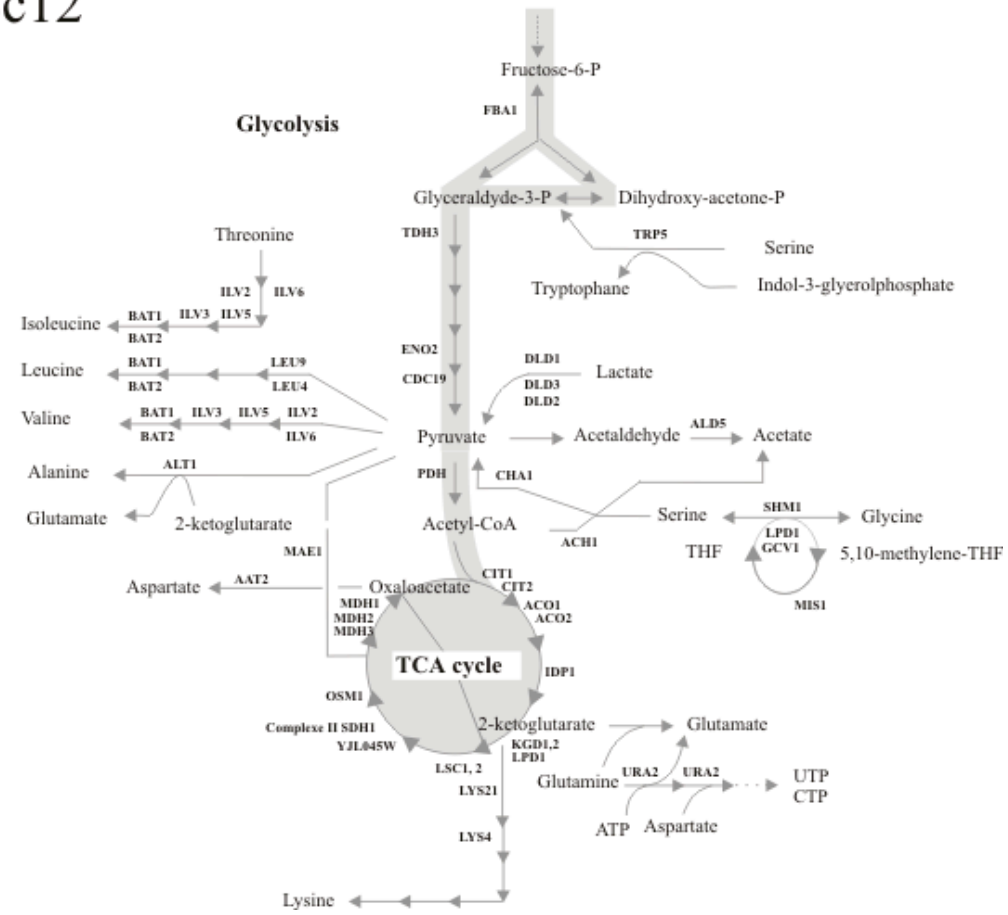
Glycolysis
Fructose-6-P
FBA1
Glyceraldyde-3-P
Dihydroxy-acetone-P
TDH3
TRP5
Serine
Tryptophane
Indol-3-glyerolphosphate
Threonine
ILV2
ILV6
Isoleucine
BAT1
ILV3
ILV5
BAT2
Leucine
LEU9
LEU4
Valine
ENO2
CDC19
DLD1
DLD3
DLD2
Lactate
Pyruvate
Acetaldehyde
ALD5
Acetate
Alanine
ALT1
Glutamate
2-ketoglutarate
PDH
CHA1
Acetyl-CoA
Serine
SHM1
Glycine
ACH1
THF
LPD1
GCV1
5,10-methylene-THF
MIS1
MAE1
Aspartate
AAT2
Oxaloacetate
CIT1
CIT2
MDH1
MDH2
MDH3
ACO1
ACO2
TCA cycle
IDP1
OSM1
Complexe II SDH1
YJL045W
2-ketoglutarate
Glutamate
KGD1,2
LPD1
LSC1, 2
LYS21
Glutamine
URA2
URA2
UTP
CTP
ATP
Aspartate
LYS4
Lysine

Sc13

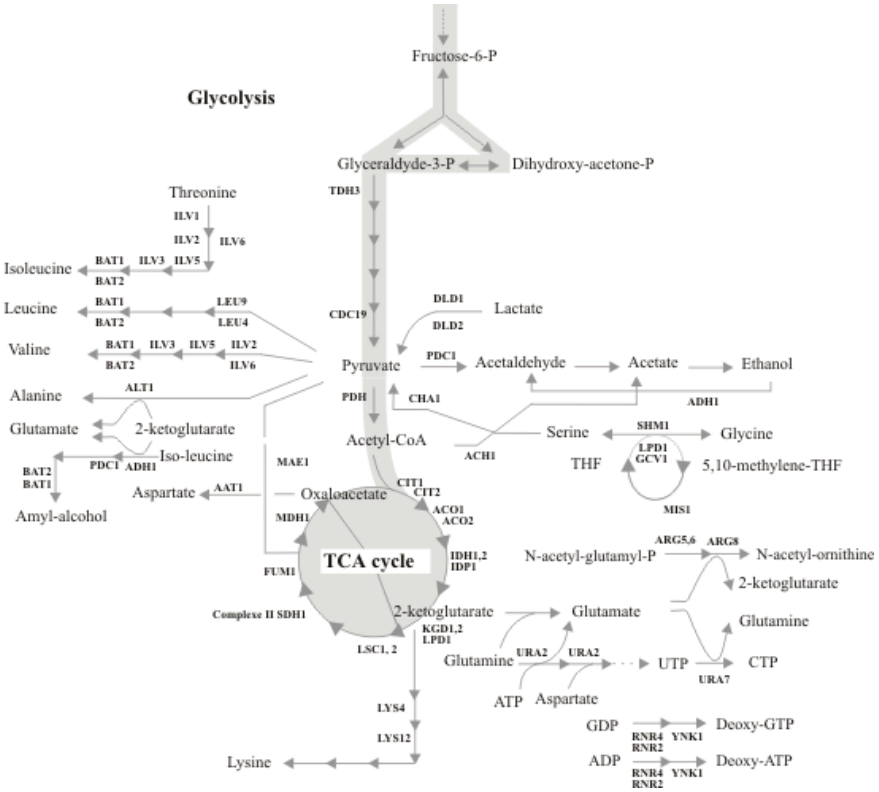
Fructose-6-P
Glycolysis
Glyceraldyde-3-P
Dihydroxy-acetone-P
TDH3
Threonine
ILV1
ILV2
ILV6
Isoleucine
BAT1
ILV3
ILV5
BAT2
Leucine
LEU9
LEU4
Valine
CDC19
DLD1
DLD2
Lactate
Pyruvate
PDC1
Acetaldehyde
Acetate
Ethanol
ADH1
Alanine
ALT1
PDH
CHA1
Glutamate
2-ketoglutarate
Acetyl-CoA
Serine
SHM1
Glycine
ACH1
Iso-leucine
PDC1
ADH1
THF
LPD1
GCV1
5,10-methylene-THF
MIS1
BAT2
BAT1
Amyl-alcohol
Aspartate
AAT1
MAE1
Oxaloacetate
CIT1
CIT2
ACO1
ACO2
MDH1
TCA cycle
IDH1,2
IDP1
FUM1
Complexe II SDH1
2-ketoglutarate
KGD1,2
LPD1
LSC1, 2
N-acetyl-glutamyl-P
ARG5,6
ARG8
N-acetyl-ornithine
2-ketoglutarate
Glutamate
Glutamine
Glutamine
URA2
URA2
UTP
CTP
URA7
ATP
Aspartate
LYS4
LYS12
Lysine
GDP
Deoxy-GTP
RNR4
YNK1
RNR2
ADP
Deoxy-ATP
RNR4
YNK1
RNR2

Sc14

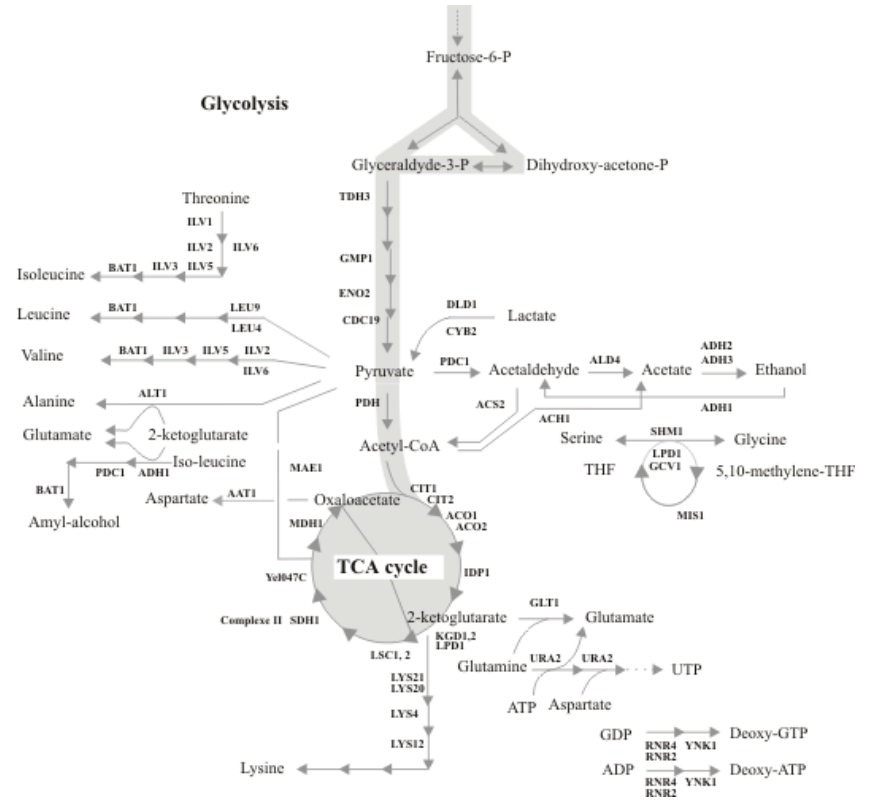
Fructose-6-P
Glycolysis
Glyceraldyde-3-P
Dihydroxy-acetone-P
TDH3
Threonine
ILV1
ILV2
ILV6
GMP1
Isoleucine
BAT1
ILV3
ILV5
ENO2
Leucine
BAT1
LEU9
LEU4
CDC19
DLD1
CYB2
Lactate
Valine
BAT1
ILV3
ILV5
ILV2
ILV6
Pyruvate
PDC1
Acetaldehyde
ALD4
Acetate
ADH2
ADH3
Ethanol
ADH1
Alanine
ALT1
PDH
ACS2
ACH1
Glutamate
2-ketoglutarate
Acetyl-CoA
Serine
SHM1
Glycine
Iso-leucine
PDC1
ADH1
MAE1
THF
LPD1
GCV1
5,10-methylene-THF
MIS1
BAT1
Aspartate
AAT1
Oxaloacetate
CIT1
CIT2
Amyl-alcohol
ACO1
ACO2
MDH1
TCA cycle
IDP1
Yel047C
Complexe II SDH1
2-ketoglutarate
GLT1
Glutamate
KGD1,2
LPD1
LSC1, 2
Glutamine
URA2
URA2
UTP
LYS21
LYS20
ATP
Aspartate
LYS4
LYS12
Lysine
GDP
Deoxy-GTP
RNR4
YNK1
RNR2
ADP
Deoxy-ATP
RNR4
YNK1
RNR2

Sc15

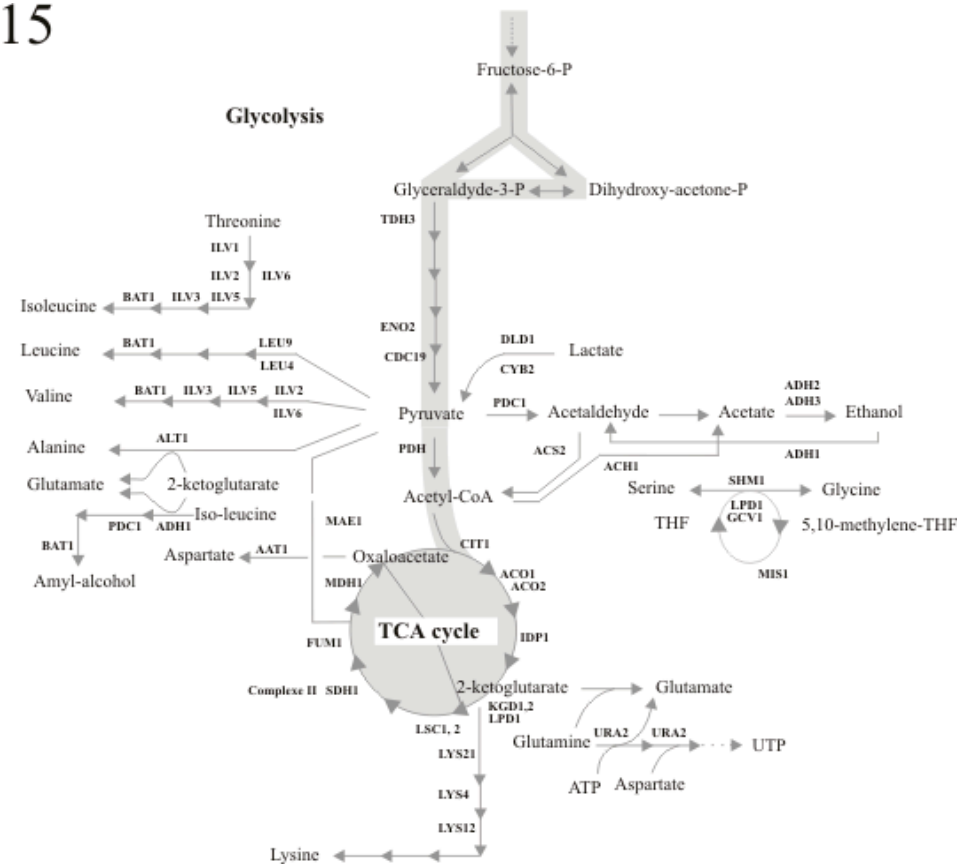
Glycolysis
Fructose-6-P
Glyceraldyde-3-P
Dihydroxy-acetone-P
TDH3
Threonine
ILV1
ILV2
ILV6
Isoleucine
BAT1
ILV3
ILV5
ENO2
CDC19
DLD1
CYB2
Lactate
Leucine
BAT1
LEU9
LEU4
Valine
BAT1
ILV3
ILV5
ILV2
ILV6
Pyruvate
PDC1
Acetaldehyde
Acetate
ADH2
ADH3
Ethanol
ADH1
ACS2
ACH1
Alanine
ALT1
PDH
Acetyl-CoA
Glutamate
2-ketoglutarate
Iso-leucine
PDC1
ADH1
BAT1
Amyl-alcohol
Aspartate
AAT1
MAE1
CIT1
Oxaloacetate
MDH1
ACO1
ACO2
TCA cycle
FUM1
IDP1
Complexe II
SDH1
2-ketoglutarate
Glutamate
KGD1,2
LPD1
LSC1, 2
Glutamine
URA2
URA2
UTP
ATP
Aspartate
LYS21
LYS4
LYS12
Lysine
Serine
SHM1
Glycine
THF
LPD1
GCV1
5,10-methylene-THF
MIS1

Sc16

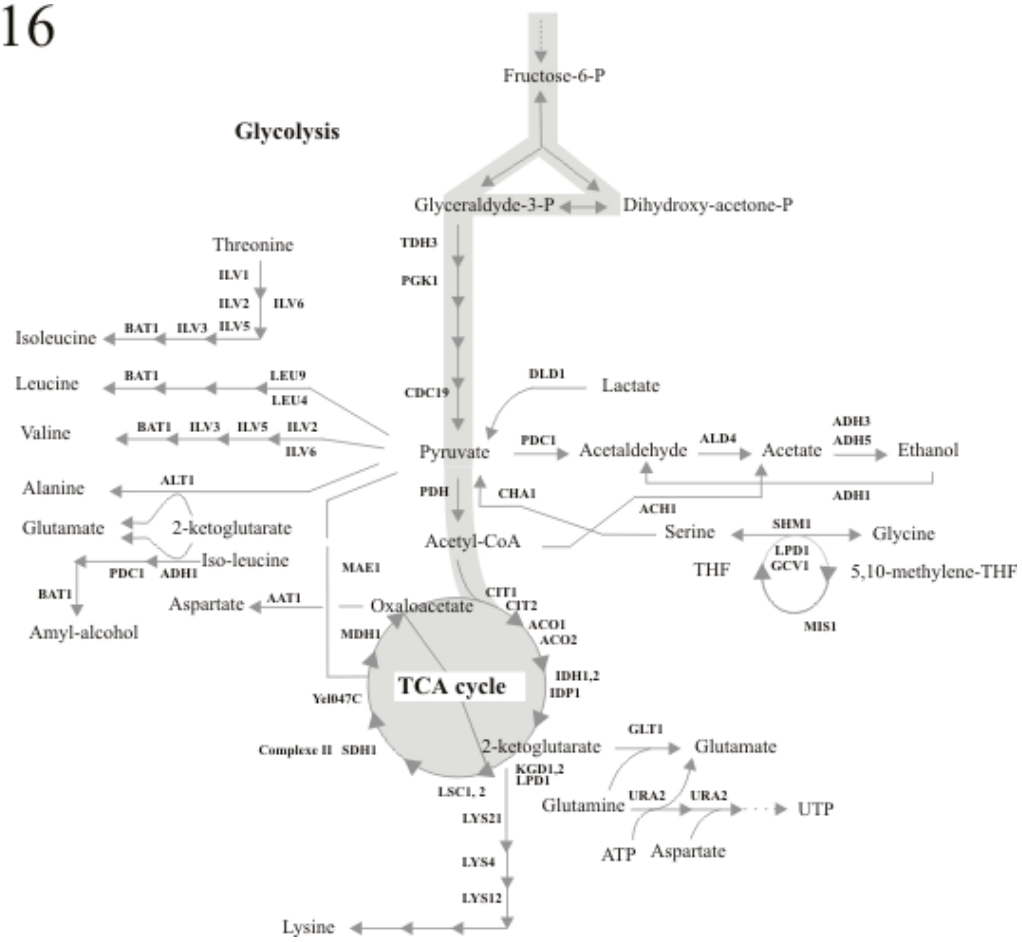
Glycolysis
Fructose-6-P
Glyceraldyde-3-P
Dihydroxy-acetone-P
TDH3
PGK1
CDC19
Threonine
ILV1
ILV2
ILV6
Isoleucine
BAT1
ILV3
ILV5
Leucine
LEU9
LEU4
Valine
ILV2
ILV6
Alanine
ALT1
Glutamate
2-ketoglutarate
Iso-leucine
PDC1
ADH1
BAT1
Amyl-alcohol
Aspartate
AAT1
DLD1
Lactate
Pyruvate
PDC1
Acetaldehyde
ALD4
Acetate
ADH3
ADH5
Ethanol
ADH1
PDH
CHA1
ACH1
Acetyl-CoA
Serine
SHM1
Glycine
THF
LPD1
GCV1
5,10-methylene-THF
MIS1
MAE1
CIT1
CIT2
Oxaloacetate
ACO1
ACO2
MDH1
IDH1,2
IDP1
TCA cycle
Yel047C
Complexe II
SDH1
2-ketoglutarate
GLT1
Glutamate
KGD1,2
LPD1
LSC1, 2
Glutamine
URA2
URA2
UTP
ATP
Aspartate
LYS21
LYS4
LYS12
Lysine

Figure S5

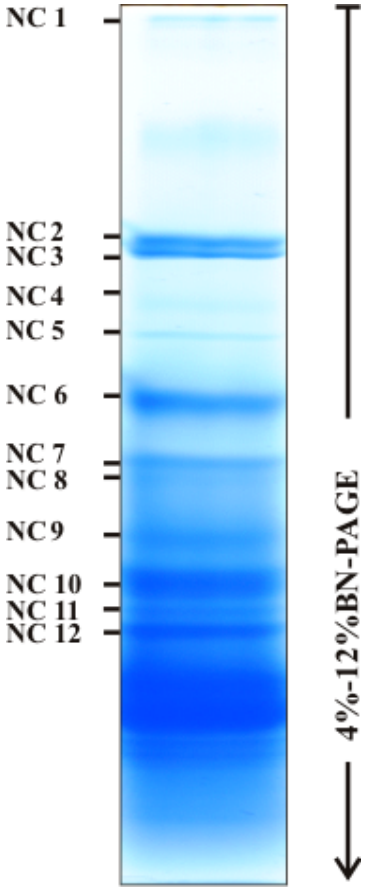

Table S1

Cellular localization	Protein number
Mitochondrial	261
Mitochondrial, Cytoplasmic	122
Cytoplasmic	65
Mitochondrial, Nuclear	23
Nuclear	21
Cytoplasmic, Nuclear	20
unknown	13
Mitochondrial, Nuclear, Cytoplasmic	9
Mitochondrial, Peroxisomal	4
Cytoplasmic, Peroxisomal	3
Vacuolar	3
Endoplasmic Reticulum	2
Mitochondrial, Cytoplasmic,Vacuolar	2
Cytoplasmic, Endoplasmic Reticulum	1
Cytoplasmic, Vacuolar, Endoplasmic Reticulum	1
Mitochondrial, Endoplasmic Reticulum	1
Mitochondrial, Extra-cellular	1
Mitochondrial, Vacuolar	1
Nuclear, Cytoplasmic	1
Nuclear, Peroxisomal	1

Table S2

Supercomplexes	SC1	SC2	SC3	SC4	SC5	SC6	SC7	SC8	SC9	SC10	SC11	SC12	SC13	SC14	SC15	SC16
SC1	54	31	19	24	18	22	25	15	22	17	16	13	27	25	20	25
SC2		167	69	84	62	77	85	67	66	50	42	43	73	87	79	59
SC3			130	97	49	79	81	66	62	57	47	38	53	57	46	57
SC4				143	58	107	103	89	77	65	55	64	73	52	62	69
SC5					69	53	59	47	38	40	34	21	37	37	36	34
SC6						145	112	102	101	69	57	48	58	67	49	57
SC7							188	108	96	98	74	58	87	91	100	92
SC8								128	83	84	62	45	66	63	55	68
SC9									138	87	67	65	47	81	71	72
SC10										127	45	47	72	74	67	74
SC11											100	52	67	61	56	60
SC12												144	72	69	69	62
SC13													222	156	143	161
SC14														226	161	149
SC15															227	150
SC16																223

Article 2 : Yeast mitochondrial RNase P, RNase Z and the RNA degradosome are part of a stable supercomplex

Rachid Daoud, Lise Forget and B. Franz Lang*

Robert-Cedergren Centre for Bioinformatics and Genomics, Department of Biochemistry, Université de Montréal, 2900 Edouard-Montpetit, Montreal, Quebec, H3T 1J4 Canada

Keywords: Mitochondria, tRNA maturation, RNA degradation, translation, type II fatty acid synthesis pathway (FAS II).

Nucleic Acids Research Advance Access published October 27, 2011

Nucleic Acids Research, 2011, 1–9
doi:10.1093/nar/gkr941

Yeast mitochondrial RNase P, RNase Z and the RNA degradosome are part of a stable supercomplex

Rachid Daoud, Lise Forget and B. Franz Lang*

Robert-Cedergren Centre for Bioinformatics and Genomics, Department of Biochemistry, Université de Montréal, 2900 Edouard-Montpetit, Montreal, Quebec, H3T 1J4 Canada

Received August 19, 2011; Revised September 30, 2011; Accepted October 12, 2011

ABSTRACT

Initial steps in the synthesis of functional tRNAs require 5′- and 3′-processing of precursor tRNAs (pre-tRNAs), which in yeast mitochondria are achieved by two endonucleases, RNase P and RNase Z. In this study, using a combination of detergent-free Blue Native Gel Electrophoresis, proteomics and *in vitro* testing of pre-tRNA maturation, we reveal the physical association of these plus other mitochondrial activities in a large, stable complex of 136 proteins. It contains a total of seven proteins involved in RNA processing including RNase P and RNase Z, five out of six subunits of the mitochondrial RNA degradosome, components of the fatty acid synthesis pathway, translation, metabolism and protein folding. At the RNA level, there are the small and large rRNA subunits and RNase P RNA. Surprisingly, this complex is absent in an *oar1*Δ deletion mutant of the type II fatty acid synthesis pathway, supporting a recently published functional link between pre-tRNA processing and the FAS II pathway—apparently by integration into a large complex as we demonstrate here. Finally, the question of mt-RNase P localization within mitochondria was investigated, by GFP-tracing of a known protein subunit (Rpm2p). We find that about equal fractions of RNase P are soluble versus membrane-attached.

INTRODUCTION

To synthesize functional tRNAs, precursor tRNAs (pre-tRNA) need to be processed at their 5′- and 3′-termini. An almost ubiquitous RNase P is responsible for endonucleolytic 5′-processing (1). Until the discovery that human and *Arabidopsis* mitochondrial RNase P are protein-only enzymes (2,3), these activities were thought to be always ribonucleo-proteins, composed of a catalytic RNA plus one or several proteins, throughout Archaea, Bacteria and eukaryotes (4–9). Processing of tRNA 3′-termini is achieved by exonucleolytic and/or endonucleolytic activities, depending on the organism and the cellular compartment (10–14). In *Escherichia coli*, processing of 3′-termini requires a multi-step process initiated by an endonucleotic cleavage, followed by exonucleolytic trimming (11). In other bacteria and most eukaryotes (including nuclear, mitochondria, and plastid) and in all Archaea, 3′-tRNA processing is an endonucleolytic cleavage catalyzed by tRNase Z that exists in two forms, a long form of 750–930 amino acids only present in Eukarya (tRNase ZL), and a short form of 280–360 amino acids (tRNaseZ S) (15).

Most information on mitochondrial (mt) pre-tRNA processing comes from studies of *Saccharomyces cerevisiae*. A highly purified form of mitochondrial RNase P (mt-RNase P) has been obtained by lysis of mitochondria in the presence of detergent and high salt, and a series of chromatographic steps. It contains the nucleus-encoded Rpm2p protein (Rpm2p; 119 kDa), and only an incomplete set of RNA fragments covering the mtDNA-encoded *RPM1* RNA subunit (mt-P RNA) of 427 nt (16–18). Yet, given that yeast mt-P RNA has a highly reduced RNA structure compared to its cytosolic counterpart (19), we strongly expect that native mt-RNase P contains more than just one protein, to compensate for the lack of RNA structure [for comparison, cytosolic RNase P contains nine proteins; (20)]. Previous studies revealed that Rpm2p is involved not only in mt-RNase P activity, but also effects mitochondrial import (21), fermentative growth (22), and transcriptional activation of several nucleus-encoded mitochondrial components (23). In addition (and most curiously), tRNA processing intersects with the type II fatty acid synthesis pathway (24). Disruption of any enzyme in the FAS II pathway leads to a defective mt-RNase P (24). One possibility to explain

this observation is that there is a structural association between mt-RNase P and FAS II that is impaired with deletion of the FAS II subunits. In fact, this led us to the hypothesis that a super-structure may combine some or all of the above-mentioned mitochondrial functions into a large physical unit. Indications that RNase P may be associated with other functions also come from mt-RNase P purification experiments. In early isolation steps, its activity co-fractionates with the tRNA 3′-processing activity (18), and purification to homogeneity is achieved at an extremely low yield, despite the use of high salt and detergent. In yeast mitochondria, 3′-tRNA processing is an endonucleotic cleavage (25), which is accomplished by a multifunctional RNase Z (11,26,27). In yeast, both the nuclear and mitochondrial forms of RNase Z are encoded by a nuclear gene (TRZ1) (15). Again, this enzyme is also implicated in ribosomal RNA maturation (26).

Controlling RNA levels (balance between RNA synthesis and degradation) is vital for both the regulation and functioning of the mitochondrial system (28–30). RNA degradation is mediated principally by (arguably) small multiprotein complexes, like the exosome in the cytoplasm of eukaryotes (31) or the degradosome in bacteria (32). The activity responsible for RNA turnover in mitochondria is a 3′- to 5′-processive exoribonuclease (33), which is organized in an RNA degradosome complex (mtEXO), as first described in *S. cerevisiae* (34). The highly purified mtEXO complex is composed of only two protein subunits, the exoribonuclease (35), and an NTP-dependent RNA helicase (related to the DExH superfamily) (36). Yet, the degradosome apparently associates with the mitochondrial ribosome, as mtEXO co-purifies with ribosomal proteins that are difficult to remove (34). These observations reinforce the hypothesis that the RNA degradosome is part of a large superstructure that associates with a variety of mitochondrial functions.

In this study, we demonstrate that mt-RNase P and tRNA Z activities are part of a large ribo-nucleoprotein complex, which also includes the RNA degradosome, five additional RNA processing proteins, plus other mitochondrial functions. We further show that the biogenesis of this complex is impaired in a mutant that is deficient in type II fatty acid synthesis, rationalizing its known pleiotropic tRNA processing phenotype discussed above.

MATERIALS AND METHODS

Cell culture and mitochondrial isolation

Saccharomyces cerevisiae (BY 4743) was kindly provided by Dr S. Michnick (Université de Montréal), and yeast GFP (Green Fluorescent Protein) constructs used in this study (MATa *his3*Δ1 *leu2*Δ0 *met15*Δ0 *ura3*Δ0 RPM2-GFP::HIS3) by Dr J. Vogel (McGill). Cells were grown to an optical density of 1.5–2.5 in a medium containing 1% yeast extract, 2% peptone, 3% glycerol and 1% galactose, pH 5.0 (YEPGal). Mitochondrial purification followed previously published procedures with slight modifications (37). Yeast cell walls were removed by digestion with glucanase, spheroplasts were disrupted by osmotic shock, and a crude mitochondrial fraction was isolated by differential centrifugation. Mitochondria were resuspended in 'washing buffer' (600 mM sucrose, 0.2 mM PMSF and 10 mM MOPS/KOH, pH 7.2) and further purified by centrifugation (60 min at 134 000*g*) through a discontinuous sucrose gradient (concentrations from top to bottom, 25%, 36% and 60%; 5 ml each). For a second purification step, the mitochondrial fraction was collected and mixed with about four times its volume of 80% sucrose, layered at the bottom of a discontinuous sucrose gradients, and purified by centrifuged at 134 000*g* for 120 min. Intact mitochondria move upwards ('flotation'), and accumulate at the interface between the 36% and 60% sucrose layers. For enhanced purity, this two-step purification of the mitochondria was repeated twice. Purified mitochondria were resuspended in buffer (600 mM sucrose, 0.2 mM PMSF and 10 mM Tricine/KOH, pH 7.2) and pelleted at 14 000*g* for 15 min. Usually, mitochondria were directly processed in further steps, but they may also be shock-frozen and kept at −80°C until use.

Extraction of mitochondria soluble matrix proteins and membrane fractions

For the extraction of matrix proteins, we adapted a previously published procedure (37,38). Mitochondria were re-suspended at 10 mg/ml in breaking buffer (600 mM sucrose, 20 mM HEPES–KOH, pH 7.4, 10 mM EDTA) and incubated for 30 min on ice in nine volumes of 20 mM HEPES–KOH, pH 7.4, 0.5 mM EDTA and 1 mM PMSF. We used three alternative ways for rupturing mitochondria, which only differ in yield but not in banding pattern or protein composition of supercomplexes. The gentlest method is to burst mitochondria through osmotic shock, by abruptly adding 10 volumes buffer. Alternatively, the mitochondrial suspension is adjusted to a final sucrose concentration of 0.45 M, incubated for 30 min on ice, and then homogenized in a Potter homogenizer for 90 s. The third method, for maximum yield of matrix proteins, involves mechanical disruption of mitochondria by shaking with an equal ratio of 125–212 µ and 425–600 µ glass beads (Sigma), in three rounds of 20 s each at 4°C. After a clarifying centrifugation at 12 000*g* for 15 min, the supernatant was subjected to centrifugation at 100 000*g*, for 2 h at 4°C. The pellet containing mitochondrial membranes was discarded, and the supernatant was subjected to a second centrifugation at 120 000*g*, for 30 min at 4°C. The matrix protein fraction (supernatant) was mostly used immediately, but may be stored at −80°C after shock-freezing. Protein concentrations were determined with the Bradford protein assay. A mitochondrial membrane fraction was prepared as described previously (39,40).

Tracking of GFP-tagged marker proteins

Soluble matrix protein complexes (1.5 mg) isolated from an Rpm2-GFP construct were separated by ultracentrifugation (16 h at 20 000*g*, Beckman SW41 rotor) on

discontinuous glycerol gradients (10–70% glycerol, in a buffer containing 20 mM HEPES–KOH pH 7.9, 50 mM KCl, 1.5 mM $MgCl_2$ and 1 mM DTT). 0.7 ml fractions were collected and analyzed for protein concentration (Bradford protein assay) and relative GFP fluorescence intensity (excitation at 488 nm, light emission between 500 and 540 nm).

Purification of mt-RNase P activity

To purify the native RNase P complex, we developed a preparative Blue Native Column Electrophoresis (NEC), which permits large-scale purification of native protein complexes. It is based on the regular blue native gel electrophoresis (BN–PAGE) protocol (41–44), using instead of a slab gel a cylindrical running chamber filled with polyacrylamide gel (e.g. 7%). The different concentrations of native polyacrylamide gel were prepared as previously published (41–44). The mitochondrial extracts (~250 µg) were separated at constant voltage (140 V and 9 mA, overnight, in a cold room 4°C), using the same electrophoresis buffers as in regular BN–PAGE. Samples were collected every 30 min from a 200 µl dialysis-cup placed at the outlet of the column. Collected fractions were assayed for mt-RNase P activity and analyzed for complexes composition with BN–PAGE.

In vitro preparation and radio-labeling of pre-tRNA^{proline}

The mitochondrial *Reclinomonas americana* pre-tRNA^{proline} substrate for the RNase P assays was prepared by *in vitro* transcription and purified as described previously (45). The tRNA^{proline} DNA ligated into pFBS/EcoRV (2.9 kb) vector with T4 DNA ligase (Roche) and amplified by PCR using 5′-GAAATTAATACGACTCACTATAGGGTAACGTACTTAATGTAAAAGGTT-3′, 5′-TGGTCGGGATGACGTGATTTGAACA-3′ and 5′-TCACTAAAGGGAACAAAAGCTGGGT-3′ primers produce respectively 5′-leader pre-tRNA^{proline} and, 5′-leader and 3′-termini pre-tRNA^{proline}. The two amplified tRNA^{proline} DNAs were used separately for two *in vitro* radio-labeled transcriptions. Two micrograms of each amplified tRNA^{proline} DNA were used for tRNA^{proline} transcription with Invitrogen T7 RNA polymerase (2 u/µl) and α P^{32} ATP (10 mCi/ml) (Perkin Elmer) as previously described (45). After an overnight incubation at 37°C, loading buffer was added and the samples were heated at 75°C for 2 min before loading on a 9% polyacrylamide/8 M urea gel (4 h, 200 V at room temperature). The 117 nt (5′-leader pre-tRNA^{proline}) and 148 nt (5′-leader and 3′-termini pre-tRNA^{proline}) RNA bands were cut out of the gel and incubated over night at 37°C in a 300 µl buffer extraction (30 µl of 1% SDS and 270 µl of H_20_2). After phenol–chloroform extraction and ethanol precipitation, the precursor RNA was 5′-labeled with α-ATP^{32}.

Activity assay of mt-RNase P

To test the mt-RNase P activity we used the same procedure as described previously (46). Radio-labeled pre-tRNA^{proline} (2000 cpm) was dissolved in 1× PA buffer (50 mM Tris–HCl, pH 7.5, 100 mM NH_4Cl, 10 mM $MgCl_2$) and incubated 30 min at 37°C, in a 15-µl mixture reaction. After incubation, 10 µl of loading buffer was added, and the sample was heated at 75°C for 2 min before loading on a 9% polyacrylamide/8 M urea gel (4 h, 200 V at room temperature). The gels were then either exposed to a Kodak film (~12 h) or a Biorad molecular imaging screen K (2 h).

The M1 RNA ribozyme was used as positive control for 5′-tRNA processing. The expression plasmid carrying the *E. coli* M1 RNA gene (provided by Sidney Altman) was used for *in vitro* transcription. For all experimental information for M1 RNA transcription and purification see (45). The primers for amplification of the *rnpB* gene were 5′-GAAATTAATACGACTCACTATAGGGAAGCTGACCAGACAGTCGC-3′ and 5′AGGTGAAACTGACCGATAAGCC 3′. The M1 RNA was activated before use, by heating (65°C for 5 min), and slow cooling to room temperature in 1× PA buffer (50 mM Tris–HCl, pH 7.5, 100 mM NH_4Cl, 10 mM $MgCl_2$). Radio-labeled pre-tRNA^{proline} (2.000 cpm) was incubated at 37°C in 10 mM Tris–HCl, pH 7.5, 100 mM $MgCl_2$, 100 mM NH_4Cl, 4% PEG, in the presence of ~10 nM M1 RNA. The total volume of the reaction is 15 µl. After 30 min, 10 µl of loading buffer was added, and the sample was heated at 75°C for 2 min before loading on a 9% polyacrylamide/8 M urea gel.

Identification of mt-RNase P RNA (RPM1) by RT–PCR

Endogenous RNA from the identified MRT complex was purified using the 'RNeasy plus' kit by QIAGEN, and RT–PCR assays were performed on 10 ng RNA with AMV reverse transcriptase (cDNA synthesis). The cDNA was amplified with the Expand High Fidelity PCR system provided by Roche. The PCR primers for RPM1 RNA amplification are 5′-TAATAGGAAAGTCATAAATAT-3′, 5′-GTAATATAT ATATATATATTGGAATAG-3′ and 5′-TTATATTATTATACAGAAATA-3′. For RT–PCR the same primers of the PCR were used in addition to 5′-AGAAATAATATTATAAATAAATATAT-3′, 5′-GGATATTATATTATAAGCA-3′ and 5′-AAGCATATTTCTGTATAATAA-3′. The expected PCR products have lengths of 51, 71, 52, 387 and 400 nt.

Blue native gel electrophoresis

Preparation of samples and of 4–14% BN–PAGE gel followed previously published procedures (41–44), except that detergents were omitted (their effect was only tested in supercomplex stability tests). Approximately 150 µg protein was loaded per well, and electrophoretic separation was performed in a Höfer (18 × 16 cm) electrophoresis chamber, at 140 V and 9 mA, overnight at 4°C.

Analysis of supercomplex composition by mass spectrometry

To identify protein complexes that form discrete bands in BN–PAGE, complex bands were cut from the gel and submitted to liquid chromatography tandem mass spectrometry (LC–MS/MS) analysis (47,48). In-gel tryptic digestion and LC–MS/MS analysis was performed by a

service at the Université de Montréal (IRIC), including functional annotation by Mascot (49).

RESULTS AND DISCUSSION

Purification of mt-RNase P without the use of detergents

To preserve the integrity of a postulated large complex that combines mt-RNase P with other mitochondrial functions, we have developed purification procedures that do not make use of detergents or other highly disruptive conditions as previously applied [such as detergent, high salt, EDTA, heat shock etc; (16–18)]. For this we start with highly purified yeast mitochondria, gently disrupt the organelles and extract a soluble matrix fraction by centrifugation, which represents ~57% of total mitochondrial proteins. When separating the soluble extract on a glycerol gradient (10–70%; for details see 'Materials and Methods' section), most of the material moves into the glycerol phase, in support of the idea that most soluble proteins are organized in large complexes. In fact, tracing of the protein subunit of mt-RNase P (Rpm2p) by *in vivo* GFP fluorescence labeling reveals that about half (54%) of the GFP-Rpm2p is in the soluble mitochondrial matrix fraction, and that most of it (81%) is associated with a high-molecular-weight complex as it migrates far into the glycerol gradient (35–40%; Figure 1). This gradient fraction also contains the bulk of RNase P activity (Supplementary Figure S1). GFP-labeled cells grow normally on non-fermentable substrates, indicating that the GFP fusion does not lead to functional disturbances.

As gradient procedures have only limited resolution, we set out to find an alternative, non-disruptive and preparative purification procedure for large protein complexes. This led us to develop a variant of BN–PAGE (50), in which all steps are performed under physiological conditions (e.g. pH 7), and in the absence of detergents (named non-denaturing polyacrylamide gel electrophoresis column, or NEC; for details see 'Materials and Methods' section). Instead of using a slab gel, preparative NEC separates in a large column with a continuous polyacrylamide gel, and fractions are continuously recovered in a dialysis cup as they leave the column. Tracking of mt-RNase P by *in vitro* cleavage of a mitochondrial pre-tRNA^{proline} precursor identifies ~70% of the total mt-RNase P activity in fractions 7–9 (with a total of 20 fractions; Figure 2A). To investigate the purity of fractions 7–9, they were separated by a second, regular slab-gel NEC that has more resolution than preparative NEC, and at a gel concentration that is optimal for separation close to the complex's size range. Several complexes were identified in all three fractions, but only one of them occurs regularly (Figure 3A), which is the putative mt-RNase P-containing complex. Therefore, for further large-scale purification, fractions 7, 8 and 9 were pooled and processed on a second preparative NEC column at a higher polyacrylamide concentration (7.5%). Under this condition, mt-RNase P activity elutes exclusively in fraction 38 (for a total of 50 samples; Figure 2B and Supplementary Figure S2). Slab-gel NEC analysis confirms that it contains a single complex (Figure 3A), which remains stable following treatments with DNase, RNase and to some degree (~50%) with a mild detergent (digitonin; Figure 3B). Taken together, we argue that this complex closely represents the *in vivo* organization of a set of soluble mitochondrial matrix proteins, combining a variety of RNA maturation and other functions as shown in the following experiments.

Association of 5′- and 3′-tRNA processing activities

The processing activity of the purified complex was subsequently tested in an *in vitro* assay, with a different pre-tRNA^{proline} substrate that has both 5′-leader and 3′-trailer extensions. We find essentially two forms of processed RNAs, the mature tRNA^{proline} and an intermediate pre-tRNA^{proline} with a 5′-leader (Figure 4), revealing the presence of a 3′-tRNA processing that is somewhat more effective than RNase P. This result is consistent with the previously observed co-fractionation of RNase P and RNase Z in early steps of yeast mt-RNase P purification (18).

Presence of RPM1 RNA and Rpm2p protein in the complex

To further characterize the homogeneity and composition of this tRNA processing complex, we tracked the presence of the known yeast mt-RNase P core RNA and protein components (i.e. the *RPM1* RNA subunit and Rpm2p). Proteomic analysis by mass spectrometry (LC–MS/MS, see 'Materials and Methods' section) shows that the Rpm2p is present only in this complex, together with a variety of other proteins (see below). Likewise, an extraction and analysis of the endogenous RNA of the purified complex demonstrate the presence of the two (un-degraded) small and large subunit rRNAs, as well as several RNAs of ~70–90 nt (Figure 5A). As expected, an RNA with the predicted size of an intact RPM1 RNA (427 nt) is absent, which is in agreement with previous investigations on purified yeast mt-RNaseP [e.g. (16)], in which only fragments of RPM1 RNA are detected. In fact, consistent with these studies, we find by RT–PCR and sequencing the same two RPM1 RNA fragments of 52, 89 and 71 nt (Figure 5B and Supplementary Figure S3). Our results thus confirm that an intact *RPM1* RNA subunit is not required for RNase P activity *in vitro* (16), and that the mt-RNase P core subunits are integrated within a large complex when isolated under non-denaturing conditions.

Protein composition of the mt-RNase P (RMT) complex

Proteomic analysis with liquid chromatography and tandem mass spectrometry (LC–MS/MS) reveals the presence of an unexpected high number of proteins (130) in the purified 'native' RNase P/RNase Z complex (confirmed by three independent analyses; Supplementary Table S1). These proteins are implicated in numerous functions including (as expected) RNA processing, but also metabolism (e.g. TCA cycle), translation (two aminoacyl–tRNA synthetases; two translation elongation factors; an incomplete set of ribosomal proteins but

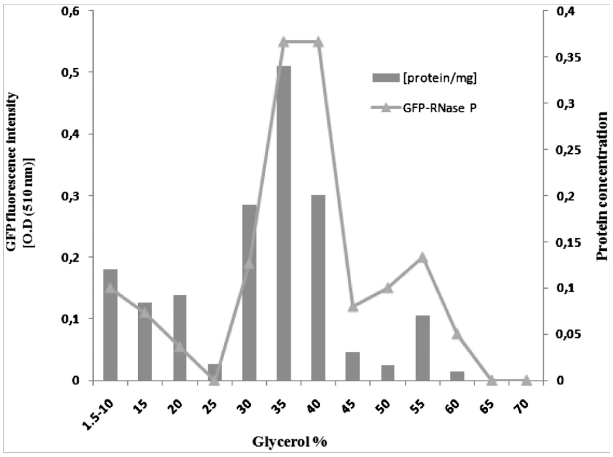

Figure 1. Density-based fractionation of mitochondrial GFP-Rpm2p. After fractionation on a discontinuous 10–70% glycerol gradient, relative GFP fluorescence absorbance/fraction identify most Rpm2-GFP with high-molecular-weight complexes.

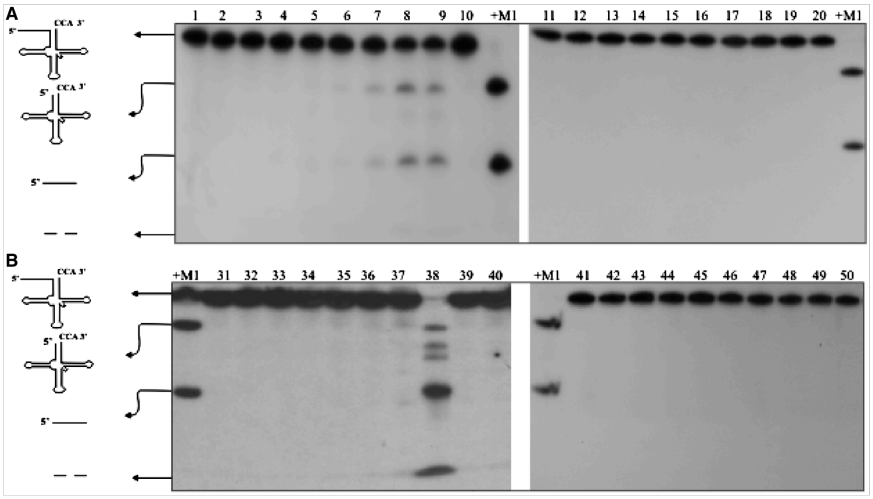

Figure 2. Purification of mt-RNase P from the mitochondrial matrix extract. Purification and assays conditions are given in 'Materials and Methods' section. Mt-RNase P activities in (**A**) correspond to a separation on a 5.5% NEC column and (B) on 7.5% NEC slab gel. Aliquots from each fraction were assayed for RNase P activity. The negative control (C–) is without and the positive control (+M1) with *E. coli* M1 RNA. The RNA corresponding to 5′-leader pre-tRNA^{proline} (117 nt), tRNA^{proline} (78 nt) and the removed 5′-leader sequence (39 nt) are indicated. Mt-RNase P activity was found in fractions 7, 8 and 9 in preparative NEC (A), and in fraction 38 only in a subsequent regular NEC separation (**B**). Note that the activity test of fraction 38 (B) was performed with more material, leading to almost complete processing of the tRNA precursor, but also to partial, unspecific cleavage of the mature tRNA into smaller fragments. With less material, the processing pattern is similar to that in (A) (Supplementary Figure S2).

un-degraded forms of the large and small rRNA subunits (Figure 5A), and others (e.g. mitochondrial genome maintenance and chaperons) (Supplementary Table S1). In the following we will refer to this complex as the 'RMT complex' (for RNA processing, metabolism, translation complex). A total of 564 physical protein–protein interactions are listed among proteins of the RMT complex in the BioGRID and SGD databases, in support of their organization in a complex.

Besides Rpm2p and tRNA Z that are involved in 5′- and 3′-tRNA maturation, we find five out of six subunits (Mtr4p; Dead-box family of ATP dependent helicase; ribosomal proteins Mrp1p, Mrpl3p, Mrpl35p and Mrpl40) of the RNA degradosome complex, as previously characterized by others (34). The remaining second catalytic subunit of the RNA degradosome (3′–5′ exoribonuclease, Dss1p) was identified only once in the three LC-MS/MS experiments, which is consistent with its low level of cellular expression [only about 1000 molecules/cell (51)]. The RNA degradosome is responsible for RNA turnover (34), but loss of function of any of its subunits also results in accumulation of RNA precursors with abnormal 5′- and 3′-termini, and stalled mitochondrial translation (33,34). Finally, the presence of five further proteins involved in rRNA and mRNA processing and RNA modification demonstrates a structural integration of most mitochondrial RNA processing activities (Nop7p; involved in rRNA processing, Mrm1p; ribose methyltransferase of the mitochondrial 21S rRNA, Hsh155p; mRNA-binding protein, Ngl1p; putative endonuclease and Prp22p; DEAH-box RNA-dependent ATPase/ATP-dependent RNA helicase).

That the RMT complex contains 22 ribosomal proteins of the large subunit and 13 of the small subunit is in agreement with the existing data that show an association of a highly purified RNA degradosome complex with four ribosomal proteins (Mrpl3p, Mrpl35p, Mrpl40 and Mrp1p) (34). Depending on the adopted experimental

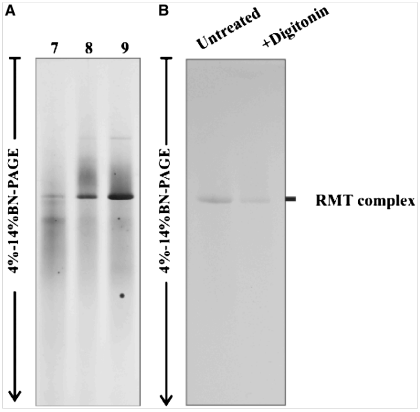

Figure 3. A homogenous, stable RMT complex. A total of 50 µg protein was loaded per lane, and after overnight electrophoresis (140 V and 9 mA; 4°C) the gel was either stained with silver nitrate (BioRad silver staining kit) in (**A**), and Serva Blue G250 in (**B**). (A) Aliquots of fractions 7, 8 and 9 (with mt-RNase P activity) from a 5.5% preparative NEC were analyzed by slab-gel NEC (4–14%) for complex composition. (B) The RMT complex (fraction 38 from 7.5% NEC) is to some degree (~50%) not dissociated by treatment (30 min) with detergent [digitonin/protein ratio (2 g/g)].

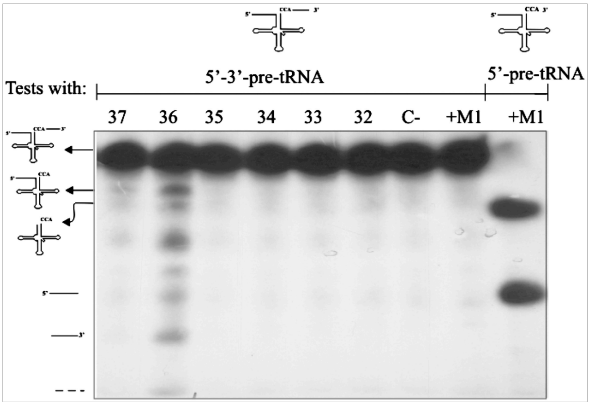

Figure 4. Association of mt-RNase P with 3′-tRNA processing activity. The RMT complex is assayed for *in vitro* processing of 5′-leader and 3′-termini pre-tRNA^{proline}. Assay conditions are given in 'Materials and Methods' section. The negative control (C–) is without addition of M1 RNA and the positive control is with M1 RNA (+M1). The RNA corresponding to 5′-leader and 3′-terminus pre-tRNA^{proline} (148 nt), 5′-leader pre-tRNA^{proline} (117 nt), tRNA^{proline} (78 nt), 5′-leader (39 nt), and 3′-trailer (31 nt) sequences are indicated. Activities of the combined mt-RNase P and 3′-tRNA processing activity were found in fractions 36 and 37.

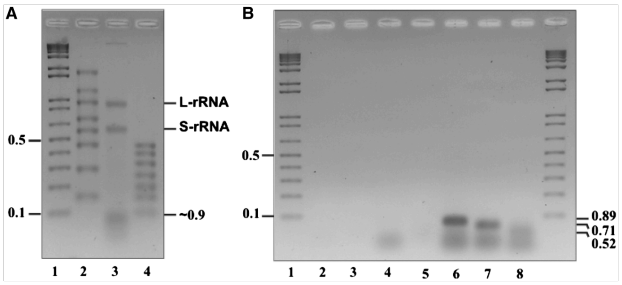

Figure 5. Two rRNAs subunits and fragments of RPM1 RNA are components of the RMT complex. (**A**) Agarose gel electrophoresis of the RNA extracted from the RMT complex. The prominent small and large S-rRNA) (L-rRNA) rRNA subunits are indicated (S-rRNA and L-rRNA). Lane 1, DNA size marker kb+ Lane 2, RNA size marker RiboRuler High Range; Lane 3, RNA extracted from RMT complex; Lane 4, RNA size marker RiboRuler Low Range. (**B**) RPM1 RNA of the RMT complex was reverse transcribed and PCR amplified using different primer combinations. Lane 1, DNA size marker kb+ lane 2, RNA control without RT–PCR amplification; lane 3, negative control with primers; lanes 4 to 8 RT–PCR products of 89, 71 and 51 nt were identified. The diffuse RNAs migrating close to 35 bp in lanes 4, 6, 7 and 8 are primers and/or primer dimers.

procedure, the mitochondrial ribosome contains about 70 proteins (52,53). The presence of only 35 mito-ribosomal proteins in the RMT complex falls short of about one half of the protein components, yet contains the un-degraded large and small subunit rRNAs (Figure 5A). This may be interpreted in two ways: (i) the RMT complex results from dissociation of a large membrane-attached complex that contains the intact ribosome. The dissociation may be caused by experimental manipulation (e.g. mechanical extraction procedure). It has been reported that the mitochondrial ribosome is attached to the inner membrane (40), which would be consistent with our result that mt-RNase P and the RMT complex is partially membrane-attached. Alternatively, (ii) the RMT complex represents a biogenesis intermediate, with an incomplete set of ribosomal proteins that are being added to the rRNA subunits.

The finding of metabolic proteins (e.g. the complete TCA cycle) and chaperons in this complex is consistent with the observed co-purification of metabolic (TCA cycle) and ribosomal proteins in enriched human mt-RNase P fractions (2). Interestingly, the RMT complex also contains several chaperons that are involved in protein maturation, modification, targeting and assembly steps.

Lack of RMT complex in a FAS II deletion mutant

A recent investigation of yeast mutants demonstrates that deficiency in any enzyme of the mitochondrial fatty acid type II biosynthetic pathway (FASII) leads to impaired 5′-tRNA processing in yeast mitochondria and an overall pleiotropic phenotype (24). Our data reveal the presence of one regular component of the pathway (Oar1p; 3-Oxoacyl-[acyl-carrier-protein] reductase; FASII biosynthesis) in the RMT complex. Two other FAS II enzymes (Htd2p and Mct1p) were also identified, but only once in the three LC-MS/MS experiments. This is probably due to their relatively low level of cellular expression (51). Consistent with the above observations, the RMT complex is no longer discernable in an Oar1 deletion mutant, and the amount of other complexes is strongly reduced (Figure 6). Our data support the interpretation that lack of FAS II enzymes indirectly affects RNAse P assembly and its activity (24), as well as enzymes in the TCA cycle (24,54). As a consequence of lacking mature

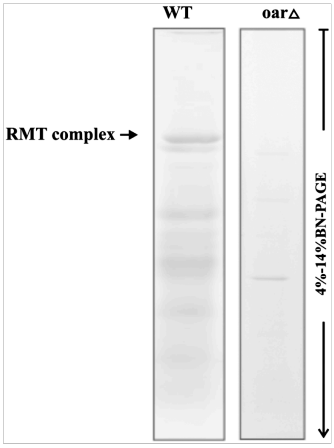

Figure 6. Biogenesis and stability of the RMT complex are affected in the yeast *oar1*Δ mutant. Soluble mitochondrial multiprotein complexes (50 µg of total protein) of the yeast wild strain and *oar1*Δ mutant were separated on linear 4–14% BN–PAGE, overnight (140 V and 9 mA; 4°C). Gels were stained with Serva Blue G250.

tRNAs and strongly reduced mitochondrial translation, FAS 2 mutants have a pleiotropic phenotype.

A membrane-attached form of mt-RNase P?

Previous publications suggest that yeast mt-RNase P is difficult to purify without the aid of detergents (16–18), and at least partially membrane-bound. Unfortunately, measuring mt-RNase P activity of mitochondrial membrane fractions is difficult because of rapid unspecific degradation of the pre-tRNA. We have therefore tracked mt-RNase P quantities by localization of its known GFP-labeled protein subunit (Rpm2p), and find that ~54% of GFP-Rpm2p is in the soluble mitochondria matrix fraction. With a mild detergent (1% digitonin) the amount of soluble GFP-Rpm2p increases to only ~68%, suggesting that the RMT complex has indeed a strong tendency for membrane attachment, but we clearly confirm that more than half is soluble, integrated with the RMT complex.

CONCLUSION

Here we show that native mt-RNase P and RNase Z activities are organized in a stable RMT supercomplex in yeast mitochondria, associated with the RNA degradosome, other RNA processing activities and several other mitochondrial functions including fatty acid synthesis, the complete TCA cycle and components of the translation machinery including a ribosome with both rRNAs but a reduced set of ribosomal proteins. Our results rationalize and further extend the surprising finding by others, that a deficiency in any component of the fatty acid type II biosynthetic pathway leads to impaired tRNA processing (24), and that deletion of genes coding for components of the RNA degradosome lead to pleiotropic defects in RNA processing and protein translation (33,34). In addition, our demonstration of stable (detergent-resistant), structural organization of metabolic activities in the RMT complex signals an end to the common belief that most metabolic enzymes are small separate enzymes that interact only casually (by diffusion) from within a pool.

SUPPLEMENTARY DATA

Supplementary Data are available at NAR Online: Supplementary Table S1, Supplementary Figures S1–S3.

ACKNOWLEDGEMENTS

The authors thank Nihade El Kraimi for discussions and valuable comments on the manuscript.

FUNDING

National Science and Engineering Research Council (NSERC) of Canada; Funding for open access charge: NSERC Canada.

Conflict of interest statement. None declared.

REFERENCES

1. Lai,L.B., Vioque,A., Kirsebom,L.A. and Gopalan,V. (2010) Unexpected diversity of RNase P, an ancient tRNA processing enzyme: challenges and prospects. *FEBS Lett.*, **584**, 287–296.
2. Holzmann,J., Frank,P., Loffler,E., Bennett,K.L., Gerner,C. and Rossmanith,W. (2008) RNase P without RNA: identification and functional reconstitution of the human mitochondrial tRNA processing enzyme. *Cell*, **135**, 462–474.
3. Gobert,A., Gutmann,B., Taschner,A., Gossringer,M., Holzmann,J., Hartmann,R.K., Rossmanith,W. and Giege,P. (2010) A single Arabidopsis organellar protein has RNase P activity. *Nat. Struct. Mol. Biol.*, **17**, 740–744.
4. Walker,S.C. and Engelke,D.R. (2008) A protein-only RNase P in human mitochondria. *Cell*, **135**, 412–414.
5. Guerrier-Takada,C., Gardiner,K., Marsh,T., Pace,N. and Altman,S. (1983) The RNA moiety of ribonuclease P is the catalytic subunit of the enzyme. *Cell*, **35**, 849–857.
6. Pannucci,J.A., Haas,E.S., Hall,T.A., Harris,J.K. and Brown,J.W. (1999) RNase P RNAs from some Archaea are catalytically active. *Proc. Natl Acad. Sci. USA*, **96**, 7803–7808.
7. Kikovska,E., Svard,S.G. and Kirsebom,L.A. (2007) Eukaryotic RNase P RNA mediates cleavage in the absence of protein. *Proc. Natl Acad. Sci. USA*, **104**, 2062–2067.
8. Cherayil,B., Krupp,G., Schuchert,P., Char,S. and Soll,D. (1987) The RNA components of Schizosaccharomyces pombe RNase P are essential for cell viability. *Gene*, **60**, 157–161.
9. Waugh,D.S. and Pace,N.R. (1990) Complementation of an RNase P RNA (rnpB) gene deletion in Escherichia coli by homologous genes from distantly related eubacteria. *J. Bacteriol.*, **172**, 6316–6322.
10. Apirion,D. and Miczak,A. (1993) RNA processing in prokaryotic cells. *Bioessays*, **15**, 113–120.
11. Morl,M. and Marchfelder,A. (2001) The final cut. The importance of tRNA 3′-processing. *EMBO Rep.*, **2**, 17–20.
12. Garber,R.L. and Altman,S. (1979) In vitro processing of B. mori transfer RNA precursor molecules. *Cell*, **17**, 389–397.
13. Engelke,D.R., Gegenheimer,P. and Abelson,J. (1985) Nucleolytic processing of a tRNAArg-tRNAAsp dimeric precursor by a homologous component from Saccharomyces cerevisiae. *J. Biol. Chem.*, **260**, 1271–1279.
14. Mayer,M., Schiffer,S. and Marchfelder,A. (2000) tRNA 3′ processing in plants: nuclear and mitochondrial activities differ. *Biochemistry*, **39**, 2096–2105.
15. Zhao,Z., Su,W., Yuan,S. and Huang,Y. (2009) Functional conservation of tRNase ZL among Saccharomyces cerevisiae, Schizosaccharomyces pombe and humans. *Biochem. J.*, **422**, 483–492.
16. Morales,M.J., Wise,C.A., Hollingsworth,M.J. and Martin,N.C. (1989) Characterization of yeast mitochondrial RNase P: an intact RNA subunit is not essential for activity in vitro. *Nucleic Acids Res.*, **17**, 6865–6881.
17. Morales,M.J., Dang,Y.L., Lou,Y.C., Sulo,P. and Martin,N.C. (1992) A 105-kDa protein is required for yeast mitochondrial RNase P activity. *Proc. Natl Acad. Sci. USA*, **89**, 9875–9879.
18. AME,J.-C. and Martin,R.P. (1993) Thèse de doctorat: Etude des mécanismes de maturation des précurseurs de tRNA dans la mitochondrie de levure: RNase P et 3′ pre-tRNase mitochondriales. Université de Strasbourg, France.
19. Seif,E.R., Forget,L., Martin,N.C. and Lang,B.F. (2003) Mitochondrial RNase P RNAs in ascomycete fungi: lineage-specific variations in RNA secondary structure. *RNA*, **9**, 1073–1083.
20. Chamberlain,J.R., Lee,Y., Lane,W.S. and Engelke,D.R. (1998) Purification and characterization of the nuclear RNase P holoenzyme complex reveals extensive subunit overlap with RNase MRP. *Genes Dev.*, **12**, 1678–1690.
21. Kassenbrock,C.K., Gao,G.J., Groom,K.R., Sulo,P., Douglas,M.G. and Martin,N.C. (1995) RPM2, independently of its mitochondrial RNase P function, suppresses an ISP42 mutant defective in mitochondrial import and is essential for normal growth. *Mol. Cell Biol.*, **15**, 4763–4770.
22. Stribinskis,V., Gao,G.J., Ellis,S.R. and Martin,N.C. (2001) Rpm2, the protein subunit of mitochondrial RNase P in Saccharomyces

cerevisiae, also has a role in the translation of mitochondrially encoded subunits of cytochrome c oxidase. *Genetics*, **158**, 573–585.
23. Stribinskis,V., Heyman,H.C., Ellis,S.R., Steffen,M.C. and Martin,N.C. (2005) Rpm2p, a component of yeast mitochondrial RNase P, acts as a transcriptional activator in the nucleus. *Mol. Cell Biol.*, **25**, 6546–6558.
24. Schonauer,M.S., Kastaniotis,A.J., Hiltunen,J.K. and Dieckmann,C.L. (2008) Intersection of RNA processing and the type II fatty acid synthesis pathway in yeast mitochondria. *Mol. Cell Biol.*, **28**, 6646–6657.
25. Chen,J.Y. and Martin,N.C. (1988) Biosynthesis of tRNA in yeast mitochondria. An endonuclease is responsible for the 3′-processing of tRNA precursors. *J. Biol. Chem.*, **263**, 13677–13682.
26. Papadimitriou,A. and Gross,H.J. (1996) Pre-tRNA 3′-processing in Saccharomyces cerevisiae. Purification and characterization of exo- and endoribonucleases. Eur. *J. Biochem.*, **242**, 747–759.
27. Vogel,A., Schilling,O., Spath,B. and Marchfelder,A. (2005) The tRNase Z family of proteins: physiological functions, substrate specificity and structural properties. *Biol. Chem.*, **386**, 1253–1264.
28. Rogowska,A.T., Puchta,O., Czarnecka,A.M., Kaniak,A., Stepien,P.P. and Golik,P. (2006) Balance between transcription and RNA degradation is vital for Saccharomyces cerevisiae mitochondria: reduced transcription rescues the phenotype of deficient RNA degradation. *Mol. Biol. Cell.*, **17**, 1184–1193.
29. Borowski,L.S., Szczesny,R.J., Brzezniak,L.K. and Stepien,P.P. (2010) RNA turnover in human mitochondria: more questions than answers? *Biochim. Biophys. Acta*, **1797**, 1066–1070.
30. Chernyakov,I., Whipple,J.M., Kotelawala,L., Grayhack,E.J. and Phizicky,E.M. (2008) Degradation of several hypomodified mature tRNA species in Saccharomyces cerevisiae is mediated by Met22 and the 5′-3′ exonucleases Rat1 and Xrn1. *Genes Dev.*, **22**, 1369–1380.
31. Butler,J.S. (2002) The yin and yang of the exosome. *Trends Cell. Biol.*, **12**, 90–96.
32. Carpousis,A.J., Vanzo,N.F. and Raynal,L.C. (1999) mRNA degradation. A tale of poly(A) and multiprotein machines. *Trends Genet.*, **15**, 24–28.
33. Gagliardi,D., Stepien,P.P., Temperley,R.J., Lightowlers,R.N. and Chrzanowska-Lightowlers,Z.M. (2004) Messenger RNA stability in mitochondria: different means to an end. *Trends Genet.*, **20**, 260–267.
34. Dziembowski,A., Piwowarski,J., Hoser,R., Minczuk,M., Dmochowska,A., Siep,M., van der Spek,H., Grivell,L. and Stepien,P.P. (2003) The yeast mitochondrial degradosome. Its composition, interplay between RNA helicase and RNase activities and the role in mitochondrial RNA metabolism. *J. Biol. Chem.*, **278**, 1603–1611.
35. Dmochowska,A., Golik,P. and Stepien,P.P. (1995) The novel nuclear gene DSS-1 of Saccharomyces cerevisiae is necessary for mitochondrial biogenesis. *Curr. Genet.*, **28**, 108–112.
36. Stepien,P.P., Margossian,S.P., Landsman,D. and Butow,R.A. (1992) The yeast nuclear gene suv3 affecting mitochondrial post-transcriptional processes encodes a putative ATP-dependent RNA helicase. *Proc. Natl Acad. Sci. USA*, **89**, 6813–6817.
37. Zahedi,R.P., Sickmann,A., Boehm,A.M., Winkler,C., Zufall,N., Schonfisch,B., Guiard,B., Pfanner,N. and Meisinger,C. (2006) Proteomic analysis of the yeast mitochondrial outer membrane reveals accumulation of a subclass of preproteins. *Mol. Biol. Cell.*, **17**, 1436–1450.
38. Meisinger,C., Sommer,T. and Pfanner,N. (2000) Purification of Saccharomcyes cerevisiae mitochondria devoid of microsomal and cytosolic contaminations. *Anal. Biochem.*, **287**, 339–342.
39. Daum,G., Bohni,P.C. and Schatz,G. (1982) Import of proteins into mitochondria. Cytochrome b2 and cytochrome c peroxidase are located in the intermembrane space of yeast mitochondria. *J. Biol. Chem.*, **257**, 13028–13033.
40. Liu,M. and Spremulli,L. (2000) Interaction of mammalian mitochondrial ribosomes with the inner membrane. *J. Biol. Chem.*, **275**, 29400–29406.
41. Schagger,H. (1995) Native electrophoresis for isolation of mitochondrial oxidative phosphorylation protein complexes. *Methods Enzymol.*, **260**, 190–202.
42. Schagger,H. and von Jagow,G. (1991) Blue native electrophoresis for isolation of membrane protein complexes in enzymatically active form. *Anal. Biochem.*, **199**, 223–231.
43. Wittig,I., Braun,H.P. and Schagger,H. (2006) Blue native PAGE. *Nat Protoc*, **1**, 418–428.
44. Wittig,I. and Schagger,H. (2007) Electrophoretic methods to isolate protein complexes from mitochondria. *Methods Cell Biol.*, **80**, 723–741.
45. Jacob,Y., Seif,E., Paquet,P.O. and Lang,B.F. (2004) Loss of the mRNA-like region in mitochondrial tmRNAs of jakobids. *RNA*, **10**, 605–614.
46. Guerrier-Takada,C. and Altman,S. (2000) Inactivation of gene expression using ribonuclease P and external guide sequences. *Methods Enzymol.*, **313**, 442–456.
47. Wessels,H.J., Vogel,R.O., van den Heuvel,L., Smeitink,J.A., Rodenburg,R.J., Nijtmans,L.G. and Farhoud,M.H. (2009) LC-MS/MS as an alternative for SDS-PAGE in blue native analysis of protein complexes. *Proteomics*, **9**, 4221–4228.
48. Fandino,A.S., Rais,I., Vollmer,M., Elgass,H., Schagger,H. and Karas,M. (2005) LC-nanospray-MS/MS analysis of hydrophobic proteins from membrane protein complexes isolated by blue-native electrophoresis. *J. Mass Spectrom.*, **40**, 1223–1231.
49. Perkins,D.N., Pappin,D.J., Creasy,D.M. and Cottrell,J.S. (1999) Probability-based protein identification by searching sequence databases using mass spectrometry data. *Electrophoresis*, **20**, 3551–3567.
50. Wittig,I. and Schagger,H. (2008) Features and applications of blue-native and clear-native electrophoresis. *Proteomics*, **8**, 3974–3990.
51. Ghaemmaghami,S., Huh,W.K., Bower,K., Howson,R.W., Belle,A., Dephoure,N., O'Shea,E.K. and Weissman,J.S. (2003) Global analysis of protein expression in yeast. *Nature*, **425**, 737–741.
52. Gan,X., Kitakawa,M., Yoshino,K., Oshiro,N., Yonezawa,K. and Isono,K. (2002) Tag-mediated isolation of yeast mitochondrial ribosome and mass spectrometric identification of its new components. *Eur. J. Biochem.*, **269**, 5203–5214.
53. Smits,P., Smeitink,J.A., van den Heuvel,L.P., Huynen,M.A. and Ettema,T.J. (2007) Reconstructing the evolution of the mitochondrial ribosomal proteome. *Nucleic Acids Res.*, **35**, 4686–4703.
54. Schonauer,M.S., Kastaniotis,A.J., Kursu,V.A., Hiltunen,J.K. and Dieckmann,C.L. (2009) Lipoic acid synthesis and attachment in yeast mitochondria. *J. Biol. Chem.*, **284**, 23234–23242.

Supplementary Information

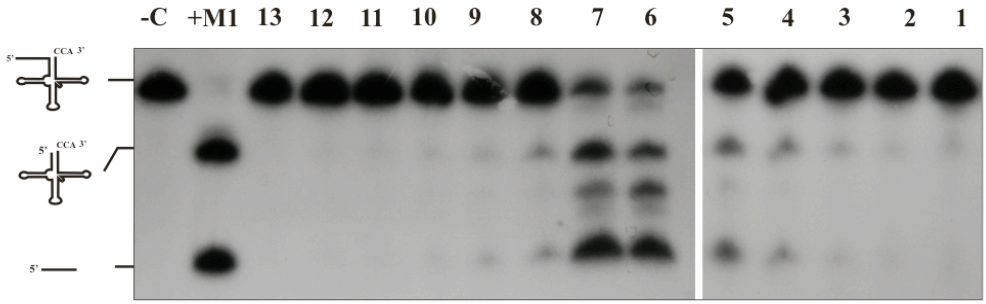

Figure S1: Gradient fractionation of a yeast mitochondrial matrix extract. After separation on a discontinuous, kinetic 10-70% glycerol gradient, aliquots from the 13 collected fractions were assayed for mt-RNase P activity. For details on purification and assay conditions see Materials and Methods. The negative control (-C) is without, and the positive control (+M1) with *E. coli* M1 RNA. The RNA corresponding to pre-tRNA^{proline} (117 nt), tRNA^{proline} (78 nt) and the removed 5' leader sequence (39 nt) are indicated. Most mt-RNase P activity was found in fractions 5, 6 and 7.

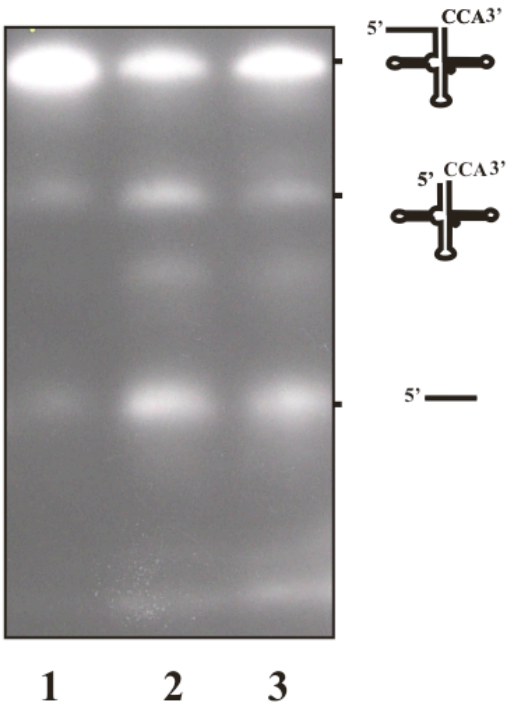

Figure S2: **Comparison of mt-RNase P activities in two consecutive NEC gel separations.** Lane 1, positive control, *E. coli* M1 RNA; lane 2, fraction 9 from first gel (5.5%); lane 3, fraction 38 from subsequent gel (7.5%), in which active fractions from the first gel were re-purified. The RNA corresponding to pre-tRNA^{proline} (117 nt), tRNA^{proline} (78 nt) and the removed 5' leader sequence (39 nt) are indicated. Equivalent protein quantities have been used for the assays, indicating a similar stoichiometry of the pre-tRNA processing products (only slightly decreased RNase P activity after re-purification).

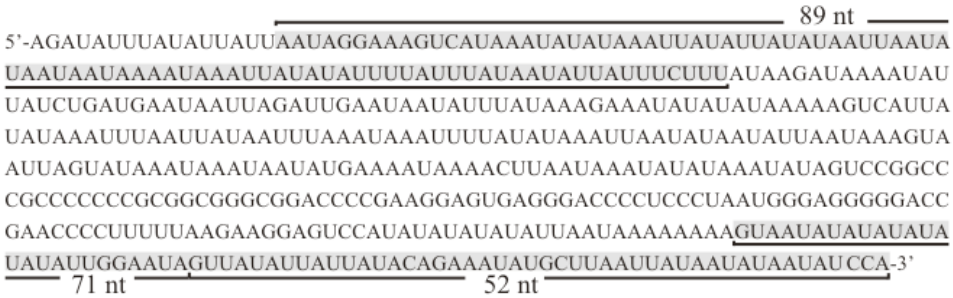

Figure S3: Identification of RPM1 RNA fragments by RT-PCR and sequencing. Three fragments (underlined) at the 5' (89 nt) and 3' end (52 and 71 nt) of RPM1 RNA were identified.

Table S1. Protein composition of the yeast mitochondrial RMT complex. First column, protein ID; second column, protein function; third column, protein name; fourth column, subcellular localization according to the SGD database (http://www.yeastgenome.org/) and ((Smith and Robinson 2009) and references therein).

Protein ID	Biological Process	Gene Name
gi|6322743	Amino acid metabolism, choline metabolism, pyrimidine synthesis	AAT1
gi|37362677	Amino acid metabolism, choline metabolism, pyrimidine synthesis	AAT2
gi|6324702	Amino acid metabolism, choline metabolism, pyrimidine synthesis	ADE2
gi|6321643	Amino acid metabolism, choline metabolism, pyrimidine synthesis	ADE3
gi|6323961	Amino acid metabolism, choline metabolism, pyrimidine synthesis	ADH2
gi|6323729	Amino acid metabolism, choline metabolism, pyrimidine synthesis	ADH3
gi|14318489	Amino acid metabolism, choline metabolism, pyrimidine synthesis	AGX1
gi|6324950	Amino acid metabolism, choline metabolism, pyrimidine synthesis	ALD4
gi|6320917	Amino acid metabolism, choline metabolism, pyrimidine synthesis	ALD5
gi|6323707	Amino acid metabolism, choline metabolism, pyrimidine synthesis	ARG7
gi|6322002	Amino acid metabolism, choline metabolism, pyrimidine synthesis	BAT1
gi|6322608	Amino acid metabolism, choline metabolism, pyrimidine synthesis	BAT2
gi|6323587	Amino acid metabolism, choline metabolism, pyrimidine synthesis	CYB2
gi|6319653	Amino acid metabolism, choline metabolism, pyrimidine synthesis	ECM31
gi|6319492	Amino acid metabolism, choline metabolism, pyrimidine synthesis	GAL7
gi|6323843	Amino acid metabolism, choline metabolism, pyrimidine synthesis	GCV2
gi|6320930	Amino acid metabolism, choline metabolism, pyrimidine synthesis	ILV1
gi|6323755	Amino acid metabolism, choline metabolism, pyrimidine synthesis	ILV2
gi|6322476	Amino acid metabolism, choline metabolism, pyrimidine synthesis	ILV3
gi|6323387	Amino acid metabolism, choline metabolism, pyrimidine synthesis	ILV5
gi|6321429	Amino acid metabolism, choline metabolism, pyrimidine synthesis	LEU1
gi|6324225	Amino acid metabolism, choline metabolism, pyrimidine synthesis	LEU4
gi|6324682	Amino acid metabolism, choline metabolism, pyrimidine synthesis	LEU9
gi|6319558	Amino acid metabolism, choline metabolism, pyrimidine synthesis	MIS1
gi|6321826	Amino acid metabolism, choline metabolism, pyrimidine synthesis	PUT2
gi|37362622	Amino acid metabolism, choline metabolism, pyrimidine synthesis	SHM1
gi|6323087	Amino acid metabolism, choline metabolism, pyrimidine synthesis	SHM2
gi|6325331	Amino acid metabolism, choline metabolism, pyrimidine synthesis	TKL1
gi|6319643	Amino acid metabolism, choline metabolism, pyrimidine synthesis	TYR1
gi|6325153	Aminoacyl-tRNA synthetases	MSD1
gi|6323950	Aminoacyl-tRNA synthetases	Ymr293c
gi|6323288	Chaperones	HSP60
gi|6323004	Chaperones	SSA2
gi|6319396	Chaperones	SSA3
gi|6320950	Chaperones	SSA4
gi|6319518	Chaperones	TCM62
gi|6322795	Fatty acid metabolism	OAR1
gi|6319481	Genome maintenance	HHF1
gi|6319482	Genome maintenance	HHT1
gi|6319470	Genome maintenance	HTA2
gi|6319471	Genome maintenance	HTB2
gi|6324562	Genome maintenance	HTZ1
gi|6322138	Genome maintenance	MMF1
gi|6319279	Glycolysis	CDC19
gi|6321693	Glycolysis	ENO1
gi|6322697	Glycolysis	GPM1
gi|6322036	Glycolysis	GUT2
gi|6322409	Glycolysis	TDH1
gi|6320255	Glycolysis	TPI1

gi|6319370	Oxidative phosphorylation	ATP1
gi|6322581	Oxidative phosphorylation	ATP2
gi|6319513	Oxidative phosphorylation	ATP3
gi|6319426	Oxidative phosphorylation	COR1
gi|6325449	Oxidative phosphorylation	QCR2
gi|6321837	Protease	AAP1
gi|9755335	Protease	Ape2
gi|82795241	Protease	APE3
gi|14318569	Protease	DUG1
gi|6319758	Protease	DUG2
gi|6324927	Regulation and signalization	MEK1
gi|6323944	RNA processing	HSH155
gi|6324775	RNA processing	MRM1
gi|6322411	RNA processing	MTR4
gi|6324531	RNA processing	NGL1
gi|6321540	RNA processing	NOP7
gi|6320849	RNA processing	PRP22
gi|6323548	RNA processing	RPM2
gi|6320016	RNA processing	TFP1
gi|6322932	RNA processing	TRZ1
gi|6321442	Transcription Factor	TFG2
gi|6320554	Translation (ribosome)	Mrp1
gi|6321521	Translation (ribosome)	MRP13
gi|6322850	Translation (ribosome)	MRP17
gi|6321782	Translation (ribosome)	MRP4
gi|6324323	Translation (ribosome)	MRP7
gi|116006497	Translation (ribosome)	MRPL15
gi|6324077	Translation (ribosome)	Mrpl17
gi|6324724	Translation (ribosome)	MRPL23
gi|6320670	Translation (ribosome)	MRPL28
gi|6323666	Translation (ribosome)	MRPL3
gi|6320528	Translation (ribosome)	Mrpl35
gi|37362666	Translation (ribosome)	MRPL49
gi|6325356	Translation (ribosome)	MRPL51
gi|6320443	Translation (ribosome)	Mrpl7
gi|6321604	Translation (ribosome)	MRPS35
gi|6323808	Translation (ribosome)	MRPS8
gi|6319622	Translation (ribosome)	MRPS9
gi|6324192	Translation (ribosome)	NAM9
gi|6320121	Translation (ribosome)	Rpl13a
gi|6321786	Translation (ribosome)	Rpl14b
gi|6323057	Translation (ribosome)	RPL15A
gi|6319444	Translation (ribosome)	Rpl19b
gi|6319378	Translation (ribosome)	RPL32
gi|6325006	Translation (ribosome)	Rpl36b
gi|6323567	Translation (ribosome)	RPL6A
gi|6321754	Translation (ribosome)	Rpl8a
gi|6322984	Translation (ribosome)	RPL8B
gi|6322271	Translation (ribosome)	Rps22a
gi|6322583	Translation (ribosome)	RPS5

gi|83578098	Translation (ribosome)	RSM18
gi|6321309	Translation (ribosome)	RSM23
gi|6322098	Translation (ribosome)	RSM25
gi|6322561	Translation (ribosome)	RSM26
gi|6321654	Translation (ribosome)	RSM27
gi|6323616	Translation (ribosome)	Yml6
gi|6322323	Translational factor	Tif2
gi|6323654	Translational elongation factor	Clu1
gi|6319594	Translational elongation factor	Tef2
gi|6320438	Transport and carrier proteins	Rtn1
gi|6320006	Transport and carrier proteins	Sec31
gi|6323335	Tricarboxylic acid cycle	Aco1
gi|6324328	Tricarboxylic acid cycle	Cit1
gi|6324993	Tricarboxylic acid cycle	Fum1
gi|6324291	Tricarboxylic acid cycle	Idh1
gi|6324709	Tricarboxylic acid cycle	Idh2
gi|6320137	Tricarboxylic acid cycle	Idp1
gi|6322066	Tricarboxylic acid cycle	Kgd1
gi|6320352	Tricarboxylic acid cycle	Kgd2
gi|6324258	Tricarboxylic acid cycle	Lat1
gi|6324716	Tricarboxylic acid cycle	Lsc1
gi|6322823	Tricarboxylic acid cycle	Mae1
gi|6322765	Tricarboxylic acid cycle	Mdh1
gi|37362644	Tricarboxylic acid cycle	Pda1
gi|6322701	Tricarboxylic acid cycle	Sdh1
gi|6322416	Tricarboxylic acid cycle	Yjl045w
gi|6323383	Unknown function	Nit3

Article 3 *: E. coli* RNase P is part of a supercomplex combining RNA processing, transcription, tRNA aminoacylation, and metabolic functions

Rachid Daoud, Lise Forget and B. Franz Lang*

Centre Robert Cedergren, Département de Biochimie, Université de Montréal, Montréal, Québec, Canada.

Keywords: RNA degradosome; PNPase; RNA polymerase; tRNA synthases.

Abstract

In *E. coli*, tRNA precursors are processed by the endonuclease RNase P to generate mature 5' termini, and 3' ends are trimmed by the concerted action of two endo- and six exonucleases. Bacterial RNase P is a ribozyme, which in its most purified form consists of a catalytic RNA plus one accessory protein. Yet, RNase P and the 3' tRNA processing activities tend to co-purify and are both involved in other RNA processing activities. They may therefore be functionally and structurally coordinated in an 'RNA processosome'. Here we show that indeed, under native conditions, concerted *in vitro* 5' plus 3' tRNA processing is associated with a large, multifunctional supercomplex of 154 proteins. The complex further includes six out of the seven proteins of the RNA degradosome, nine aminoacyl-tRNA synthases, RNA polymerase plus four transcription factors, eleven ribosomal proteins and four translation factors, components of protein folding and maturation, and a small set of metabolic enzymes. Apparently, not only is RNA processing coordinated, but it is structurally connected to aminoacylation, transcription and other cellular functions.

Introduction

Processing of tRNA precursors (pre-tRNAs) is a ubiquitous, essential cellular function that occurs in virtually all species of the three domains of life, including eukaryotic organelles. Exceptions are in a few Archaea, and in organelles that import all tRNAs from the cytoplasm (e.g., (Yermovsky-Kammerer and Hajduk 1999; Randau, Schroder et al. 2008)). Properly maturated tRNAs are essential, because only these are aminoacylated and available for protein translation.

In *E. coli*, 5' tRNA processing is accomplished by an endonuclease called RNase P (Altman, Kirsebom et al. 1995), which in its highly purified form consists of an autocatalytic RNA (P-RNA; 377 nt) and a 14 kDa accessory RNA-binding protein subunit that serves structural purposes (Stark, Kole et al. 1978; Baer and Altman 1985; Brown and Pace 1992). Yet, it has long been known that in early steps of RNase P purification, most of its activity sediments together with ribosomes (Robertson, Altman et al. 1972), indicating its potential integration into a large complex of about ribosomal size. To purify a much smaller, two-component RNase P from *E. coli* cells, dissociation of the large complex from this high-molecular weight fraction is achieved by high salt concentration (500 mM NH4Cl; 55% ammonium sulfate) (Stark, Kole et al. 1978; Baer and Altman 1985; Brown and Pace 1992), followed by a series of steps that result in isolation of the two-component RNase P, albeit at a low yield (Stark, Kole et al. 1978; Baer and Altman 1985; Brown and Pace 1992). Given this information, it is tempting to speculate that native RNase P is tightly integrated with numerous other cellular functions like the 3'tRNA processing activity (Deutscher 1990; Li and Deutscher 1994; Morl and Marchfelder 2001).

In *E. coli,* 3' tRNA processing is a multi-step process initiated by endonucleolytic cleavage with two endonucleases (RNase III and E), followed by trimming with six exonucleases (RNases II, BN, D, PH, PNPase and T; for a review see (Morl and Marchfelder 2001)). Like RNase P

(Alifano, Rivellini et al. 1994; Mohanty and Kushner 2007), these enzymes are not strictly tRNA-specific (Deutscher 1990; Li and Deutscher 1994), but also implicated in processing of polycistronic mRNAs, rRNAs precursors etc. (Alifano, Rivellini et al. 1994; Carpousis 2007; Mohanty and Kushner 2007), supporting the idea of an extended form of an RNA degradosome (Li and Deutscher 1996; Deutscher 2006; Carpousis 2007). In fact, a highly purified RNA degradosome complex contains RNase E, PNPase, DEAH-box proteins (RhlBp), but intriguingly, also proteins unrelated to RNA turnover like the molecular chaperones DnaK and GroEL, enolase (glycolysis pathway), polyphosphate kinase (PPK), subunits β, β' and α of RNA polymerase, subunits E1 and E2 of pyruvate dehydrogenase, and a few other proteins (Prud'homme-Genereux, Beran et al. 2004; Regonesi, Del Favero et al. 2006; Carpousis 2007). Whether or not these seemingly unrelated proteins are contaminants or integral components of a large multi-functional complex remains to be demonstrated.

In this investigation we show that *E. coli* RNase P and 3' tRNA processing enzymes are indeed organized in a large protein complex of about ribosome size as suggested by their co-fractionation (Robertson, Altman et al. 1972), and that they are linked with the RNA degradosome the transcription machinery and other cellular processes.

Results and Discussion

Purification of 5' tRNA processing activity

In order to preserve the integrity of a potential multi-protein complex including RNase P, we developed an alternative to published procedures that apply a series of columns and high-salt treatments (500 mM NH_4Cl, and ammonium sulfate at 55%) (Stark, Kole et al. 1978; Baer and Altman 1985; Brown and Pace 1992). These conditions are likely to dissociate large complexes, and after removal of salt, proteins may aggregate unspecifically. Indeed, following ammonium sulfate precipitation of an *E. coli* extract, we find with a detergent-free variant of the Blue Native Electrophoresis (BN-PAGE) (Schagger and von Jagow 1991; Wittig, Braun et al. 2006) an unspecific smear of protein aggregates that overlays an otherwise distinct pattern of protein complexes (not shown). Therefore, to minimize preparative artifacts, we developed a new Preparative Native Gel Stripe PAGE without detergent (PNGS-PAGE), directly from soluble *E. coli* protein extracts. The original protocol developed by Schägger and collaborators (Wittig, Braun et al. 2006) requires use of detergents, as it was optimized for the purification of otherwise insoluble membrane complexes. Details on the PNGS-PAGE protocol are described and discussed in an accompanying publication (DR and BFL, manuscript under review). Briefly, preparative separation is achieved on a discontinuous series of native polyacrylamide (PA) gel stripes (4-14 %) that are separated from each other by glycerol buffer (60%), permitting easy recuperation of fractions that contain complexes. By applying this technology, a few complexes (usually 1-4 per fraction) with similar migration properties may be pre-purified and isolated.

In the current investigation, we focus on the purification of a complex that contains RNase P, by tracking active fractions with an *in vitro* assay (5' processing of pre-$tRNA^{proline}$). Most of the activity (~90%) was identified in fraction 6 (between 7% and 8% PA on PNGS-PAGE; Fig. 1A). When analyzing the active fraction on a detergent-free variant of slab-gel BN-PAGE

(Wittig and Schagger 2008), only a single complex is confirmed (Fig. 1B). It remains stable when treating with DNase, RNase and mild detergents like digitonin (2g/g), and to some degree even to Triton X-100 (2.5%) (Fig. 1B).Taken together, these experiments provide evidence that this RNase P complex is homogenous (migrating as a sharp, discrete band in PA electrophoresis), stable, and unlikely the result of unspecific protein aggregation, potentially mediated by DNA or RNA. Homogeneity of the RNase P complex is further seen in electron microscopy experiments (not shown). In the following we will refer to this complex as the 'RAMT complex' (for RNA processing, aminoacylation of tRNA, Metabolism, Transcription complex, for more details see below).

Presence of RNase P RNA and the accessory C5p protein in the RAMT complex

In *E. coli*, the highly purified form of RNase P contains two components, an autocatalytic RNA (P-RNA; also called M1 RNA; 377 nt in length) and the small accessory RNA-binding protein C5p (Stark, Kole et al. 1978; Baer and Altman 1985; Brown and Pace 1992). An analysis of the RAMT complex (~200 ng protein) for the presence of nucleic acids demonstrates the presence of RNAs in a size range between ~120 to 380 nt (~10 ng in total), with a prominent band corresponding to M1 RNA (337 nt), and minor bands at 120 and 250 nt. In fact, this RNA pattern is apparently identical to the one that develops over time in an *in-vitro* transcribed M1 control sample (Fig. 2A), due to an intrinsic instability. This implies that RAMT complex contains only M1 RNA with its usual degradation products. RT-PCR analysis and sequencing of the 377 nt RNA that was isolated from the RNase P complex further confirms the M1 RNA identity (Fig. 2B). Finally, a proteomic analysis (LC-MS-MS) of the complex identifies C5p, together with a variety of other proteins as presented in the following. Taken together, we demonstrate that

the two-component RNase P core is integrated within RAMT complex of about ribosome-size.

Association of 5'and 3' tRNA processing activities

One of the six *E. coli* exonucleases RNase II, BN, D, PH, PNPase and T are sufficient for maturation of the 3' terminus pre-tRNA (Kelly and Deutscher 1992)(Deutscher 1990; Li and Deutscher 1994; Morl and Marchfelder 2001). The 3' tRNA processing activity of the RAMT complex was tested in an *in vitro* assay, with a pre-tRNA^{proline} substrate that has both 5' leader and 3' trailer extensions. In fact, this complex accurately processes 5' and 3' tRNA termini (Fig. 3, lane 7). A 30 minute treatment with a mild detergent (digitonin/ protein ratio 2g/g, a condition used for solubilization and dissociation of mitochondrial membrane complexes; (Wittig, Braun et al. 2006)(Eubel, Braun et al. 2005)) does not affect its activity (Fig. 3, lane 6), nor as shown above its stability (Fig. 1C). It is interesting that the tRNA processing intermediates include tRNA^{proline} plus either, 5' leader or 3' trailer (Fig. 3), in line with previous results demonstrating that 5' and 3' processing may occur independently (Li and Deutscher 1996). Our results are further consistent with co-fractionation of *E. coli* RNase P and 3' tRNA processing activity in early steps of purification (Deutscher 1990; Li and Deutscher 1994; Morl and Marchfelder 2001).

Proteomic analysis shows that PNPase is the only 3' tRNA processing exonuclease that is regularly identified in this purified complex (for more details on protein composition see below), suggesting that tRNA processing is a primary role of PNPase. Yet, it may be replaced by any of the five other listed exonucleases that are not integrated into this complex. Another enzyme that is involved in tRNA processing but that is not present in the complex is the CCA-adding enzyme [ATP(CTP):tRNA nucleotidyl transferase], which catalyzes the post-transcriptional regeneration of the CCA 3' terminus of tRNAs in *E. coli* (Sprinzl and Cramer 1979; Solari and Deutscher 1982) and

most other bacteria. This is not surprising as the CCA-adding enzyme is not essential for viability of *E. coli*, as CCA is encoded in its tRNA genes (Zhu and Deutscher 1987).

It has been suggested that tRNA aminoacylation in *E. coli* occurs is closely coordinated with a transcription/ 3′ tRNA maturation step (Gegenheimer and Apirion 1981; Apirion 1983); and likewise, that RNase P cleaves some polycistronic mRNAs and pre-tRNA co-transcriptionally (Alifano, Rivellini et al. 1994; Mohanty and Kushner 2007). The idea that tRNA processing, transcription and translation may be coordinated is consistent with our findings that RNase P and PNPase co-exist in the RAMT complex with the core RNA polymerase (subunits α_2, β and β'), 4 transcription factors, 9 aminoacyl-tRNA synthetases, 4 translation factors and 11 ribosomal proteins (Table S1), and with two recent studies demonstrating physical coupling of initial transcription and translation steps in bacteria (Gegenheimer and Apirion 1981; Apirion 1983; Burmann, Schweimer et al. 2010; Proshkin, Rahmouni et al. 2010).

Protein composition of the RAMT complex

Proteomic analysis with liquid chromatography, tandem mass spectrometry (LC-MS/MS) reveals the presence of a high number of proteins (154) in the purified RAMT complex (confirmed by four independent analyses; Table S1). These proteins are implicated in numerous functions including (as expected) RNA processing, but also metabolism (e.g., TCA cycle and glycolysis enzymes), transcription (RNA polymerase (subunits α_2, β and β') and four transcription factors), translation (11 ribosomal proteins although no ribosomal rRNAs, Fig. 2A; and nine tRNA synthetases) and others like chaperons (e.g., DnaK and GroEL that are known components of the RNA degradosome, see below) and genome maintenance (e.g., type II

topoisomerase and DNA polymerase I). The latter two enzymes are key players in replication, and in transcription when the DNA helix is unwound (Watt and Hickson 1994; Reckinger, Jeong et al. 2007) (Table S1).

Besides 5' tRNA processing (C5p; subunit of RNase P) we find six out of the seven core subunits of the RNA degradosome complex (Carpousis 2007), including a DEAH-box protein (RhlBp), PNPase, molecular chaperons DnaK and GroEL, enolase and polyphosphate kinase (PPK) (Table 1). The seventh component, RNase E, was present in only two out of four independent analyses of the RAMT complex, indicating that its association with the RNA degradosome might be variable. In fact, the list of degradosome proteins identified in publications differs substantially from one paper to another, from 4 to 22 subunits (Feng, Huang et al. 2001; Prud'homme-Genereux, Beran et al. 2004; Regonesi, Del Favero et al. 2006; Carpousis 2007), an indication for a much larger complex integrating various cellular functions. Proteins that were identified in purified RNA degradosome preparations from various laboratories include RNA polymerase, the pyruvate dehydrogenase complex (subunits E1, E2 and E3), ribosomal proteins (S1 and S3) and transketolase 2 (Feng, Huang et al. 2001; Prud'homme-Genereux, Beran et al. 2004; Regonesi, Del Favero et al. 2006; Carpousis 2007). All of these have been also found in the RAMT complex (Table S1).

Taken together, our data confirm that the RNA degradosome is associated with RNA processing activities in general, in agreement with other investigations (Alifano, Rivellini et al. 1994; Li and Deutscher 1996; Deutscher 2006; Carpousis 2007; Mohanty and Kushner 2007). In addition, we present an attractive explanation for the substantial compositional differences in degradosome composition reported by various laboratories, as well as that some of these reported protein components (such as enolase) are functionally unrelated to RNA degradation (yet identified in all investigations). The common ground is integration of the degradosome into a large stable complex, together with a variety of associated cellular functions.

Conclusions

Here we demonstrate the structural and functional coupling of 5' and 3' tRNA processing in *E. coli*, and their physical association in a stable supercomplex with other RNA processing activities, aminoacylation, transcription, as well as some elements of translation, chaperons and metabolism. The number of documented cases where functionally related activities are structurally integrated is definitely on the rise (e.g., ribosome, transcription complexes, proteasome, RNA degradosome, editosome, glycolysis complex, etc). Indeed, structural integration of related functions and pathways may turn out to be a principle. With new BN-PAGE technology now available that allows purification of native complexes up to (and potentially beyond) 50 MDa (Strecker, Wumaier et al. ; Strecker, Wumaier et al. 2010), analyses of such super-structures may become a next structural biology frontier.

Acknowledgements

We thank Elias Seif, Gertraud Burger and Nihade Elkarimi for valuable comments on the manuscript, and the National Science and Engineering Research Council (NSERC) of Canada (Grant number194560) and the Canadian Research Chair Program for financial support.

References

Alifano, P., F. Rivellini, et al. (1994). "Ribonuclease E provides substrates for ribonuclease P-dependent processing of a polycistronic mRNA." Genes Dev **8**(24): 3021-3031.

Altman, S., L. A. Kirsebom, et al. (1995). Recent studies of RNase P. tRNA Structure, Biosynthesis, and Functions. D. Soll and U. RajBhandry. Washington DC, American Society for Microbiology Press**:** 67-78.

Apirion, D. (1983). "RNA processing in a unicellular microorganism: implications for eukaryotic cells." Prog Nucleic Acid Res Mol Biol **30**: 1-40.

Baer, M. and S. Altman (1985). "A catalytic RNA and its gene from Salmonella typhimurium." Science **228**(4702): 999-1002.

Brown, J. W. and N. R. Pace (1992). "Ribonuclease P RNA and protein subunits from bacteria." Nucleic Acids Res **20**(7): 1451-1456.

Burmann, B. M., K. Schweimer, et al. (2010). "A NusE:NusG complex links transcription and translation." Science **328**(5977): 501-504.

Carpousis, A. J. (2007). "The RNA degradosome of Escherichia coli: an mRNA-degrading machine assembled on RNase E." Annu Rev Microbiol **61**: 71-87.

Deutscher, M. P. (1990). "Ribonucleases, tRNA nucleotidyltransferase, and the 3' processing of tRNA." Prog Nucleic Acid Res Mol Biol **39**: 209-240.

Deutscher, M. P. (2006). "Degradation of RNA in bacteria: comparison of mRNA and stable RNA." Nucleic Acids Res **34**(2): 659-666.

Eubel, H., H. P. Braun, et al. (2005). "Blue-native PAGE in plants: a tool in analysis of protein-protein interactions." Plant Methods **1**(1): 11.

Fandino, A. S., I. Rais, et al. (2005). "LC-nanospray-MS/MS analysis of hydrophobic proteins from membrane protein complexes isolated by blue-native electrophoresis." J Mass Spectrom **40**(9): 1223-1231.

Feng, Y., H. Huang, et al. (2001). "Escherichia coli poly(A)-binding proteins that interact with components of degradosomes or impede RNA decay mediated by polynucleotide phosphorylase and RNase E." J Biol Chem **276**(34): 31651-31656.

Gegenheimer, P. and D. Apirion (1981). "Processing of procaryotic ribonucleic acid." Microbiol Rev **45**(4): 502-541.

Guerrier-Takada, C. and S. Altman (2000). "Inactivation of gene expression using ribonuclease P and external guide sequences." Methods Enzymol **313**: 442-456.

Jacob, Y., E. Seif, et al. (2004). "Loss of the mRNA-like region in mitochondrial tmRNAs of jakobids." RNA **10**(4): 605-614.

Kelly, K. O. and M. P. Deutscher (1992). "The presence of only one of five exoribonucleases is sufficient to support the growth of Escherichia coli." J Bacteriol **174**(20): 6682-6684.

Li, Z. and M. P. Deutscher (1994). "The role of individual exoribonucleases in processing at the 3' end of Escherichia coli tRNA precursors." J Biol Chem **269**(8): 6064-6071.

Li, Z. and M. P. Deutscher (1996). "Maturation pathways for E. coli tRNA precursors: a random multienzyme process in vivo." Cell **86**(3): 503-512.

Mohanty, B. K. and S. R. Kushner (2007). "Ribonuclease P processes polycistronic tRNA transcripts in Escherichia coli independent of ribonuclease E." Nucleic Acids Res **35**(22): 7614-7625.

Morl, M. and A. Marchfelder (2001). "The final cut. The importance of tRNA 3'-processing." EMBO Rep **2**(1): 17-20.

Perkins, D. N., D. J. Pappin, et al. (1999). "Probability-based protein identification by searching sequence databases using mass spectrometry data." Electrophoresis **20**(18): 3551-3567.

Proshkin, S., A. R. Rahmouni, et al. (2010). "Cooperation between translating ribosomes and RNA polymerase in transcription elongation." Science **328**(5977): 504-508.

Prud'homme-Genereux, A., R. K. Beran, et al. (2004). "Physical and functional interactions among RNase E, polynucleotide phosphorylase and the cold-shock protein, CsdA: evidence for a 'cold shock degradosome'." Mol Microbiol **54**(5): 1409-1421.

Randau, L., I. Schroder, et al. (2008). "Life without RNase P." Nature **453**(7191): 120-123.

Reckinger, A. R., K. S. Jeong, et al. (2007). "RecA can stimulate the relaxation activity of topoisomerase I: Molecular basis of topoisomerase-mediated genome-wide transcriptional responses in Escherichia coli." Nucleic Acids Res **35**(1): 79-86.

Regonesi, M. E., M. Del Favero, et al. (2006). "Analysis of the Escherichia coli RNA degradosome composition by a proteomic approach." Biochimie **88**(2): 151-161.

Robertson, H. D., S. Altman, et al. (1972). "Purification and properties of a specific Escherichia coli ribonuclease which cleaves a tyrosine transfer ribonucleic acid presursor." J Biol Chem **247**(16): 5243-5251.

Schagger, H. (1995). "Native electrophoresis for isolation of mitochondrial oxidative phosphorylation protein complexes." Methods Enzymol **260**: 190-202.

Schagger, H. and G. von Jagow (1991). "Blue native electrophoresis for isolation of membrane protein complexes in enzymatically active form." Anal Biochem **199**(2): 223-231.

Solari, A. and M. P. Deutscher (1982). "Subcellular localization of the tRNA processing enzyme, tRNA nucleotidyltransferase, in Xenopus laevis oocytes and in somatic cells." Nucleic Acids Res **10**(14): 4397-4407.

Sprinzl, M. and F. Cramer (1979). "The -C-C-A end of tRNA and its role in protein biosynthesis." Prog Nucleic Acid Res Mol Biol **22**: 1-69.

Stark, B. C., R. Kole, et al. (1978). "Ribonuclease P: an enzyme with an essential RNA component." Proc Natl Acad Sci U S A **75**(8): 3717-3721.

Strecker, V., Z. Wumaier, et al. (2010). "Large pore gels to separate mega protein complexes larger than 10 MDa by blue native electrophoresis: Isolation of putative respiratory strings or patches." Proteomics.

Strecker, V., Z. Wumaier, et al. (2010). "Large pore gels to separate mega protein complexes larger than 10 MDa by blue native electrophoresis: isolation of putative respiratory strings or patches." Proteomics **10**(18): 3379-3387.

Watt, P. M. and I. D. Hickson (1994). "Structure and function of type II DNA topoisomerases." Biochem J **303 (Pt 3)**: 681-695.

Wessels, H. J., R. O. Vogel, et al. (2009). "LC-MS/MS as an alternative for SDS-PAGE in blue native analysis of protein complexes." Proteomics **9**(17): 4221-4228.

Wittig, I., H. P. Braun, et al. (2006). "Blue native PAGE." Nat Protoc **1**(1): 418-428.

Wittig, I. and H. Schagger (2007). "Electrophoretic methods to isolate protein complexes from mitochondria." Methods Cell Biol **80**: 723-741.

Wittig, I. and H. Schagger (2008). "Features and applications of blue-native and clear-native electrophoresis." Proteomics **8**(19): 3974-3990.

Yermovsky-Kammerer, A. E. and S. L. Hajduk (1999). "In vitro import of a nuclearly encoded tRNA into the mitochondrion of *Trypanosoma brucei*." Mol Cell Biol **19**(9): 6253-6259.

Zhu, L. and M. P. Deutscher (1987). "tRNA nucleotidyltransferase is not essential for Escherichia coli viability." EMBO J **6**(8): 2473-2477.

Figures and Tables

Figure 1: Purification of a stable *E. coli* RAMT complex.

(**A**) RNase P activity (assayed for processing of 5' leader pre-tRNA^{proline}) of fractions separated by PNGS-PAGE. Corresponding bands are the 5' leader pre-tRNA^{proline} (117 nt), tRNA^{proline} (78 nt) and the removed 5' leader sequence (39 nt). RNase P activity was identified only in fraction 6. Lane 6+digitonin: RNase P from fraction 6 after 30 minutes treatments with digitonin (2g/g protein). The negative control (C-) is without addition of *in-vitro* transcribed *E. coli* M1 RNA, and the positive control is cleavage with M1 (+M1).

(B) The RAMT complex (fraction 6) was separated on a 4-14% high-resolution slab-gel BN-PAGE. It remains stable in the presence of digitonin (2g/g protein; treatment of 30 minutes), and partially stable with Triton X-100 (2.5%). The amounts of complex loaded correspond to 40 µg protein for the untreated, and 80 µg each for the detergent-treated samples. The gel was stained with Serva Blue G250.

Figure 2: Identification of M1 RNA within the RAMT complex.

(A) Agarose gel separation of RNAs that were extracted from the RAMT complex (purified from fraction 6). The prominent band at 377 nucleotides corresponds to M1 RNA and its degradation products (including bands at 250 and 120 nt). Lane 1, DNA size marker kbp+; Lane 2, *in-vitro* transcribed M1 control sample. Lane 3, RNA extracted from the RAMT complex; Lane 4, RNA size marker RiboRuler Low Range; Lane 5, RNA size marker RiboRuler High Range.

(B) RNA purified from the RAMT complex was reverse transcribed and PCR amplified using two different primers combination covers most of the M1

RNA, and a shorter variant. Lane 1 and 5, DNA size marker kbp+; Lanes 2 and 3, RT-PCR products of 377 and 302 nucleotides were identified; Lane 4, RNA control without RT-PCR.

Figure 3: Association of RNase P and 3' tRNA processing activities.
Assay conditions for 5' and 3' tRNA processing are given in Materials and Methods. The indicated tRNA processing intermediates were extracted from the gel, amplified by RT-PCR, and sequenced to confirm their identity (not shown). Lanes: 1, negative control (C-) with 5' leader pre-tRNA^{proline}; 2, positive control (M1 + 5' leader pre-tRNA^{proline}); 3, negative control (C-) with 5' leader and 3' trailer pre-tRNA^{proline}; 4, M1 + 5'leader and 3' trailer pre-tRNA^{proline}. For conditions of digitonin treatment see legend of figure 1. The negative control (C-) is without addition of M1 RNA, and the positive control is cleavage with M1 RNA (+M1).

Figure 1:

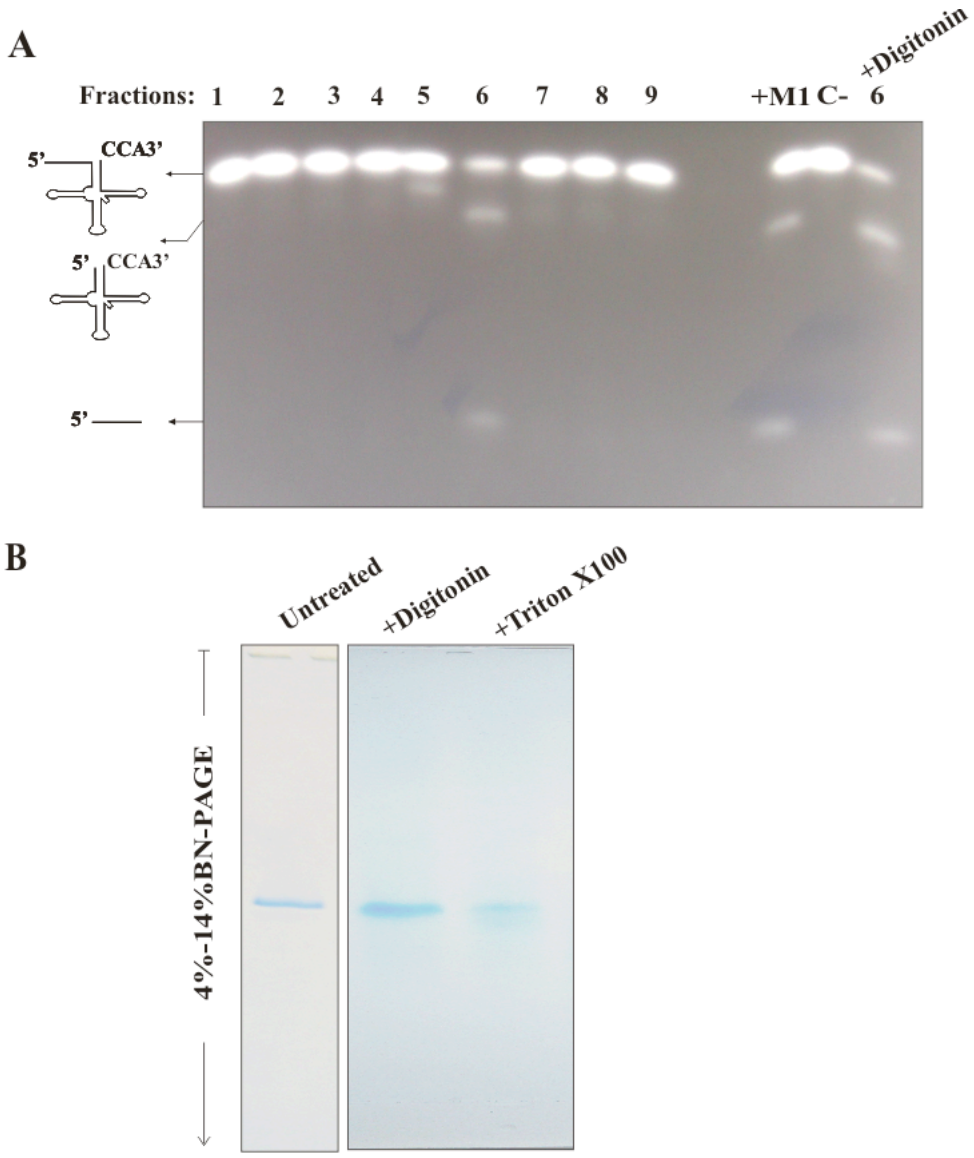
A
Fractions: 1 2 3 4 5 6 7 8 9 +M1 C- +Digitonin 6
5' CCA3'
5' CCA3'
5'
B
Untreated
+Digitonin
+Triton X100
4%-14%BN-PAGE

Figure 2.

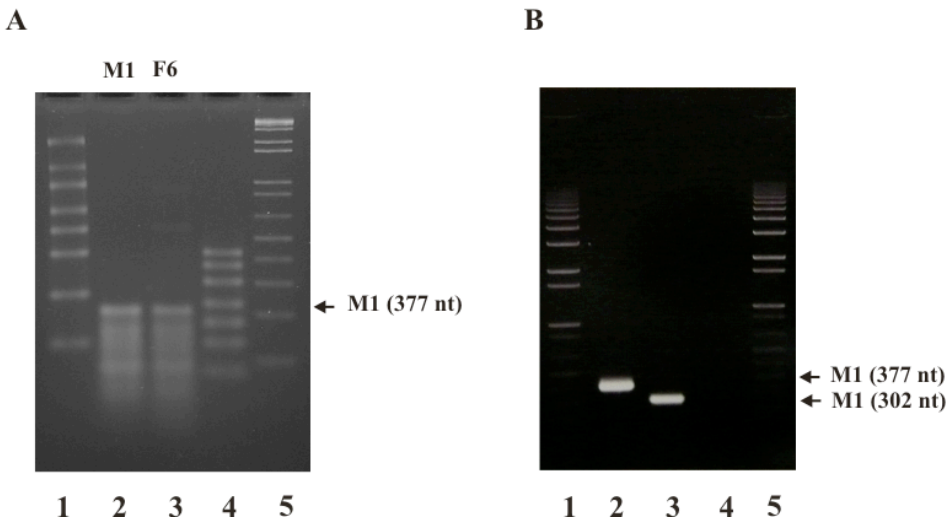

Figure 3.

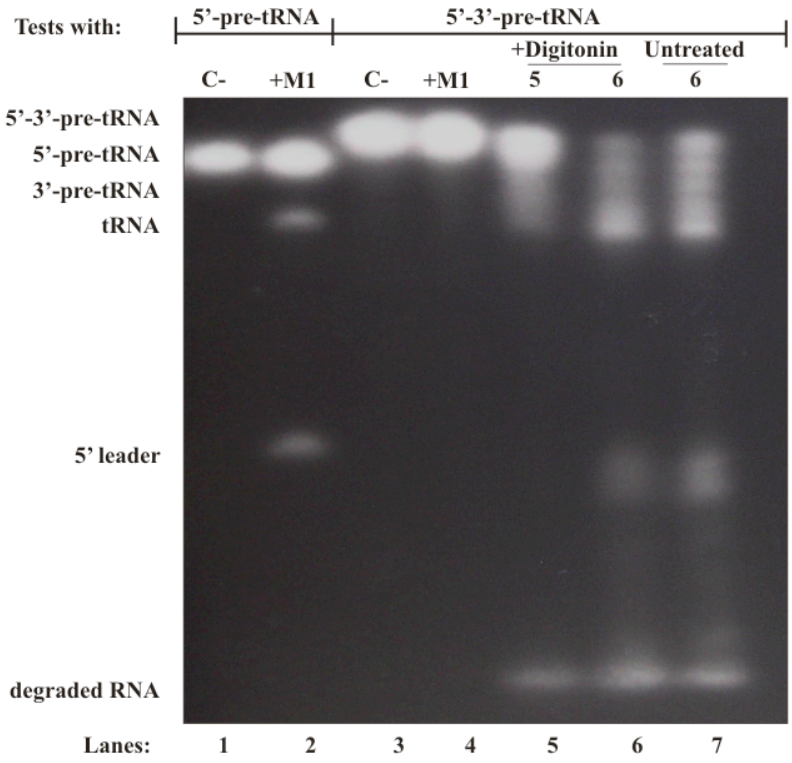
Tests with:
5'-pre-tRNA
5'-3'-pre-tRNA
+Digitonin
Untreated
C-
+M1
C-
+M1
5
6
6
5'-3'-pre-tRNA
5'-pre-tRNA
3'-pre-tRNA
tRNA
5' leader
degraded RNA
Lanes:
1
2
3
4
5
6
7

Materials and Methods

E. coli culture and extraction of soluble proteins

E. coli was grown on complete medium for 12 hours by shaking (100 rpm) at 37°C. Procedures for *E. coli* soluble proteins extraction were followed as published (Robertson, Altman et al. 1972). All operations were carried out at 4°C. Five grams of *E. coli* were disrupted with 10 g of alumina with a previously chilled (-4°C) mortar and pestle until a paste was formed. 10 mL of extraction buffer (50 mM Tris-HCl, pH 7.5, 600 mM NH_4Cl, 10 mM $MgCl_2$, 6 mM 2-mercaptoethanol and 1 mM PMSF) was added, together with 10 pg/mL pancreatic DNase. After 30 min at 4°C, the sample was cleared by subsequent centrifugations for 10 min at 15,000 g, and 40 min at 30,000 g, and the supernatant was kept on ice until further use.

RAMT complex purification

To separate the RAMT complex, we developed a new technique based on alternation of a discontinued gradient of native polyacrylamide gel (4-14%) and glycerol buffer (60% glycerol, 50 mM Tricine, 15 mM Bis-Tris). The different concentrations of native polyacrylamide gel are prepared as previously published procedure (Schagger and von Jagow 1991; Schagger 1995; Wittig, Braun et al. 2006; Wittig and Schagger 2007). After cast and polymerization of 1.5 ml of 14% polyacrylamide gel we add 1 ml of 60% glycerol buffer. Then, 1.5 ml of 13% polyacrylamide gel is cast and after polymerization 1 ml of 60% glycerol buffer is added. In the same way final discontinued gradient is prepared step-by-step following the example of [14% polyacrylamide gel -glycerol-13% polyacrylamide gel] casting gel. Gels were run in Hoefer (18 x 16 cm) electrophoresis chambers.40-100 µg of proteins/ fraction are loading *per* line on the gel, which was run at 140 V and 9 mA, overnight, in a cold room 4 ^{0}C. 18 total fractions of ~1 ml are collected.

***In vitro* preparation and radio-labeling of pre-tRNA^{proline}**

The mitochondrial *Reclinomonas americana* tRNA^{proline} substrates for RNase P assays were prepared by *in vitro* transcription and purified as described previously (Jacob, Seif et al. 2004). The tRNA^{proline} DNA was legated into pFBS/EcoRV (2.9 kb) vector with T4 DNA ligase (Roche) and amplified by PCR using 5'-GAAATTAATACGACTCACTATAGGGTAACGTACTTAATGTAAAAG GTT-3', 5'-TGGTCGGGATGACGTGATTTGAACA-3' and 5'-TCACTAAAGGGAACAAAAGCTGGGT-3' primers to product respectively 5' leader pre-tRNA^{proline} and, 5' leader and 3' termini pre-tRNA^{proline}. The two amplified tRNA^{proline} DNA were used separately for two *in vitro* radio-labeled transcriptions. 2 μg of each amplified tRNA^{proline} DNA were using to tRNA^{proline} transcriptions with Invitrogen T7 RNA polymerase (2u/μl) and α P ^{32} ATP (10 mCi/ml) (PerkinsElmers) as described (Jacob, Seif et al. 2004). After overnight incubation at 37°C of the two reactions mixtures, the loading buffer is added and the samples was heated at 75°C for 2 min before loading on a 9% polyacrylamide/8M urea gel (4 hours, 200V at room temperature). The 117 nucleotides (5' leader pre-tRNA^{proline}) and 148 nucleotides (5' leader and 3 termini pre-tRNA^{proline}) bands were cut and overnight incubated at 37°C in a 300 μl buffer extraction (30 μl of 1% SDS and 270 μl of H_20_2). After phenol/chloroform extraction and ethanol precipitation, the labeled 5'-end α P^{32} pre-tRNA^{proline} and, 5' leader and 3' termini α P^{32} pre-tRNA^{proline} were ready to be used as substrates to measure RNase P activity.

RNase P activity assays

To test the RNase P activity we us the same procedure described previously (Guerrier-Takada and Altman 2000). Radio-labeled pre-tRNA^{proline} (2,000 cpm) is dissolved in 1X PA buffer (50 mM Tris-HCl, pH 7.5, 100 mM

NH_4Cl, 10 mM $MgCl_2$) and incubated 30 minutes at 37°C with purified fractions in a 15-µl mixture reaction. After incubation, 10 µL of loading buffer was added, and the sample was heated at 75°C for 2 min before loading on a 9% polyacrylamide/8M urea gel (4 hours, 200V at room temperature). The electrophoresis 9% gels were then 12 hours exposed to a Kodak film or exposed for 2 hours on a Biorad molecular imaging screen K (#1707841), and images were developed using the Biorad molecular imager FX and analyzed by the ‘’Quantity One’’ software.

The M1 RNA ribozyme is using for the positive control for 5’ leader pre-tRNA processing. The expression plasmid carrying the *E. coli* M1 RNA gene (provided by Sidney Altman’s laboratory) was used for *in vitro* transcription. For all experimental information on M1 RNA transcription and purification see the published procedure (Jacob, Seif et al. 2004). The primers using to amplify the *rnpB* gene are 5'-GAAATTAATACGACTCACTATAGGGAAGCTGACCAGACAGTCGC-3' and 5’AGGTGAAACTGACCGATAAGCC 3’. For the M1 RNA 5’ leader pre-$tRNA^{proline}$ tests, the M1 RNA was activated by heating (65°C for 5 min), and cooling it slowly to room temperature in 1X PA buffer (50 mM Tris-HCl, pH 7.5, 100 mM NH_4Cl, 10 mM $MgCl_2$). Radio-labeled pre-$tRNA^{proline}$ (2.000 cpm) were incubated at 37°C in 10 mM Tris-HCl, pH 7.5, 100 mM $MgCl_2$, 100 mM NH_4Cl, 4% PEG, and in the presence about10 nM M1 RNA. The total reaction volume was 15 µL. After 30 minutes, 10 µL of loading buffer was added, and the sample was heated at 75°C for 2 min before loading on a 9% polyacrylamide/8M urea gel.

Identification of *E. coli* RNase P RNA (M1 RNA) by RT-PCR

Endogenous M1 RNA subunit from the identified RNA complex were purified using the RNeasy plus kit by QIAGEN and RT-PCR assays were performed on 10 ng RNA with AMV reverse transcriptase (cDNA synthesis). The cDNA was amplified with the Expand High Fidelity PCR system

provided by Roche, at an annealing temperature of 55 °C, for 30 cycles. The PCR primers for M1 RNA amplification are 5'GAAGCTGACCAGACAGTCGC 3' and 5'AGGTGAAACTGACCGATAAGCC 3'. For RT-PCR we use the same primers of the PCR in addition 5' AAGCTGACCAGACAGTCGC 3'and 5' CTCCATAGGGCAGGGTGCCAGGTA 3'. The expected PCR products have lengths of 302 and 377 nucleotides.

Blue Native Gel Electrophoresis (BN-PAGE)

Sample preparation and 4-14% BN-PAGE gel followed previously published procedures (Schagger and von Jagow 1991; Schagger 1995; Wittig, Braun et al. 2006; Wittig and Schagger 2007), except that detergents were omitted (except in stability tests of supercomplexes). Approximately 50 µg proteins were loaded per well and electrophoretic separation was performed in a Hoefer (18 x 16 cm) electrophoresis chamber, at 140 V and 9 mA, overnight at 4^0C.

Analysis of supercomplex composition by mass spectrometry

To identify proteins that form discrete bands in BN-PAGE, bands were cut from the gel and submitted to liquid chromatography tandem mass spectrometry (LC-MS/MS) analysis (Fandino, Rais et al. 2005; Wessels, Vogel et al. 2009). In-gel tryptic digestion and LC-MS/MS analysis was performed by a service at the Université de Montréal (IRIC), including functional annotation by Mascot (Perkins, Pappin et al. 1999). Details of the procedures are as follows.

The gel pieces were digested by trypsin (50 mM ammonium bicarbonate for 8 hours at 37ºC), and peptides were extracted three times with 90% acetonitrile (ACN) in 0.5 M urea. Combined extracts were dried and

resuspended in 5% ACN, 0.2% formic acid (FA) prior to mass-spectrometry analyses. Peptides were separated on a 150 μm ID, 10 cm reversed-phase nano-LC column (Jupiter C18, 3 μm, 300 Å, Phenomex) with a loading buffer of water with 0.2% formic acid (FA). Peptide elution was achieved using a gradient of 5%–60% ACN (0.2% FA) in 56 min. The nano-LC column was coupled to an LTQ-Orbitrap mass spectrometer (Thermo Fisher Scientific), and samples were injected in an interleaved manner. The mass spectrometer was operated in a data-dependent acquisition mode with a 1 s survey scan at 60,000 resolution, followed by three product ion scans (MS/MS) in the ion trap for the most abundant precursors above a threshold of 10,000 counts.

The conventional MS spectra (survey scan) were acquired in profile mode at a resolution of 60,000 at m/z 400. MS/MS spectra were acquired in the ion trap using collision-induced dissociation (CID) only or by combining CID and electron transfer dissociation (ETD) with supplemental activation mode in a decision tree data-dependent fashion for multiply charged ions exceeding a threshold of 10,000 counts. Mass calibration used an internal lock mass (protonated $(Si(CH_3)_2O))_6$; m/z 445.12057) and typically provided mass accuracy within 10 ppm for precursor ion mass measurements. The centroided MS/MS data were merged into single peak-list files and searched with the Mascot search engine v2.0.2 (Mascot 2.3) against the combined forward and reversed NCBI 2006/03/03 database (3.310.354 sequences) to obtain a false discovery rate < 1%. The mass tolerance on precursor and fragment ions was set to ± 0.03 and ± 0.5 Daltons, The threshold score for accepting individual spectra was 25 (Mascot score). The carbamidomethyl (C), deamidation (NG), oxidation (O) and phosphorylation (STY) modification were considered. Peptide clusters were aligned with mascot identification files to assign sequence identity. Expression analyses were performed on proteins identified by at least 2 different peptide sequences across triplicate analyses.

Table S1: Protein composition of the *E. coli* RAMT complex. Only those proteins identified by at least 2 peptides are reported in four independent analyses. First column, protein ID; second column, protein name; third column, protein function.

Protein ID	Protein Description	Protein Function
gi|38491472	Chaperon GroEL	Chaperon
gi|145774	Heat shock protein 70	Chaperon
gi|147549	Disulfide isomerases and chaperone	Chaperon
gi|459233	Heat shock protein DnaJ/Hsp40	Chaperon
gi|145774	Molecular chaperone DnaK	Chaperon
gi|3114400	Protease HslV and the ATPase/chaperone HslU	Chaperon
gi|1799995	Protein disaggregation chaperone	Chaperon
gi|52139759	Type I fimbrial chaperone	Chaperon
gi|146535	Catalase HP1	Detoxification
gi|1742829	Hydroperoxidase HPII	Detoxification
gi|640119	Superoxide Dismutase	Detoxification
gi|85676705	Bacterioferritin; iron storage and detoxification protein	Detoxification
gi|12516566	DNA gyrase; subunit A; type II topoisomerase	Genome maintenance
gi|13364262	DNA polymerase I (exhibits 3' to 5' and 5' to 3' exonuclease activity)	Genome maintenance
gi|1742069	DNA topoisomerase I; omega subunit	Genome maintenance
gi|26108407	Exodeoxyribonuclease III	Genome maintenance
gi|85675977	GTPase involved in cell partioning and DNA repair	Genome maintenance
gi|83588489	Single-stranded DNA-binding protein	Genome maintenance
gi|13359624	2;3;4;5-tetrahydropyridine-2-carboxylate N-succinyltransferase	metabolism
gi|146011	5;10-methylene-tetrahydrofolate dehydrogenase/5; 10-methenyl-dtetrahydrofolate cyclo-hydrolase	metabolism
gi|42585	Adenylosuccinate lyase; succinyl-AMP lyase	metabolism
gi|38492452	Aldo-keto reductases	metabolism
gi|229501	Asparaginase	metabolism
gi|640095	Aspartate/ornithine carbamoyltransferase	metabolism
gi|75194228	Aspartokinases	metabolism
gi|43064	Bifunctional aspartokinase/homoserine dehydrogenase 1	metabolism
gi|26106353	Carbamoyl-phosphate synthase large chain	metabolism
gi|12517021	Bifunctional chorismate mutase/prephenatedehydratase	metabolism
gi|26109196	Cysteine synthase A	metabolism
gi|42498	Gamma-glutamyl phosphate reductase	metabolism
gi|42497	Glutamate 5-kinase	metabolism
gi|26108180	Glutamate decarboxylase	metabolism
gi|146124	Glutamate dehydrogenase	metabolism
gi|26110127	Keto-acid formate acetyltransferase	metabolism
gi|75188019	NADPH-dependent glutamate synthase beta chain	metabolism
gi|13363305	L-asparaginase II	metabolism
gi|13359893	Pyrroline-5-carboxylate reductase	metabolism
gi|7767020	Serine-glycine hydroxymethyltransferase (SHMT)	metabolism
gi|229278	Aspartate carbamoyltransferase, regulatory subunit	metabolism
gi|12513576	Glucosamine-6-phosphate deaminase	metabolism
gi|12514962	Oligopeptide transport; periplasmic binding protein	metabolism
gi|75187609	Protein-disulfide isomerase	metabolism
gi|563868	Enolase; phosphopyruvate hydratase	metabolism
gi|10120774	Glyceraldehyde 3-Phosphate Dehydrogenase	metabolism
gi|396292	Glycerol dehydrogenase	metabolism
gi|12518878	Phosphoenolpyruvate carboxylase	metabolism
gi|42377	Phosphoglucose isomerase (PGI)	metabolism
gi|66360693	Phosphoglycerate Dehydrogenase	metabolism
Pentose phosphate	Transaldolase A	metabolism
gi|75233904	Dihydroxyacetone kinase	metabolism
gi|20149796	Phosphoglycerate Mutase	metabolism
gi|2392285	Fructose-Bisphosphate Aldolase	metabolism
gi|40904	Adenylate kinase (ADK)	metabolism
gi|1742901	PrkA serine protein kinase	metabolism
gi|5822346	Enoyl-[acyl-carrier-protein]	metabolism
gi|757842	UDP-sugar hydrolase	metabolism
gi|26106818	6;7-dimethyl-8-ribityllumazine synthase	metabolism
gi|2392785	Asparaginase	metabolism
gi|21104353	Beta-D-galactosidase	metabolism
gi|12516679	Erythronate-4-phosphate dehydrogenase	metabolism
gi|26108577	Ferritin 1; Transport of small molecules	metabolism
gi|26110579	Glutamate decarboxylase alpha	metabolism
gi|146157	Glutamine synthetase	metabolism
gi|7435996	GTP cyclohydrolase I	metabolism
gi|13362648	Hypothetical protein	metabolism
gi|995518	Beta-D-galactosidase	metabolism

gi|75238587	NADPH:quinone reductase and related Zn-dependent oxidoreductases	metabolism
gi|75229016	Nucleoside-diphosphate-sugar epimerases	metabolism
gi|147379	Phosphoribosylpyrophosphate synthetase	metabolism
gi|75243108	Phosphotransacetylase	metabolism
gi|75234185	Polyketide synthase modules and related proteins	metabolism
gi|13363598	Putative dehydrogenase	metabolism
gi|75214842	Pyruvate kinase	metabolism
gi|42479	Thiol:disulfide interchange protein dsbA	metabolism
gi|13364247	Ubiquinone biosynthesis: putative oxidoreductase	metabolism
gi|402694	Formyltetrahydrofolate deformylase (tgs)	metabolism
gi|13359564	GMP reductase	metabolism
gi|46015751	Guanylate Kinase	metabolism
gi|75255057	Phosphoribosylpyrophosphate synthetase	metabolism
gi|21730872	Uridine Phosphorylase	metabolism
gi|13362622	2-oxoglutarate decarboxylase	metabolism
gi|13359578	Aconitate hydrase B	metabolism
gi|1651427	Pyruvate formate lyase I	metabolism
gi|1009025	Pyruvate oxidase	metabolism
gi|75258891	E3 Dihydrolipoamide dehydrogenase component of pyruvate/2-oxoglutarate dehydrogenase complex	metabolism
gi|75242076	Aconitase A	metabolism
gi|13364640	Putative acyl coenzyme A dehydrogenase	metabolism
gi|12519165	Adenylosuccinate synthetase	metabolism
gi|13360203	Citrate synthase	metabolism
gi|434011	E2 Dihydrolipoamide acetyltransferase component of pyruvate dehydrogenase complex	metabolism
gi|146048	Fumarase	metabolism
gi|37953594	Isocitrate dehydrogenase	metabolism
gi|26111215	Isocitrate lyase	metabolism
gi|443367	Malate Dehydrogenase	metabolism
gi|13361549	NAD-linked malate dehydrogenase	metabolism
gi|26109236	NADP-dependent malic enzyme	metabolism
gi|83584560	E1 Dehydrogenase component of pyruvate dehydrogenase complex	metabolism
gi|85675970	Phosphoglucosamine mutase	metabolism
gi|41627	Inosine-5'-monophosphate dehydrogenase	metabolism
gi|42377	Glucose-6-phosphate isomerase	metabolism
gi|13364510	Quinone oxidoreductase	OXPHOS
gi|91074831	F1 ATP synthase; beta-subunit	OXPHOS
gi|43264	F1 ATP synthase; alpha-subunit	OXPHOS
gi|75256211	Succinate dehydrogenase/fumarate reductase; flavoprotein subunit	OXPHOS
gi|24050810	Succinyl-CoA synthetase; beta subunit	OXPHOS
gi|1651324	Succinyl-CoA synthetase; NAD(P)-binding; alpha subunit	OXPHOS
gi|7245738	ATP-dependent protease ATP-binding subunit HslU	Protease
gi|3318866	Caseinolytic protease (ClpP)	Protease
gi|75209207	Di- and tripeptidases	Protease
gi|1778540	Cold shock-like protein: RNA-binding motif bind poly-pyrimidine region	RNA processing
gi|299362	Helicases (DEAH-box proteins)	RNA processing
gi|551833	Polynucleotide phosphorilase PNPase	RNA processing
gi|1805561	Polyphosphate kinase; component of RNA degradosome	RNA processing
gi|40866	ATPase; RNA helicase	RNA processing
gi|581220	Ribonuclease P protein component; C5p	RNA processing
gi|85674314	DNA-binding transcriptional regulator	Transcription
gi|1742647	DNA-binding transcriptional regulator RstA	Transcription
gi|42799	DNA-directed RNA polymerase subunit alpha	Transcription
gi|409789	DNA-directed RNA polymerase; beta'-subunit	Transcription
gi|396326	DNA-directed RNA polymerase; beta-subunit	Transcription
gi|7766952	Rob Transcription Factor	Transcription
gi|75188633	Transcriptional antiterminator	Transcription
gi|75514625	Transcriptional regulator	Transcription
gi|1942723	Translation elongation Factor EF-TU	Translation
gi|12519129	Translation elongation factor P (EF-P)	Translation
gi|75255006	Translation elongation factors (GTPases)	Translation
gi|1651556	Peptidase T	Translation
gi|42814	Ribosomal protein L11	Translation
gi|42981	Ribosomal protein L5	Translation
gi|24054564	Ribosomal protein L7/L12	Translation
gi|223035	Ribosomal protein L10	Translation
gi|83584813	Ribosomal protein L11	Translation
gi|6980397	Ribosomal Protein L25	Translation
gi|42842	Ribosomal protein S2	Translation
gi|75208452	Ribosomal protein S5	Translation
gi|223404	Ribosomal Proteins S1	Translation
gi|223572	Ribosomal protein L9	Translation
gi|42832	Ribosomal protein S3	Translation
gi|42146	Translation initiation factor IF-2	Translation
gi|1942954	Glutaminyl-tRNA Synthetase	tRNA amino-acylation
gi|1800083	Alanyl-tRNA synthetase	tRNA amino-acylation
gi|41015	Aspartate-tRNA ligase	tRNA amino-acylation
gi|146222	Glycyl-tRNA synthetase alpha subunit	tRNA amino-acylation
gi|146223	Glycyl-tRNA synthetase beta subunit	tRNA amino-acylation
gi|75187681	L-asparaginase/archaeal Glu-tRNAGln amidotransferase subunit D	tRNA amino-acylation
gi|85675086	Phenylalanine tRNA synthetase; alpha subunit	tRNA amino-acylation
gi|1742793	Phenylalanine tRNA synthetase; beta subunit	tRNA amino-acylation
gi|26108368	Phenylalanyl-tRNA synthetase alpha chain	tRNA amino-acylation
gi|75256711	Phenylalanyl-tRNA synthetase beta subunit	tRNA amino-acylation
gi|13361893	Threonine tRNA synthetase	tRNA amino-acylation
gi|775154	Tryptophan synthase alpha subunit	tRNA amino-acylation
gi|75188158	Tryptophanyl-tRNA synthetase	tRNA amino-acylation
gi|12515629	Tyrosine tRNA synthetase	tRNA amino-acylation
gi|12516326	Putative ATPase	Uncharacterized
gi|75514816	Uncharacterized protein conserved in bacteria	Uncharacterized

CHAPITRE 3. Discussion et Conclusions

Supercomplexes multifonctionnels dans la matrice de la mitochondrie et chez *E. coli*

Les résultats présentés dans les chapitres 2, 3 et 4 révèlent l'organisation de protéines solubles en supercomplexes multifonctionnels stables, dans la mitochondrie et dans *E. coli* (publication 1). En d'autres termes, contrairement à la perception classique, les fonctions cellulaires telles que le métabolisme semblent êtres organisées en superstructures multifonctionnelles. Ces résultats sont appuyés par les données récentes (p. ex AP-MS, IPPs) qui suggèrent des interconnexions de la transcription, la traduction, le métabolisme et la régulation (Krause, von Mering et al. 2004; Kuhner, van Noort et al. 2009; Burmann, Schweimer et al. 2010; Proshkin, Rahmouni et al. 2010). En effet, les supercomplexes caractérisés n'incluent pas seulement des protéines de diverses fonctions, mais ils ont en commun un noyau de protéines en majorité métabolique (incluant le cycle TCA) et énergétique (p. ex F1ATPase, Cor1p, Cor2p et Sdh1p). A travers chacun des supercomplexes, ce noyau est associé soit à la traduction (ribosome, tRNA synthétases et facteurs de traduction), soit au maintien de l'intégrité de l'ADN (ADN polymérase, histones et facteurs de transcription), soit à la maturation et au repliement des protéines, ou à différentes combinaisons de ces dernières fonctions (publication 1). Ceci suggère que les voies métaboliques et énergétiques fournissent *in situ* les éléments nécessaires comme l'énergie sous forme d'ATP, les acides aminés, les deoxyribonucleotides et les ribonucleotides pour le fonctionnement optimal des autres fonctions cellulaires. Ainsi par exemple, l'ARN polymérase (Rpo41p et Mtf1p) et la machinerie de réplication (ADN polymérase (MIP1), primase (Pri2p) et ribonucléase H1) sont spécifiquement associés à la voie de biosynthèse des nucléotides (UTP, CTP, deoxy-ATP et deoxy-GTP) dans le supercomplexe SC13 de la levure (publication 1). Ce supercomplexe qui comporte 20 des 22 protéines connues pour être associé aux nucléoïdes (responsables du maintien de l'ADN mitochondrial) (Chen, Wang et al. 2005). Ce résultat représente

une évidence du couplage étroit de la synthèse des précurseurs d'ADN et de la réplication en complexe multienzymatique et multiprotéique "réplitase" (Prem veer Reddy and Pardee 1980; Alberts 1987; Wheeler, Ray et al. 1996; Murthy and Reddy 2006).

Le concept de l'organisation des enzymes métaboliques en complexes multi-protéiques nommés métabolon (p. ex le cycle de Krebs et la glycolyse) reste controversé à cause du peu d'évidences expérimentales en sa faveur (Welch 1977; Srere 1987; Winkel 2004; Williamson and Sutcliffe 2010). Nos résultats présentés dans le chapitre 1 démontrent ce concept par le biais de l'association des protéines du cycle TCA, de la biosynthèse des acides aminés et des lipides avec la pyruvate déshydrogénase (PDH) au sein des supercomplexes (p. ex. SC3 et SC8 chez la levure, CF4 et CF10 chez *B. oleracea*, EC16 et EC18 chez *E.* coli). D'autre part, en accord avec l'identification récente de l'interaction de la malate déshydrogénase (enzyme du cycle TCA) avec le complexe *bc1* (Wang, Yu et al. 2010), et de l'isovaleryl-CoA déshydrogénase (biosynthèse des lipides) avec le complexe I (Reifschneider, Goto et al. 2006; Wang, Mohsen et al. 2010) nos résultats révèlent que le métabolon est associé à la phosphorylation oxydative, évidemment *via* la F1 ATPase (complexe V), Cor1p et Cor2p (complexe III) et Sdh1p (complexe II) (publication 1). En fait selon nos données, ces sous-unités de l'OXPHOS font partie du noyau commun entre les supercomplexes.

Dynamique des supercomplexes suite aux changements métaboliques

L'expression des protéines (induction versus dégradation) des machines moléculaires est étroitement régulée en réponse aux stimulis cellulaires et aux conditions de croissance telles les changements métaboliques. Dans cette étude, nous avons vérifié l'effet de la répression catabolique du glucose chez la levure, qui est connue pour affecter l'expression des protéines de la majorité des fonctions incluant l'induction des enzymes de la glycolyse et la répression des protéines de l'OXPHOS (Kolkman, Olsthoorn et al. 2005). En

accord avec les changements dûs à cette répression, seulement deux supercomplexes mitochondriaux sont identifiés (publication 1). Les analyses protéomiques de ces deux supercomplexes SC1-glucose et SC2-glucose révèlent qu'ils incluent seulement une partie des enzymes du cycle TCA (PDH, Cit1p, Aco1p, Idh1p, Idh2p et Idp1p) requises pour lier la glycolyse (correspondant aux protéines de la phase de trois carbones uniquement), le métabolisme des acides aminées (leucine, valine, aspartate, glutamate, ornithine, citruline, serine et glycine), des lipides et de l'acétate (publication 1). Les protéines de l'OXPHOS (p. ex F1-ATPase et Sdh1) n'y sont plus identifiées. Ces résultats suggèrent que les supercomplexes sont dynamiques et que leur composition en protéines dépend des stimulis et de la régulation cellulaire.

Effet de l'inactivation de la voie de biosynthèse des lipides de type II sur les assemblages des supercomplexes

Nous suggérons que la plupart des effets pléiotropiques (importantes modifications globales phénotypiques) sont causées par des mutations de protéines et/ou par l'action des inhibiteurs qui perturbent la structure et l'assemblage des supercomplexes. Ces perturbations déclencheraient des cascades de dysfonctionnement du métabolisme et des autres processus biologiques. Chez la levure, nos résultats révèlent que l'inactivation de la voie de biosynthèse des lipides de type II (FASII) perturbe l'assemblage et/ou la biogenèse du supercomplexe SC3 de la RNase P (le supercomplexe est absent dans le mutant oar1Δ) (publications 1 et 2). Ceci est en accord avec l'accumulation des 5' pré-ARNt mitochondriaux non matures, un effet qui est causé par la délétion de n'importe quelle gène de la voie de FASII (Schonauer, Kastaniotis et al. 2008). Ce résultat suggère que d'autres effets pléiotropiques peuvent être de nature structural entre les protéines comme c'est le cas de la RNase P et la protéine Oar1p.

Supercomplexes versus large complexes

Chez la levure, les 16 supercomplexes mitochondriaux ont beaucoup de protéines en communs (p. ex; 80% des protéines en commun entre SC6 et SC7, et 87% entre SC5 et SC7) (publication 1). Deux interprétations pourraient expliquer ces résultats:

i) les supercomplexes sont des unités fonctionnelles possédant un noyau commun qui inclue le cycle TCA et les chaperons. Ainsi, en fonction de la régulation cellulaire d'autres protéines et/ou des fonctions différentes (ex biosynthèse des acides aminés et des lipides, et l'OXPHOS) vont êtres rajoutées à ce noyau. Toutefois, certains de ces supercomplexes pourraient refléter une étape précise de l'assemblage des autres supercomplexes. Ainsi par exemple, dans le cas du ribosome, il est connu que certains facteurs pré-ribosomiques restent associés aux sous-unités au cours de l'étape de la biogenèse, et d'autres s'associent de manière transitoire pour accomplir leur fonction, ensuite ils se dissocient. À cause de cette variation de la composition des particules pré-ribosomiques, les complexes protéiques purifiés (p. ex. par AP-MS) sont des mélanges de plusieurs complexes distincts, chacun reflétant une étape de l'assemblage (Saveanu, Namane et al. 2003).

ii) les supercomplexes pourraient être le résultat de la dissociation d'un très grand complexe. Ainsi, nos analyses par le BN-PAGE révèlent qu'après 48 heures d'électrophorèse continue à 160 volts, des mégacomplexes arrivent à entrer dans le gel mais restent bloqués au niveau du gel de concentration (3,5%). Pour l'instant nous n'avons pas encore fait des analyses plus poussées sur la composition et la stabilité de ces mégacomplexes. En terme de présence des très grands complexes, nos résultats sont en accord avec la description en 2010 de l'observation dans la mitochondrie d'un très grand complexe dont la taille peut atteindre 45 MDa et

dont la composition et la fonction restent inconnues (Strecker, Wumaier et al. 2010).

Association de la RNase P avec les enzymes de la maturation d'ARNt en 3' chez la levure et chez *E. coli*

Dans la mitochondrie de la levure nous avons caractérisé pour la première fois un supercomplexe de 130 protéines incluant la Rpm2p (protéine de la RNase P (Morales, Wise et al. 1989)) et la tRNA Z (maturation en 3' des pré-ARNt (Morl and Marchfelder 2001; Spath, Canino et al. 2007)) et qui est capable de la maturation des pré-ARNt en 5'et 3' (publication 2).

D'autre part, l'identification de six enzymes du métabolisme d'ARN (Mtr4p, Prp22p, Nop7p, Ngl1p, Mrm1p et Hsh155p) dans ce supercomplexe suggère l'association de la voie de maturation des pré-ARNt avec la dégradation des ARN mitochondriaux, puisque nous avons identifié cinq des six sous-unités du 'RNA dégradosome mitochondriale' (la Mtr4p; ATP dépendent 3'-5' RNA helicase of the Dead-box family, et les Mrpl3p, Mrpl35p, Mrpl40 et Mrp1p (protéines ribosomiques mitochondriales)) (Dziembowski, Piwowarski et al. 2003) (publication 2). Toute fois, l'association de la voie de maturation des pré-ARNt avec celle des ARNr est aussi possible puisque nous avons identifié Nop7p, Mrm1p et Hsh155p qui sont impliquées dans le métabolisme des ARNr et que le 'RNA dégradosome mitochondriale' semble impliqué dans la stabilisation des ARNr et des ARNm (la délétion de l'une de ces deux protéines catalytiques aboutit à l'accumulation des pré-ARNr et des pré-ARNm en 3' et 5' dans la mitochondrie (Dziembowski, Piwowarski et al. 2003)).

D'autre part, l'identification de 35 protéines ribosomiques, les deux sous-unités d'ARN ribosomiques et 3 facteurs de traduction dans ce supercomplexe suggère une éventuelle association de la voie de maturation des pré-ARNt et des ARNr, avec le RNA dégradosome et le ribosome. Toutefois, bien que l'association du 'RNA dégradosome mitochondriale' avec

le ribosome a été suggérée suite à sa co-fraction avec les protéines Mrpl3p, Mrpl35p, Mrpl40 et Mrp1p (Dziembowski, Piwowarski et al. 2003), nous jugeons que d'autres évidences expérimentales supplémentaires (p. ex cross-linking) sont nécessaires, surtout, pour essayer d'identifier toutes les protéines ribosomiques et pas seulement une partie comme c'est le cas dans notre étude et celle de Dziembowski.

Chez *E. coli*, nous avons caractérisé un supercomplexe similaire (154 protéines), capable de la maturation des pré-ARNt en 5' et 3'. Ce dernier inclut en plus de la sous-unité ARN et de la protéine C5p de la RNase P: la PNPase, le complexe du 'RNA degradosome' (toutes les protéines déjà rapportée (Carpousis 2007)), l'ARN polymérase, quatre facteurs de transcription, neuf aminoacyl-tRNA synthétases, onze protéines ribosomiques, des chaperons et certaines protéines métaboliques (publication 3). Ainsi, nos résultats supposent l'association physique de la voie de maturation et d'aminoacylation des ARNt avec celle de la dégradation des ARN. D'autre part, l'identification de l'ARN polymérase (sous-unités α_2, β and β') et de 4 facteurs de transcription avec la RNase P dans ce supercomplexe est supporté par la révélation plus récente du rôle de la RNase P dans le clivage de certains ARNm et pré-ARNt directement après leurs transcription (Alifano, Rivellini et al. 1994; Mohanty and Kushner 2007). Dans le but d'apporter plus d'évidences expérimentales de la fonctionnalité de l'ARN polymérase, nous avons fait des essais de la transcription *in vitro*, mais à cause de la présence de DNases et du RNA degradosome les résultats n'ont pas été concluants.

Chez *E. coli*, l'association de la RNase P avec le ribosome a été suggérée suite à son identification dans le culot des ribosomes (Robertson, Altman et al. 1972). En accord avec ce résultat, nous avons aussi identifié un tel supercomplexe dans le culot des ribosomes; toutefois, puisqu'il comporte seulement 4 facteurs de traduction et 11 protéines ribosomiques nous supposons que cette présence conjointe peut être la conséquence de la grande

taille de ce supercomplexe et non pas une évidence de l'association de la RNase P avec le ribosome. La possibilité que ce supercomplexe soit le résultat de la dissociation d'un mégacomplexe contenant le ribosome au complet est envisageable cependant des expérimentations supplémentaires sont nécessaires.

Nouvelles protéines mitochondriales

Dans le cas de la levure et de *B. oleracea* nous avons identifié de nouvelles protéines mitochondriales (132 de plus que celles actuellement reconnues dans la mitochondrie de la levure) (publication 1). Ces dernières incluent des protéines que l'on présume mitochondriales. Nos résultats chez la levure révèlent pour la première fois l'association de la primase (Pri2p) et la ribonucléase H1 (Rnh1p, dégradation des fragments d'Okazaki) avec l'ADN polymérase (MIP1) dans le supercomplexe SC3. D'autre part, nos résultats chez *B. oleracea* fournissent un premier aperçu de la machinerie de réplication mitochondriale. Ainsi, les supercomplexes CF6 et CF12 contiennent, en plus de l'ADN gyrase (sous-unités A et B) et de plusieurs protéines nécessaires à la maintenance du génome mitochondriale, deux ADN polymérase différentes (POLE1Bp (Ronceret, Guilleminot et al. 2005) et AT4G32700 (Inagaki, Suzuki et al. 2006)) (publication 1). Contrairement aux attentes, les ADN polymérases identifiées ne sont pas connues pour être situées dans les mitochondries (Ronceret, Guilleminot et al. 2005; Inagaki, Suzuki et al. 2006).

La localisation mitochondriale (non pas une contamination de protéines d'origines différentes par agrégation non-spécifique) de ces extra-protéines est appuyée par cinq évidences: (i) l'extrait matriciel est obtenu a partir des mitochondries ultra-pures, (ii) un traitement par la trypsine des mitochondries intactes avant l'élimination des membranes externes et internes, (iii) les protéines supplémentaires font partie des supercomplexes identifiés, (iv) comparativement à l'analyse directe de mitochondries intactes,

les protéines faiblement exprimées sont efficacement identifiées vue qu'elles sont enrichies dans les bandes des supercomplexes, et (v) la délétion de certaines de ces protéines causent des défauts mitochondriaux graves (exemple de Egd2p et Gln4p (Ludmerer and Schimmel 1985; George, Beddoe et al. 1998)). Pour appuyer la localisation mitochondriale de ces nouvelles protéines l'utilisation de l'imagerie cellulaire avec de séquences Tag fluorescentes pourrait s'avérer utile.

Universalité des supercomplexes

Le couplage physique de fonctions tels que le métabolisme, la traduction et la transcription en supercomplexes semble être universel, puisque présent dans les mitochondries des champignons (ex *Saccharomyces cerevisiae, Aspergillus nidulans* et *Neurospora crassa*), des animaux (ex *Bos taurus*), des plantes (*B. oleracea* et *Arabidopsis thaliana*) et chez les bactéries (ex *E. coli*) à partir des quelles les mitochondries descendent (publication 1). La composition des supercomplexes chez les champignons et les animaux est comparable a celle de levure, toute fois, chez les plantes et *E. coli* ils comportent des différences notables. Ainsi par exemple, chez *B. oleracea* les supercomplexes incluent des enzymes spécifiques à la voie de biosynthèse des sucres et des métabolites secondaires, des protéines de la famille des lectines (impliquées souvent dans le mécanisme de défense des plantes), et des protéines pentatricopeptides (PPR, souvent impliquées dans l'édition des ARN mitochondriaux; (Okuda, Chateigner-Boutin et al. 2009)).

Perspectives

Nos résultats de l'organisation en supercomplexes offrent de nouvelles hypothèses et des projets dont certains font l'objet d'études en cours avec des résultats préliminaires :

i. Compréhension de la nature de certains effets pléiotropiques qui sont dus a des mutations et/ou délétions spécifiques. Chez la levure par exemple, nous avons montré que la désactivation de la voie FASII perturbe l'assemblage et/ou la biogenèse du supercomplexe mitochondrial de la RNase P (publication 2). Ainsi il serait intéressant de tester les conséquences d'autres délétions pléiotropiques.

ii. Validation de l'organisation en supercomplexes *in vivo.* Pour ce faire nous avons commencé des essais de co-localisation des protéines (étiquetées par des séquences GFP ou YFP) qui font partie du même supercomplexe.

iii. Perturbation de l'assemblage et/ou de la composition des supercomplexes par l'étude de l'effet :

- Délétion d'une ou de plusieurs protéines des voies métaboliques et/ou des processus connectées au sein du même supercomplexe. Par exemple, vérifier si par la délétion du gène de la glutamate déshydrogénase (enzyme qui lie le cycle TCA et la voie de biosynthèse du glutamate et glutamine) on sera capable «d'éliminer» toutes les enzymes de cette voie de biosynthèse.

- Perturbation de la traduction, la transcription et la réplication par des inhibiteurs (ex bromure d'éthidium (transcription) et l'érythromycine (traduction)) dans le but de mieux comprendre l'effet spécifique sur l'organisation en complexe dans les cellules.

iv. Essai de la canalisation métabolique au sein des métabolons identifiés. Après la purification des supercomplexes nous envisageons d'utiliser des substrats isotopiques pour tester la canalisation métabolique au sein du cycle TCA et des voies qui sont reliées comme la biosynthèse du glutamate. Ainsi, nous supposons que la génération d'un produit final en absence d'échanges

d'intermédiaires métaboliques provenant du substrat précurseur avec le milieu extérieur serait un indicateur de la canalisation métabolique.

v. Études de l'ultrastructure des supercomplexes par la microscopie électronique et par la tomographie (en collaboration avec la Dr. Isabelle Rouiller (Anatomy and Cellular Biology, McGill)).

Bibliographie

Acin-Perez, R., M. P. Bayona-Bafaluy, et al. (2004). "Respiratory complex III is required to maintain complex I in mammalian mitochondria." Mol Cell **13**(6): 805-815.

Adelmant, G. and J. A. Marto (2009). "Protein complexes: the forest and the trees." Expert Rev Proteomics **6**(1): 5-10.

Alberts, B. (1998). "The cell as a collection of protein machines: preparing the next generation of molecular biologists." Cell **92**(3): 291-294.

Alberts, B. M. (1987). "Prokaryotic DNA replication mechanisms." Philos Trans R Soc Lond B Biol Sci **317**(1187): 395-420.

Alifano, P., F. Rivellini, et al. (1994). "Ribonuclease E provides substrates for ribonuclease P-dependent processing of a polycistronic mRNA." Genes Dev **8**(24): 3021-3031.

An, S., R. Kumar, et al. (2008). "Reversible compartmentalization of de novo purine biosynthetic complexes in living cells." Science **320**(5872): 103-106.

Apirion, D. and A. Miczak (1993). "RNA processing in prokaryotic cells." Bioessays **15**(2): 113-120.

Baer, M. and S. Altman (1985). "A catalytic RNA and its gene from Salmonella typhimurium." Science **228**(4702): 999-1002.

Bentley, D. L. (2005). "Rules of engagement: co-transcriptional recruitment of pre-mRNA processing factors." Curr Opin Cell Biol **17**(3): 251-256.

Bouwmeester, T., A. Bauch, et al. (2004). "A physical and functional map of the human TNF-alpha/NF-kappa B signal transduction pathway." Nat Cell Biol **6**(2): 97-105.

Brown, J. W. and N. R. Pace (1992). "Ribonuclease P RNA and protein subunits from bacteria." Nucleic Acids Res **20**(7): 1451-1456.

Buratowski, S. (2005). "Connections between mRNA 3' end processing and transcription termination." Curr Opin Cell Biol **17**(3): 257-261.

Burmann, B. M., K. Schweimer, et al. (2010). "A NusE:NusG complex links transcription and translation." Science **328**(5977): 501-504.

Butland, G., J. M. Peregrin-Alvarez, et al. (2005). "Interaction network containing conserved and essential protein complexes in Escherichia coli." Nature **433**(7025): 531-537.

Carpousis, A. J. (2007). "The RNA degradosome of Escherichia coli: an mRNA-degrading machine assembled on RNase E." Annu Rev Microbiol **61**: 71-87.

Castano, J. G., J. A. Tobian, et al. (1985). "Purification and characterization of an endonuclease from Xenopus laevis ovaries which accurately processes the 3' terminus of human pre-tRNA-Met(i) (3' pre-tRNase)." J Biol Chem **260**(15): 9002-9008.

Chen, X. J., X. Wang, et al. (2005). "Aconitase couples metabolic regulation to mitochondrial DNA maintenance." Science **307**(5710): 714-717.

Cherayil, B., G. Krupp, et al. (1987). "The RNA components of Schizosaccharomyces pombe RNase P are essential for cell viability." Gene **60**(2-3): 157-161.

Chien, C. T., P. L. Bartel, et al. (1991). "The two-hybrid system: a method to identify and clone genes for proteins that interact with a protein of interest." Proc Natl Acad Sci U S A **88**(21): 9578-9582.

Condon, C. (2007). "Maturation and degradation of RNA in bacteria." Curr Opin Microbiol **10**(3): 271-278.

Cornish-Bowden, A., M. L. Cardenas, et al. (2004). "Understanding the parts in terms of the whole." Biol Cell **96**(9): 713-717.

Coughlin, D. J., J. A. Pleiss, et al. (2008). "Genome-wide search for yeast RNase P substrates reveals role in maturation of intron-encoded box C/D small nucleolar RNAs." Proc Natl Acad Sci U S A **105**(34): 12218-12223.

Deutscher, M. P. (2006). "Degradation of RNA in bacteria: comparison of mRNA and stable RNA." Nucleic Acids Res **34**(2): 659-666.

Diaz, F., H. Fukui, et al. (2006). "Cytochrome c oxidase is required for the assembly/stability of respiratory complex I in mouse fibroblasts." Mol Cell Biol **26**(13): 4872-4881.

Dobson, C. M. (2004). "Chemical space and biology." Nature **432**(7019): 824-828.

Dubrovsky, E. B., V. A. Dubrovskaya, et al. (2004). "Drosophila RNase Z processes mitochondrial and nuclear pre-tRNA 3' ends in vivo." Nucleic Acids Res **32**(1): 255-262.

Dudkina, N. V., J. Heinemeyer, et al. (2006). "Respiratory chain supercomplexes in the plant mitochondrial membrane." Trends Plant Sci **11**(5): 232-240.

Dudkina, N. V., R. Kouril, et al. (2010). "Structure and function of mitochondrial supercomplexes." Biochim Biophys Acta **1797**(6-7): 664-670.

Dziembowski, A., J. Piwowarski, et al. (2003). "The yeast mitochondrial degradosome. Its composition, interplay between RNA helicase and RNase activities and the role in mitochondrial RNA metabolism." J Biol Chem **278**(3): 1603-1611.

Ellis, R. J. (2001). "Macromolecular crowding: obvious but underappreciated." Trends Biochem Sci **26**(10): 597-604.

Engelke, D. R., P. Gegenheimer, et al. (1985). "Nucleolytic processing of a tRNAArg-tRNAAsp dimeric precursor by a homologous component from Saccharomyces cerevisiae." J Biol Chem **260**(2): 1271-1279.

Evans, D., S. M. Marquez, et al. (2006). "RNase P: interface of the RNA and protein worlds." Trends Biochem Sci **31**(6): 333-341.

Ewing, R. M., P. Chu, et al. (2007). "Large-scale mapping of human protein-protein interactions by mass spectrometry." Mol Syst Biol **3**: 89.

Folichon, M., V. Arluison, et al. (2003). "The poly(A) binding protein Hfq protects RNA from RNase E and exoribonucleolytic degradation." Nucleic Acids Res **31**(24): 7302-7310.

French, S. L., T. J. Santangelo, et al. (2007). "Transcription and translation are coupled in Archaea." Mol Biol Evol **24**(4): 893-895.

Garber, R. L. and S. Altman (1979). "In vitro processing of B. mori transfer RNA precursor molecules." Cell **17**(2): 389-397.

Gavin, A. C., P. Aloy, et al. (2006). "Proteome survey reveals modularity of the yeast cell machinery." Nature **440**(7084): 631-636.

Gavin, A. C., M. Bosche, et al. (2002). "Functional organization of the yeast proteome by systematic analysis of protein complexes." Nature **415**(6868): 141-147.

Gavin, A. C., K. Maeda, et al. (2010). "Recent advances in charting protein-protein interaction: mass spectrometry-based approaches." Curr Opin Biotechnol.

Gavin, A. C. and G. Superti-Furga (2003). "Protein complexes and proteome organization from yeast to man." Curr Opin Chem Biol **7**(1): 21-27.

George, R., T. Beddoe, et al. (1998). "The yeast nascent polypeptide-associated complex initiates protein targeting to mitochondria in vivo." Proc Natl Acad Sci U S A **95**(5): 2296-2301.

Ghaemmaghami, S., W. K. Huh, et al. (2003). "Global analysis of protein expression in yeast." Nature **425**(6959): 737-741.

Giege, P., J. L. Heazlewood, et al. (2003). "Enzymes of glycolysis are functionally associated with the mitochondrion in Arabidopsis cells." Plant Cell **15**(9): 2140-2151.

Gobert, A., B. Gutmann, et al. (2010). "A single Arabidopsis organellar protein has RNase P activity." Nat Struct Mol Biol **17**(6): 740-744.

Graham, J. W., T. C. Williams, et al. (2007). "Glycolytic enzymes associate dynamically with mitochondria in response to respiratory demand and support substrate channeling." Plant Cell **19**(11): 3723-3738.

Grandi, P., V. Rybin, et al. (2002). "90S pre-ribosomes include the 35S pre-rRNA, the U3 snoRNP, and 40S subunit processing factors but predominantly lack 60S synthesis factors." Mol Cell **10**(1): 105-115.

Granneman, S. and S. J. Baserga (2005). "Crosstalk in gene expression: coupling and co-regulation of rDNA transcription, pre-ribosome assembly and pre-rRNA processing." Curr Opin Cell Biol **17**(3): 281-286.

Gray, M. W. and W. F. Doolittle (1982). "Has the endosymbiont hypothesis been proven?" Microbiol Rev **46**(1): 1-42.

Grundy, F. J. and T. M. Henkin (2006). "From ribosome to riboswitch: control of gene expression in bacteria by RNA structural rearrangements." Crit Rev Biochem Mol Biol **41**(6): 329-338.

Grunewald, K., O. Medalia, et al. (2003). "Prospects of electron cryotomography to visualize macromolecular complexes inside cellular compartments: implications of crowding." Biophys Chem **100**(1-3): 577-591.

Guerrier-Takada, C., K. Gardiner, et al. (1983). "The RNA moiety of ribonuclease P is the catalytic subunit of the enzyme." Cell **35**(3 Pt 2): 849-857.

Hall, D. and M. Hoshino (2010). "Effects of macromolecular crowding on intracellular diffusion from a single particle perspective." Biophys Rev **2**(1): 39-53.

Hartmann, R. K., M. Gossringer, et al. (2009). "The making of tRNAs and more - RNase P and tRNase Z." Prog Mol Biol Transl Sci **85**: 319-368.

Hartwell, L. H., J. J. Hopfield, et al. (1999). "From molecular to modular cell biology." Nature **402**(6761 Suppl): C47-52.

Ho, Y., A. Gruhler, et al. (2002). "Systematic identification of protein complexes in Saccharomyces cerevisiae by mass spectrometry." Nature **415**(6868): 180-183.

Holzle, A., S. Fischer, et al. (2008). "Maturation of the 5S rRNA 5' end is catalyzed in vitro by the endonuclease tRNase Z in the archaeon H. volcanii." RNA **14**(5): 928-937.

Holzmann, J., P. Frank, et al. (2008). "RNase P without RNA: identification and functional reconstitution of the human mitochondrial tRNA processing enzyme." Cell **135**(3): 462-474.

Hubscher, U., G. Maga, et al. (2002). "Eukaryotic DNA polymerases." Annu Rev Biochem **71**: 133-163.

Inagaki, S., T. Suzuki, et al. (2006). "Arabidopsis TEBICHI, with helicase and DNA polymerase domains, is required for regulated cell division and differentiation in meristems." Plant Cell **18**(4): 879-892.

Jorgensen, K., A. V. Rasmussen, et al. (2005). "Metabolon formation and metabolic channeling in the biosynthesis of plant natural products." Curr Opin Plant Biol **8**(3): 280-291.

Kassenbrock, C. K., G. J. Gao, et al. (1995). "RPM2, independently of its mitochondrial RNase P function, suppresses an ISP42 mutant defective in mitochondrial import and is essential for normal growth." Mol Cell Biol **15**(9): 4763-4770.

Kikovska, E., S. G. Svard, et al. (2007). "Eukaryotic RNase P RNA mediates cleavage in the absence of protein." Proc Natl Acad Sci U S A **104**(7): 2062-2067.

Kocher, T. and G. Superti-Furga (2007). "Mass spectrometry-based functional proteomics: from molecular machines to protein networks." Nat Methods **4**(10): 807-815.

Kohn, K. W., M. I. Aladjem, et al. (2006). "Molecular interaction maps of bioregulatory networks: a general rubric for systems biology." Mol Biol Cell **17**(1): 1-13.

Kolkman, A., M. M. Olsthoorn, et al. (2005). "Comparative proteome analysis of Saccharomyces cerevisiae grown in chemostat cultures limited for glucose or ethanol." Mol Cell Proteomics **4**(1): 1-11.

Krause, R., C. von Mering, et al. (2004). "Shared components of protein complexes--versatile building blocks or biochemical artefacts?" Bioessays **26**(12): 1333-1343.

Krogan, N. J., G. Cagney, et al. (2006). "Global landscape of protein complexes in the yeast Saccharomyces cerevisiae." Nature **440**(7084): 637-643.

Kruger, E., P. M. Kloetzel, et al. (2001). "20S proteasome biogenesis." Biochimie **83**(3-4): 289-293.

Kuhner, S., V. van Noort, et al. (2009). "Proteome organization in a genome-reduced bacterium." Science **326**(5957): 1235-1240.

Kusmierczyk, A. R. and M. Hochstrasser (2008). "Some assembly required: dedicated chaperones in eukaryotic proteasome biogenesis." Biol Chem **389**(9): 1143-1151.

Lai, L. B., A. Vioque, et al. (2010). "Unexpected diversity of RNase P, an ancient tRNA processing enzyme: challenges and prospects." FEBS Lett **584**(2): 287-296.

Lang, B. F., M. W. Gray, et al. (1999). "Mitochondrial genome evolution and the origin of eukaryotes." Annu Rev Genet **33**: 351-397.

Li, Y. and S. Altman (2003). "A specific endoribonuclease, RNase P, affects gene expression of polycistronic operon mRNAs." Proc Natl Acad Sci U S A **100**(23): 13213-13218.

Li, Y. and S. Altman (2004). "In search of RNase P RNA from microbial genomes." RNA **10**(10): 1533-1540.

Li, Z. and M. P. Deutscher (1996). "Maturation pathways for E. coli tRNA precursors: a random multienzyme process in vivo." Cell **86**(3): 503-512.

Ludmerer, S. W. and P. Schimmel (1985). "Cloning of GLN4: an essential gene that encodes glutaminyl-tRNA synthetase in Saccharomyces cerevisiae." J Bacteriol **163**(2): 763-768.

Martin, J.-C. A. a. R. P. (1993). Etude des mecanismes de maturation des precurseurs de tRNA dans la mitochondria de levure: RNase P et 3' PRE-tRNase mitochondriales. Biologie moleculaire. Strastbourg, France, Strastbourg. **Doctorat**.

Mayer, M., S. Schiffer, et al. (2000). "tRNA 3' processing in plants: nuclear and mitochondrial activities differ." Biochemistry **39**(8): 2096-2105.

Miller, O. L., Jr., B. A. Hamkalo, et al. (1970). "Visualization of bacterial genes in action." Science **169**(943): 392-395.

Mohanty, B. K. and S. R. Kushner (2007). "Ribonuclease P processes polycistronic tRNA transcripts in Escherichia coli independent of ribonuclease E." Nucleic Acids Res **35**(22): 7614-7625.

Morales, M. J., C. A. Wise, et al. (1989). "Characterization of yeast mitochondrial RNase P: an intact RNA subunit is not essential for activity in vitro." Nucleic Acids Res **17**(17): 6865-6881.

Morl, M. and A. Marchfelder (2001). "The final cut. The importance of tRNA 3'-processing." EMBO Rep **2**(1): 17-20.

Murthy, S. and G. P. Reddy (2006). "Replitase: complete machinery for DNA synthesis." J Cell Physiol **209**(3): 711-717.

Okuda, K., A. L. Chateigner-Boutin, et al. (2009). "Pentatricopeptide repeat proteins with the DYW motif have distinct molecular functions in RNA editing and RNA cleavage in Arabidopsis chloroplasts." Plant Cell **21**(1): 146-156.

Ovadi, J. and V. Saks (2004). "On the origin of intracellular compartmentation and organized metabolic systems." Mol Cell Biochem **256-257**(1-2): 5-12.

Pan, T. and T. Sosnick (2006). "RNA folding during transcription." Annu Rev Biophys Biomol Struct **35**: 161-175.

Pandit, S., D. Wang, et al. (2008). "Functional integration of transcriptional and RNA processing machineries." Curr Opin Cell Biol **20**(3): 260-265.

Pannucci, J. A., E. S. Haas, et al. (1999). "RNase P RNAs from some Archaea are catalytically active." Proc Natl Acad Sci U S A **96**(14): 7803-7808.

Papadimitriou, A. and H. J. Gross (1996). "Pre-tRNA 3'-processing in Saccharomyces cerevisiae. Purification and characterization of exo- and endoribonucleases." Eur J Biochem **242**(3): 747-759.

Parrish, J. R., K. D. Gulyas, et al. (2006). "Yeast two-hybrid contributions to interactome mapping." Curr Opin Biotechnol **17**(4): 387-393.

Peck-Miller, K. A. and S. Altman (1991). "Kinetics of the processing of the precursor to 4.5 S RNA, a naturally occurring substrate for RNase P from Escherichia coli." J Mol Biol **221**(1): 1-5.

Pereira-Leal, J. B., A. J. Enright, et al. (2004). "Detection of functional modules from protein interaction networks." Proteins **54**(1): 49-57.

Pettersson, G. (1991). "No convincing evidence is available for metabolite channelling between enzymes forming dynamic complexes." J Theor Biol **152**(1): 65-69.

Prem veer Reddy, G. and A. B. Pardee (1980). "Multienzyme complex for metabolic channeling in mammalian DNA replication." Proc Natl Acad Sci U S A **77**(6): 3312-3316.

Proshkin, S., A. R. Rahmouni, et al. (2010). "Cooperation between translating ribosomes and RNA polymerase in transcription elongation." Science **328**(5977): 504-508.

Pu, S., J. Vlasblom, et al. (2007). "Identifying functional modules in the physical interactome of Saccharomyces cerevisiae." Proteomics **7**(6): 944-960.

Randau, L., I. Schroder, et al. (2008). "Life without RNase P." Nature **453**(7191): 120-123.

Reddy, G. P. and R. S. Fager (1993). "Replitase: a complex integrating dNTP synthesis and DNA replication." Crit Rev Eukaryot Gene Expr **3**(4): 255-277.

Reddy, G. P. and C. K. Mathews (1978). "Functional compartmentation of DNA precursors in T4 phage-infected bacteria." J Biol Chem **253**(10): 3461-3467.

Reddy, G. P., A. Singh, et al. (1977). "Enzyme associations in T4 phage DNA precursor synthesis." Proc Natl Acad Sci U S A **74**(8): 3152-3156.

Reifschneider, N. H., S. Goto, et al. (2006). "Defining the mitochondrial proteomes from five rat organs in a physiologically significant context using 2D blue-native/SDS-PAGE." J Proteome Res **5**(5): 1117-1132.

Robertson, H. D., S. Altman, et al. (1972). "Purification and properties of a specific Escherichia coli ribonuclease which cleaves a tyrosine transfer ribonucleic acid presursor." J Biol Chem **247**(16): 5243-5251.

Ronceret, A., J. Guilleminot, et al. (2005). "Genetic analysis of two Arabidopsis DNA polymerase epsilon subunits during early embryogenesis." Plant J **44**(2): 223-236.

Samanta, M. P., W. Tongprasit, et al. (2006). "Global identification of noncoding RNAs in Saccharomyces cerevisiae by modulating an essential RNA processing pathway." Proc Natl Acad Sci U S A **103**(11): 4192-4197.

Saveanu, C., A. Namane, et al. (2003). "Sequential protein association with nascent 60S ribosomal particles." Mol Cell Biol **23**(13): 4449-4460.

Schonauer, M. S., A. J. Kastaniotis, et al. (2008). "Intersection of RNA processing and the type II fatty acid synthesis pathway in yeast mitochondria." Mol Cell Biol **28**(21): 6646-6657.

Spath, B., G. Canino, et al. (2007). "tRNase Z: the end is not in sight." Cell Mol Life Sci **64**(18): 2404-2412.

Spirin, V. and L. A. Mirny (2003). "Protein complexes and functional modules in molecular networks." Proc Natl Acad Sci U S A **100**(21): 12123-12128.

Srere, P. A. (1987). "Complexes of sequential metabolic enzymes." Annu Rev Biochem **56**: 89-124.

Stark, B. C., R. Kole, et al. (1978). "Ribonuclease P: an enzyme with an essential RNA component." Proc Natl Acad Sci U S A **75**(8): 3717-3721.

Strecker, V., Z. Wumaier, et al. (2010). "Large pore gels to separate mega protein complexes larger than 10 MDa by blue native electrophoresis:

isolation of putative respiratory strings or patches." Proteomics **10**(18): 3379-3387.

von Mering, C., R. Krause, et al. (2002). "Comparative assessment of large-scale data sets of protein-protein interactions." Nature **417**(6887): 399-403.

Vonck, J. and E. Schafer (2009). "Supramolecular organization of protein complexes in the mitochondrial inner membrane." Biochim Biophys Acta **1793**(1): 117-124.

Walker, S. C. and D. R. Engelke (2006). "Ribonuclease P: the evolution of an ancient RNA enzyme." Crit Rev Biochem Mol Biol **41**(2): 77-102.

Walker, S. C. and D. R. Engelke (2008). "A protein-only RNase P in human mitochondria." Cell **135**(3): 412-414.

Wang, Q., L. Yu, et al. (2010). "Cross-talk between mitochondrial malate dehydrogenase and the cytochrome bc1 complex." J Biol Chem **285**(14): 10408-10414.

Wang, Y., A. W. Mohsen, et al. (2010). "Evidence for physical association of mitochondrial fatty acid oxidation and oxidative phosphorylation complexes." J Biol Chem **285**(39): 29834-29841.

Waugh, D. S. and N. R. Pace (1990). "Complementation of an RNase P RNA (rnpB) gene deletion in Escherichia coli by homologous genes from distantly related eubacteria." J Bacteriol **172**(11): 6316-6322.

Weiner, A. M. (2004). "tRNA maturation: RNA polymerization without a nucleic acid template." Curr Biol **14**(20): R883-885.

Welch, G. R. (1977). "On the role of organized multienzyme systems in cellular metabolism: a general synthesis." Prog Biophys Mol Biol **32**(2): 103-191.

Wheeler, L. J., N. B. Ray, et al. (1996). "T4 phage gene 32 protein as a candidate organizing factor for the deoxyribonucleoside triphosphate synthetase complex." J Biol Chem **271**(19): 11156-11162.

Williamson, M. P. and M. J. Sutcliffe (2010). "Protein-protein interactions." Biochem Soc Trans **38**(4): 875-878.

Winkel, B. S. (2004). "Metabolic channeling in plants." Annu Rev Plant Biol **55**: 85-107.

Wittig, I. and H. Schagger (2009). "Supramolecular organization of ATP synthase and respiratory chain in mitochondrial membranes." Biochim Biophys Acta **1787**(6): 672-680.

Wodak, S. J., S. Pu, et al. (2009). "Challenges and rewards of interaction proteomics." Mol Cell Proteomics **8**(1): 3-18.

Wolin, S. L. and T. Cedervall (2002). "The La protein." Annu Rev Biochem **71**: 375-403.

Wool, I. G. (1996). "Extraribosomal functions of ribosomal proteins." Trends Biochem Sci **21**(5): 164-165.

Wu, X. M., H. Gutfreund, et al. (1991). "Substrate channeling in glycolysis: a phantom phenomenon." Proc Natl Acad Sci U S A **88**(2): 497-501.

Xiong, Y. and T. A. Steitz (2006). "A story with a good ending: tRNA 3'-end maturation by CCA-adding enzymes." Curr Opin Struct Biol **16**(1): 12-17.

Yang, L. and S. Altman (2007). "A noncoding RNA in Saccharomyces cerevisiae is an RNase P substrate." RNA **13**(5): 682-690.

Yermovsky-Kammerer, A. E. and S. L. Hajduk (1999). "In vitro import of a nuclearly encoded tRNA into the mitochondrion of *Trypanosoma brucei*." Mol Cell Biol **19**(9): 6253-6259.

Zangrossi, S., F. Briani, et al. (2000). "Transcriptional and post-transcriptional control of polynucleotide phosphorylase during cold acclimation in Escherichia coli." Mol Microbiol **36**(6): 1470-1480.

Zhou, H. X., G. Rivas, et al. (2008). "Macromolecular crowding and confinement: biochemical, biophysical, and potential physiological consequences." Annu Rev Biophys **37**: 375-397.